The Dissertation Committee for Claire Genevieve Griffin Certifies that this is the approved version of the following dissertation:

Dissolved organic matter in major rivers across the Pan-Arctic from remote sensing

Committee:

James W. McClelland, Supervisor

Karen E. Frey

Wayne S. Gardner

Zhanfei Liu

Gerald C. Shank

Dissolved organic matter in major rivers across the Pan-Arctic from remote sensing

by

Claire Genevieve Griffin, B.A.

Dissertation

Presented to the Faculty of the Graduate School of

The University of Texas at Austin

in Partial Fulfillment

of the Requirements

for the Degree of

Doctor of Philosophy

The University of Texas at Austin
May 2016

Acknowledgements

Dissolved organic matter in major rivers across the Pan-Arctic from remote sensing

Claire Genevieve Griffin, Ph.D.

The University of Texas at Austin, 2016

Supervisor: James W. McClelland

Climate-driven changes in Arctic hydrology and biogeochemistry are impacting transport of water and water-borne material from land to ocean. This includes massive amounts of organic matter that are mobilized and exported from the pan-Arctic watershed via rivers each year. Dissolved organic matter (DOM), an important part of the Arctic carbon cycle, has received growing attention in recent years, yet long-term studies of riverine biogeochemistry remain rare in these remote and logistically challenging regions. Remote sensing of chromophoric dissolved organic matter (CDOM, the portion of the DOM pool that absorbs light), provides a unique opportunity to investigate variations in DOM in major Arctic rivers over multiple decades. CDOM is a useful proxy for dissolved organic carbon (DOC) and is essential to photochemical processes in surface waters. This dissertation presents the development and application of remote sensing regression models across six major Arctic rivers: the Kolyma, Lena, Mackenzie, Ob', Yenisey and Yukon. Frozen, archival samples of CDOM were used to develop calibration data for remote sensing regressions. Remote sensing methods estimated CDOM with R^2 of 85% across all rivers, although individual rivers varied in their predictability in association with sediment loading and hydrology. As with previous studies of Arctic systems, concentrations and export of CDOM and DOC were highest

during spring freshet in most of these rivers. Interannual variability in DOM export may be linked to the Arctic Oscillation. Within the Mackenzie, Ob', and Yenisey rivers, observations of DOM concentration and export were extended back to the 1980s, the first known empirical records of this length for Arctic rivers that span both continents. Although no pan-Arctic trends in CDOM export were detected, there is some evidence of long-term changes in riverine DOM. For example, discharge-specific CDOM concentrations decreased in the Yenisey River and increased in the Ob' River. Additionally, CDOM concentrations increased over the past ~30 years within the Mackenzie River. This dissertation also includes results from experiments used to quantify the effects of cryopreservation on CDOM analyses, and potential approaches for ameliorating freezing effects. These experiments showed that freezing for preservation introduces some error into CDOM measurements, although these effects vary between river systems. Sonication may improve CDOM measurements in some river systems, but the effects of both cryopreservation and sonication should be quantified on a case-by-case basis. Overall, this dissertation work demonstrates that 1) remote sensing of CDOM is a viable tool for tracking fluvial DOM in the major Arctic rivers, 2) only the Mackenzie River showed significant increases in CDOM concentration from the 1980s to present and 3) long-term changes in discharge-specific CDOM concentrations have occurred in the Yenisey and Ob' rivers. These long-term trends cannot be definitively linked to climate change, but may be related to effects of warming on permafrost, hydrology, and biogeochemistry within in Arctic watersheds with consequences for carbon cycling on both regional and global scales.

Table of Contents

List of Tables

List of Figures

Introduction

Rivers across the Arctic are integral to biogeochemical and hydrological processes, as they transport large amounts of freshwater and organic matter from land to sea. Aquatic ecosystems feature prominently across the Arctic landscape, with as much as 16% of permafrost-influenced land surface classified as fluvial, lotic, or wetlands [*Lehner and Doll*, 2004; *Vonk et al.*, 2015]. The presence of permafrost throughout high-latitudes limits groundwater processes, contributing to the extensive surface freshwater systems in the Arctic that link land to sea. Arctic rivers deliver approximately 10% of the world's freshwater discharge, and as much as $10 - 20\%$ of global riverine dissolved organic matter (DOM) to an ocean basin containing only ~1% of global ocean volume [*Menard and Smith*, 1966; *Aagard and E.C. Carmack et al.*, 1989; *Stein and MacDonald,* 2003; *Harrison et al.*, 2005; *Holmes et al.*, 2012].

Streams and rivers throughout the Arctic are hotspots of biogeochemical cycling as labile material is metabolized by microbial processes [*Denfeld et al.*, 2013; *Mann et al.*, 2015; *Spencer et al.*, 2015; *Vonk et al.*, 2015]. Riverine dissolved organic carbon (DOC) may be converted into greenhouse gases such as carbon dioxide or methane, while dissolved organic nitrogen (DON) can also be remineralized. DOM, often rich in DON, is a potentially important source of both energy and nutrients to coastal ecosystems in the Arctic [*Garneau et al.*, 2008; *Dunton et al.*, 2012; *Tank et al.*, 2012b; *Le Fouest et al.*, 2013]. Experimental and observational data support a significant portion of DOM in Arctic rivers is labile over relatively short time frames, even from large rivers where much of the organic matter was once presumed to be refractory [*Holmes et al.*, 2008; *Alling et al.*, 2010; *Mann et al.*, 2012]. Additionally, photochemical processes can enhance the transformation and mineralization of DOM, as Arctic rivers are often highly

colored with large amounts of chromophoric dissolved organic matter (CDOM) [*Xie et al.*, 2006; *Osburn et al.*, 2009; *Le Fouest et al.*, 2013]. Alternatively, some of this terrestrially-derived DOC may be delivered into the deep waters via ocean circulation or sediments through flocculation, removing carbon from cycling at the ocean or land surface for centuries [*Raymond and Bauer*, 2001; *Dittmar and Kattner*, 2003; *Benner et al.*, 2004; *Battin et al.*, 2009].

Most of the DOM in Arctic rivers is allochthonous, making riverine quantity and quality DOM responsive to terrestrial watershed characteristics such as soil type or permafrost extent. As such, the dramatic climatic changes currently underway in the Arctic will result in alterations to DOM mobilization, transformation, and transport pathways which ultimately could lead to changes in the amount of riverine DOM delivered to the Arctic Ocean. Widespread permafrost throughout high northern latitudes currently stores ~50% of global soil organic carbon stocks [*Tarnocai et al.*, 2009; *Hugelius et al.*, 2013a]. These permafrost soils have been relatively stable for millennia in many areas, with some permafrost regions dominated by yedoma (wind-blown dust deposits) that date to the late Pleistocene [*Hugelius et al.*, 2013b]. Additional high-latitude soil organic carbon has been stored in non-permafrost peatlands, which also may be hundreds or thousands of years old [*Kremenetski et al.*, 2003; *Beilman et al.*, 2009]. Recent warming throughout the Arctic Ocean watershed has raised concerns that these large carbon stocks are vulnerable to climate change, and rivers represent a major pathway through which carbon may be mobilized [*Schuur et al.*, 2015; *Vonk et al.*, 2015].

Already, climate has had significant impacts on river hydrology and chemistry within the Arctic [*Peterson et al.*, 2006; *White et al.*, 2007]. Over the course of the 20th century and into the 21st, many large Arctic rivers, particularly in Siberia, have shown substantial increases in discharge that cannot be accounted for by fire or dam building

[*Peterson et al.*, 2002; *McClelland et al.*, 2004]. Rather, increased discharge is associated with an accelerated hydrological cycle, where warmth and moisture are transported poleward as a result of increased atmospheric energy and global warming. Within these highly seasonal major Arctic rivers, discharge and DOM concentrations are tightly correlated [*Finlay et al.*, 2006; *Raymond et al.*, 2007; *Holmes et al.*, 2012]. Thus, increased river discharge may be associated with an increase in DOM export. However, warming climate may lead to fundamental changes in couplings between hydrology and biogeochemistry as permafrost thaws, microbial activities change, and vegetation productivity and composition shift. For instance, space-for-time substitutions across western Siberia indicate additional carbon release from permafrost peatlands may be expected independent of discharge as temperatures increase and permafrost destabilizes [*Frey and Smith*, 2005]. Alternatively, permafrost thaw may lead to deeper hydrological flowpaths that bypass organic-rich surface layers for deeper mineral soils, and longer residence times that allow for greater microbial re-working of DOM [*Walvoord and Striegl*, 2007; *Pokrovsky et al.*, 2015]. Such processes may already have occurred in the Yukon River, where discharge-normalized DOC has decreased from the 1970s to 2000s [*Striegl et al.*, 2005].

Despite the importance of rivers to Arctic biogeochemical cycles, there have been few efforts to establish long-term records of riverine organic matter or nutrients. These remote regions are logistically difficult and expensive to study, particularly during spring freshet and fall when ice and snow may be present. The highly seasonal nature of these rivers requires sampling across the hydrograph to adequately characterize fluxes of organic matter and nutrients. The Arctic Great Rivers Observatory (Arctic-GRO), originally established as Pan Arctic River Transport of Nutrients, organic mattER, and suspended Sediments (PARTNERS), began monitoring in 2003 in order to provide

3

baseline assessments of biogeochemical characteristics in rivers across the pan-Arctic [*McClelland et al.*, 2008]. The six rivers included, the Kolyma, Lena, Mackenzie, Ob', Yenisey, and Yukon rivers, represent over half of annual discharge and roughly two-thirds of the Arctic Ocean watershed. The Yukon River is included, although it flows into the Bering Sea, because Yukon River water contributes to relatively low salinity Pacific waters entering the Arctic Ocean through the Bering Strait. These data have provided valuable insights into the seasonality of water-borne constituent fluxes, and the quantity and quality of organic matter and nutrients.

Arctic-GRO provides an unprecedented archive of biogeochemical data from major Arctic rivers. However, data from these rivers remains relatively sparse compared to many temperate systems. Arctic-GRO collects field data roughly six times a year on each river, and only extends from 2003 to the present – not a lengthy enough record to assess climate-driven trends in DOM concentration or export. Only a few other rivers in the Arctic have been routinely sampled over the course of several decades. The Kuparuk River, one of the most intensively studied Arctic rivers, has shown a near five-fold increase in nitrate export over a thirty year time span, although there was little associated change in DOC flux [*McClelland et al.*, 2007]. The Mackenzie River has shown an increase in DOC concentration and flux since the 1970s, as well [*Tank et al.,* in review]. However, these examples remain rare instances of long-term biogeochemical monitoring within Arctic rivers.   Satellite remote sensing offers a potential tool to develop continuous records of DOM concentrations and fluxes, as well as assessments of spatial variability within these rivers.

Remote sensing techniques have been used to map CDOM in a variety of complex aquatic environments, including Arctic estuaries and rivers [*Belanger et al.*, 2008; *Matsuoka et al.*, 2012; *Fichot et al.*, 2013]. Landsat Thematic Mapper and

Enhanced Thematic Mapper Plus (TM and ETM+, respectively) provide records of multispectral reflectance data extending to the 1980s in some regions. These sensors have been used to estimate CDOM in a Siberian river during summer, and lakes throughout temperate and boreal latitudes on decadal time scales [*Olmanson et al.*, 2008, 2014; *Griffin et al.*, 2011; *Kutser*, 2012]. In the Arctic, CDOM (the portion of DOM that absorbs light) has proven to be a useful proxy of DOC [*Spencer and Aiken*, 2009; *Frey et al.*, 2016]. Thus, remote sensing methods may be used to extend time series of CDOM and DOC concentration and flux within major Arctic rivers which may then be related to other environmental indices such as the Arctic Oscillation. Furthermore, these long-term records of CDOM concentration can be related to historical records of water flow to investigate whether the discharge-constituent relationships have altered through time as a consequence of regional climate change.

The dissertation research presented here aims to expand our knowledge of riverine DOM across the Pan-Arctic using remote sensing and laboratory techniques, ultimately building multi-decadal records of CDOM concentration and flux from satellite reflectance data (Figure I. 1). Chapter One presents regressions relating discharge-modeled CDOM concentrations to Landsat reflectance data from six major Arctic rivers from 2000 – 2013, based upon data collected through Arctic-GRO. The possible drivers behind differences between river-specific models' success are discussed, including linkages to seasonality, hydrology and sediment loading. Chapter Two applies the remote sensing models developed in Chapter One to the entire clear-sky satellite record for the Kolyma, Lena, Mackenzie, Ob', Yenisey, and Yukon rivers. In the Mackenzie, Ob', and Yenisey rivers this record extends to the 1980s, although with some data gaps. These are the first known multi-decadal observations of CDOM that span the North American and Eurasian continents in the Arctic. Satellite-derived CDOM estimates are

coupled with water discharge data to calculate flux and investigate possible trends. Chapter Three presents experimental results from both Arctic and Texas rivers that test the impacts of freezing CDOM samples for preservation, and whether sonication or filtration after thaw can correct for these effects. These experiments were motivated by a general need to understand the best methods to archive CDOM and treat samples collected from remote regions where immediate analysis is impractical.
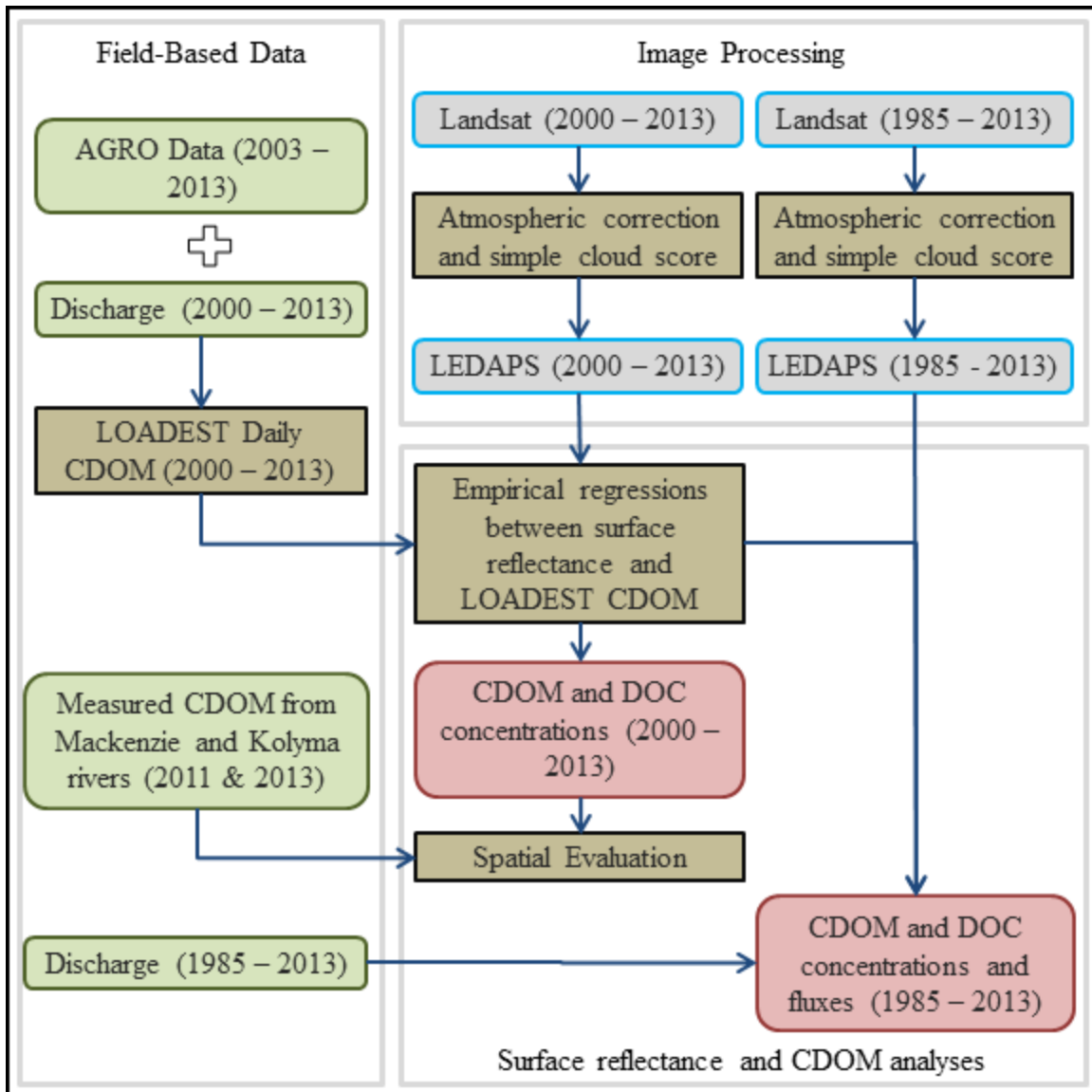
Figure I.1   Flow-chart of the methodology used in Chapters One and Two. Field data
from Arctic-GRO was used with discharge to model daily CDOM using
LOADEST. We used LEDAPS and a simple cloud score to develop datasets
of surface reflectance for each river. Surface reflectance from 2000 – 2013
was regressed against LOADEST-modeled CDOM to develop time series of
CDOM and DOC concentrations and fluxes.

Chapter One: Estimating Dissolved Organic Matter Concentrations in Major Arctic Rivers Using Landsat Data

ABSTRACT

While there is increasing recognition of the role riverine biogeochemical constituents play in coastal Arctic waters, efforts to monitor biogeochemistry were stymied by the remote nature of many rivers. Although recent programs have established routine monitoring over the past decade, such efforts are not yet long-lived enough to assess the impacts of regional climate change on organic matter concentrations or fluxes. Satellite remote sensing offers long-term datasets which may be used to estimate organic matter concentrations through space and time. Here, we present regression-based models relating Landsat reflectance data to chromophoric dissolved organic matter (CDOM) in the six largest rivers draining the pan-Arctic watershed (the Kolyma, Lena, Mackenzie, Ob', Yenisey, and Yukon rivers). Regression models explain as much as 84% of the variability in CDOM from remotely sensed data. High concentrations of total suspended solids (TSS) did not interfere with the remote sensing of CDOM in the Yukon River, but did appear to confound estimates of CDOM in the Mackenzie River. CDOM absorbance is a common proxy for dissolved organic carbon (DOC), particularly in aquatic systems dominated by terrestrial organic matter. Our results corroborate recent studies highlighting the importance of seasonal drivers in CDOM and DOC concentrations. The remote sensing of CDOM offers an opportunity to monitor the role of rivers in a rapidly changing system as a result of regional warming.

1. INTRODUCTION

Rivers transport over 3300 km^3 of water to the Arctic Ocean, representing 11% of total riverine discharge into an ocean basin containing 1% of global ocean volume [*Menard and Smith*, 1966; *Aagard and E.C. Carmack et al.*, 1989]. As such, terrestrial processes that impact the delivery of water and water-borne materials help determine the physical, chemical, and biological structure of the Arctic Ocean. Riverine dissolved organic carbon (DOC) in particular is an important component of the Arctic carbon cycle, linking terrestrial and marine systems [*Cooper et al.*, 2005; *Manizza et al.*, 2011; *Holmes et al.*, 2012]. Dissolved organic matter (DOM) in major Arctic rivers is largely allochthonous, sourced from modern vegetation and a smaller fraction from ancient permafrost soils [*Neff et al.*, 2006; *Raymond et al.*, 2007; *Guo et al.*, 2010; *Mann et al.*, 2012]. Impacts from rapid climate change, such as thawing permafrost [*Striegl et al.*, 2005; *Frey and McClelland*, 2009], an accelerated hydrological cycle [*White et al.*, 2007], and increased fire activity [*Elmquist et al.*, 2008; *Stubbins et al.*, 2015], influence the concentrations and composition of DOM in Arctic rivers. As a result, there is some evidence that riverine DOC export may increase over the next century[*McGuire et al.*, 2010]. Recent studies have established that DOC from Arctic rivers can be highly labile [*Gustafsson et al.*, 2011; *Wickland et al.*, 2012; *Mann et al.*, 2015; *Frey et al.*, 2016] and non-conservative losses of DOC have been observed along Arctic shelves [*Alling et al.*, 2010]. These losses are likely driven by both biological utilization and photochemical interactions with chromophoric dissolved organic matter (CDOM) [*Bélanger et al.*, 2006; *Stedmon et al.*, 2011; *Le Fouest et al.*, 2013]. CDOM, the portion of the DOM pool that absorbs light at a given wavelength, is a useful proxy for DOC concentrations and important for photochemical transformations [*Hu et al.*, 2002; *Spencer et al.*, 2012].

Although many questions remain about the fate of DOM in the coastal ocean, monitoring established in 2003 has led to an estimate of approximately 35 Tg C transported by Arctic rivers annually [*McClelland et al.*, 2008; *Holmes et al.*, 2012]. The Arctic Great Rivers Observatory (Arctic-GRO; 2009 – present), originally established as the Pan Arctic River Transport of Nutrients, organic mattER, and suspended Sediments (PARTNERS; 2003 – 2007) project, samples the six largest Arctic rivers across the hydrograph. These rivers – the Kolyma, Lena, Mackenzie, Ob', Yenisey and Yukon – deliver over 50% of annual river discharge and DOC flux to the Arctic Ocean [*Holmes et al.*, 2012]. Arctic river discharge and chemistry are highly seasonal and can vary widely from year to year. Seasonally explicit sampling across many years is therefore required to detect changes in DOM concentration and fluxes that may be driven by climate change. Despite the successes of the Arctic-GRO, there are logistical constraints to this sampling program. Samples are only collected from one location at each river, and the rivers are only sampled a few times (approximately 6) each year. Satellite remote sensing potentially allows for additional "sampling" during the ice-free season, observations throughout several hundred km^2 of the river basin, and a longer time series than currently available from on-the-ground sampling.

Satellite imagery has been used over the past decade to map CDOM remotely in a number of optically complex waters [*Menken et al.*, 2006; *Belanger et al.*, 2008; *Kutser*, 2012; *Fichot et al.*, 2013; *Brezonik et al.*, 2014]. Although not originally designed for remote sensing of inland waters, the Landsat Thematic Mapper and Landsat Enhanced Thematic Mapper Plus (Lansat TM and ETM+, respectively) have been used to estimate suspended sediment, chlorophyll, turbidity, and CDOM in lakes, rivers and the coastal ocean [*Olmanson et al.*, 2008; *Griffin et al.*, 2011; *Lobo et al.*, 2014; *Joshi and Sa*, 2015]. Admittedly, Landsat TM and ETM+ are limited by lower sensitivity and spectral

resolution than ocean color sensors or newer platforms such as Sentinel-2 or Landsat Operational Land Imager (OLI), making estimations of CDOM difficult in very dark waters with little water-leaving radiance [*Kutser et al.*, 2005; *Palmer et al.*, 2015]. Despite these limitations, Landsat TM and ETM+'s high spatial resolution (30m pixels) and long-term dataset (1984 – present) make these sensors the best option for monitoring many inland waters. Approaches fall into two basic categories: analytical or semi-analytical versus empirical. Analytical and semi-analytical methods use the measured inherent optical properties of a water body, while empirical methods relate measured CDOM absorbance with satellite data.

Here, we present an empirical approach relating CDOM in the six largest Arctic rivers to Landsat reflectance data. The regression-based models presented here represent the first Pan-Arctic assessment of DOM in rivers from satellite remote sensing. Using Landsat imagery, we have estimated CDOM in the six largest Arctic rivers from 424 dates from May through October, 2000 – 2013. These tools allow retrospective monitoring of CDOM from the largest Arctic rivers, potentially extending back to the 1980s.

2. METHODS

2.1 Data Collection and Analysis

Field samples were collected between 2003 and 2013 for the six largest rivers draining the Arctic Ocean watershed (Kolyma, Lena, Mackenzie, Ob', Yenisey and Yukon rivers), as part of the Arctic-GRO and PARTNERS projects (www.arcticgreatrivers.org). Depth-integrated cross-sectional sampling was conducted at downstream locations on each river, capturing 96% of drainage from their combined watersheds [*Holmes et al.*, 2012]. Comparisons of surface samples and depth-integrated

samples from the Arctic-GRO/PARTNERS sites have demonstrated that DOC and other dissolved constituents are evenly distributed throughout the water column at these sites [*Raymond et al.*, 2007; *Holmes et al.*, 2012]. For more details on sample collection, see previous publications from Arctic-GRO/PARTNERS [*Raymond et al.*, 2007; *Holmes et al.*, 2012; *Walker et al.*, 2013]. These sampling campaigns explicitly address the highly seasonal nature of Arctic rivers, with targeted sampling during spring freshet, throughout the ice-free period, and under-ice [*McClelland et al.*, 2008]. Additional samples, used in this study for model validation, were collected in field campaigns from the Mackenzie (2011) and Kolyma (2013), in the spring shortly after ice break-up on each river. These surface samples from approximately 0.5 meter depth, were collected and stored in polycarbonate or HDPE bottles, 1 – 2 liters volume, and processed within hours of collection.

Arctic-GRO and PARTNERS DOC and CDOM samples were filtered within 2-4 hours of sample collection through 0.45 µm capsule filters into pre-cleaned, pre-rinsed HDPE bottles and shipped frozen to the Woods Hole Research Center (WHRC). DOC samples from PARTNERS (2003 – 2006) were measured for concentration at the National Ocean Sciences Atomic Mass Spectrometry (AMS) facility at Woods Hole Oceanographic Institute or the AMS facility at University of Arizona [*Raymond et al.*, 2007; *Holmes et al.*, 2012]. All Arctic-GRO DOC samples were measured at the WHRC using a Shimadzu (TOC-V) organic carbon analyzer. Absorbance was measured at WHRC using a Shimadzu UV-1800 with a 1 cm quartz cuvette, from wavelengths 200 – 800 nm at 1 nm intervals. Whole water samples were shipped to the Marine Biological Laboratory for total suspended sediment (TSS) analyses. These samples were filtered onto pre-weighed Whatman GF/F filters and weighed after drying for 24 hours at 60°C.

The volume of water passing through each filter was recorded, and TSS concentrations were calculated from the paired mass and volume data.

Additional field samples from 2011 and 2013 were filtered through 0.45 μm capsule filters into pre-cleaned, pre-rinsed polycarbonate bottles. CDOM was measured immediately after filtration using an Ocean Optics USB4000 UV-VIS spectrophotometer on the Mackenzie River. A Shimadzu UV-1800 located at the Northeast Science Station in Cherskiy, Russia was used for CDOM in 2013 for Kolyma river samples. In both cases, absorbance was measured from 200-800 nm through a 1 cm quartz cuvette. DOC was frozen and shipped to WHRC for analysis from Mackenzie river samples. Kolyma samples from 2013 were stored frozen until analyzed with a Shimadzu (TOC-V) at the Northeast Science Station. Absorbance was converted to absorption coefficients using Equation 1:

$$a(\lambda) = 2.303 A(\lambda)/l \ (1)$$

where $a(\lambda)$ is the absorption coefficient at a given wavelength, $A(\lambda)$ is the absorbance at a given wavelength and l is the path length in meters [*Hu et al.*, 2002]. Absorbance at 375 nm was used for subsequent LOADEST modeling and remote sensing applications, as full absorbance scans were not available for PARTNERS data from 2003 - 2006.

2.2 LOADEST Modeling

Despite the rich dataset provided by PARTNERS and Arctic-GRO, there are only 8 – 25 instances per river where ground sampling corresponds within 3 days of an ice-free and cloud-free Landsat satellite overpass. Landsat sensors (Landsat 5 TM and Landsat 7 ETM+, in this study) are high resolution (30m) multispectral sensors with a 16 day return interval. Because Landsat sensors are polar-orbiting, at high latitudes 2-3 scenes often overlap any particular point, so that there is more frequent coverage. Still,

the frequent clouds and long ice-covered season limit the number of open water scenes available, and there are only 4-5 ice-free samples from the field available per river per year.

To address this limitation in the available data, we estimated daily CDOM concentrations for 2000 – 2013 using the US Geological Survey (USGS) Load Estimator (LOADEST) [*Runkel et al.*, 2004]. LOADEST uses relationships between constituent concentrations (measured periodically) and river water discharge (measured continuously) to generate daily estimates. LOADEST has been used in multiple studies to estimate concentrations and fluxes of biogeochemical parameters based on PARTNERS and ArcticGRO data [*Raymond et al.*, 2007; *Holmes et al.*, 2012; *Tank et al.*, 2012b], and other studies of CDOM flux [*Spencer et al.*, 2013]. LoadRunner version 2.1 (http://environment.yale.edu/loadrunner) was used to automate LOADEST runs.

Discharge data (2000 – 2013) was collected by the USGS (Yukon), Water Survey of Canada (Mackenzie), and Roshydromet (Federal Service for Hydrometeorology and Environmental Monitoring in Russia; Kolyma, Lena, Ob' and Yenisey). The Yukon River only includes data from April 2001 onwards. On the Ob', Yukon and Mackenzie rivers, discharge gauging stations coincide with biogeochemical constituent collection. On the Yenisey and Kolyma, gauging stations are 160 km and 250 km upstream of constituent sampling, respectively. Discharge gauging occurs 520 km downstream of constituent sampling on the Lena. We used corrections of 1 (Yenisey), 2 (Kolyma) and 4 (Lena) days to account for the lag times between gauging and sample collection [*Holmes et al.*, 2012], applied before running LOADEST.

LOADEST contains multiple regression models, some of which include variables to account for seasonality. All models that include long-term time functions were excluded from analyses. DOC concentrations were also modeled using LOADEST, for

validation purposes. LOADEST model 6 (Equation 2, below), was the best at predicting both CDOM and DOC concentrations for all rivers, and includes terms that account for seasonality (the terms with sine and cosine functions).

$$\text{Ln (Conc)} = a0 + a1\ \text{LnQ} + a2\ \text{LnQ2} + a3\ \text{Sin} (2\ \pi\ \text{dtime}) + a4\ \text{Cos} (2\ \pi\ \text{dtime}) \quad (2)$$

Where flux is calculated in m^2/d for CDOM and kg/d for DOC, Q is water discharge in cubic feet per second, LnQ equals Ln (Q) minus center of Ln (Q), and d_{time} is decimal time minus center of decimal time. The centering procedure for both discharge and time aims to avoid multicollinearity. Models were assessed based on their prediction of concentrations, rather than fluxes (Table 1). The resulting concentration estimates are from the adjusted maximum likelihood output.

2.3 Landsat Image Processing

We used the Landsat Ecosystem Disturbance Adaptive Processing System (LEDAPS) data, from Google Earth Engine which calculates surface reflectance for Landsat 5 TM and 7 ETM+ [*Masek et al.*, 2006; *Hansen et al.*, 2013]. Recent studies estimating DOM or suspended sediments from Landsat in optically complex waters have used a dark-object correction [*Chavez*, 1996; *Griffin et al.*, 2011]; the FLAASH (Fast Line-of-sight Atmospheric Analysis of Spectral Hypercubes) module from the ENVI software package [*Joshi and Sa*, 2015]; a dark-pixel correction combined with a radiative transfer model [*Lobo et al.*, 2014]; and top-of-atmosphere (TOA) reflectance with no further atmospheric correction [*Kallio et al.*, 2008; *Kutser*, 2012]. Many of these methods require, or are greatly improved by, field-collected radiometric data and atmospheric data from monitoring stations. However, this study focuses on remote locations and historical data collected without any concomitant atmospheric or radiometric measurements. LEDAPS, also a data product from USGS, applies the 6S

radiative transfer model (Second Simulation of a Satellite Signal in the Solar Spectrum) to ortho-rectified Landsat data, with auxiliary ozone data from the NASA GSFC Ozone Monitoring Instrument or Total Ozone Mapping spectrometer and gridded atmospheric data from the National Centers for Environmental Prediction (NCEP) [*Masek et al.*, 2006; *Schmidt et al.*, 2013]. We also modeled CDOM concentrations on select rivers using the TOA reflectances (Yenisey), a dark object correction (Yenisey), and FLAASH corrected surface reflectances (Lena). LEDAPS performed the same or better than these other options (*unpublished data*).

Over 420 Landsat TM and ETM+ scenes from 2000 – 2013 were used in remote sensing analyses. Scenes with 30% or less cloud cover were used, all with clear-sky conditions over sampling locations. Only scenes from May 15th – October 15th were included, with scenes from shoulder seasons visually inspected to insure no interference from floating ice. A 3-pixel-wide cross-section at the sampling site for each river was digitized and used to extract mean reflectance for the area of interest (AOI). In images from Landsat 7 ETM+ post-2003, a failure of the Scan Line Corrector (SLC) caused data gaps in each image; however, because each cross section spans hundreds of meters in these large rivers, data were missing from only ~25% or less of the AOI in these images. River masks were created using the Hansen et al [2013] dataset which includes a water layer. A simple cloud score method based on the thermal band removed clouds [*Hansen et al.*, 2013].

Samples from 2011 and 2013, collected separately from Arctic-GRO sampling, are used here to evaluate whether regression models based upon temporal variability can be extrapolated across space. These samples came from main stems, tributaries, and channels of the Mackenzie and Kolyma rivers. These samples were collected shortly after ice breakup on each river, within approximately a two week period. In the Mackenzie,

16

most samples that corresponded with cloud-free Landsat imagery were collected from channels in the extensive delta, and a handful of samples from tributaries or the main stem of the river. Kolyma river samples were more evenly split, with five samples from major tributaries and four samples from different sections of the main stem of the river. Only samples from rivers 90m wide or more are used here, to avoid edge effects. AOIs consisted of a 30m buffer around each sampling point, from which reflectance was extracted. In cases where samples were collected from land, AOIs were artificially moved offshore to avoid edge effects. All samples corresponded within ± 3 days of Landsat imagery, most often on the same day as a satellite flyover. After applying the appropriate regression model from Table 2, Landsat-derived CDOM values were compared to on-the-ground measurements.

2.4 Statistical Analysis

All statistical analyses were performed in R software (https://www.r-project.org/). Although we might expect CDOM to have the largest effect on reflectance in the blue band (B1) of Landsat, given the exponential decrease in CDOM absorbance as wavelength increases from 200 – 800 nm, most previous studies depend on a combination of the green and red bands (B2 and B3) [*Kallio et al.*, 2008; *Kutser*, 2012; *Joshi and Sa*, 2015]. Some previous studies had success using B1 and B4 (near infrared band; NIR), as well [*Brezonik et al.*, 2005; *Griffin et al.*, 2011; *Olmanson et al.*, 2016]. Bands 1-4 and band ratios were tested in exhaustive iterations of linear and multiple linear regressions against the LOADEST CDOM a_{375} results, grouped by river (Table 2). Additionally, we performed the same analysis across all rivers (Table 2). All Landsat CDOM values reported hereafter refer to absorbance at 375 nm. Multiple linear regressions ultimately were the most successful, evaluated based on Schwartz's Bayesian Information Criteria

(BIC) and R^2. BIC includes a penalty term for increasing the number of variables in a regression in order to avoid overfitting; while useful for model selection, BIC is not generally used to compare between different datasets. If BIC and R^2 were similar between differing models for the same river system, the model with only one band ratio or the least number of variables was selected.

3. RESULTS

3.1 DOM measurements and LOADEST modeling

CDOM absorption is a common proxy for DOC concentrations in inland waters, including Arctic rivers [*Osburn and Stedmon*, 2011; *Stedmon et al.*, 2011; *Frey et al.*, 2016]. Using all available Arctic-GRO data from 2004 – 2014, DOC and a_{375} correlate strongly across all rivers (Figure 2; $R^2 = 0.88$, n = 248). DOC ranges from 2.1 mg/L C to 23.5 mg/L C with a mean of 7.6 mg/L C; CDOM a_{375} ranges 1.1 m^{-1} to 29.7 m^{-1} with a mean of 9.7 m^{-1}. The highly seasonal nature of Arctic hydrology and ecosystem productivity drives much of this wide variation in DOM concentrations, as opposed to differences between river systems.

Much of the seasonal variation in DOM can be predicted using LOADEST. LOADEST's ability to predict CDOM concentrations in the six Arctic-GRO rivers ranged from R^2 (expressed as a percentage) of 45% to 89%, using Model 6 (Table 2). Of these, the Ob' and Mackenzie rivers are the least predictable with 45% and 53% of CDOM variance explained by the LOADEST model. The Yukon, Yenisey, and Kolyma all have R^2 of 70-73% , while 89% of CDOM variance can be explained by LOADEST in the Lena river. Model 6, which includes variables to account for seasonality, has also been used successfully for a variety of river-borne constituents in previous Arctic-GRO studies [*Holmes et al.*, 2012; *Stubbins et al.*, 2015; *Mann et al.*, 2016]. Here, model

coefficients a_0 and a_1 are significant and a_2 is non-significant for all rivers. Coefficient a_3 is significant for the Kolyma, Lena, Mackenzie, and Yukon rivers and non-significant for the Ob' and Yenisey. With the exception of the Ob', coefficient a_4 is significant for all rivers.

LOADEST modeling of DOC concentrations explain overall less of DOM variance than the CDOM models, with the largest divergence in the Mackenzie where R^2 drops from 53% to 31% and the Lena decreasing from 89% to 74%. The Yukon River is the exception, with R^2 increasing from 70% to 80% between CDOM and DOC models. Although this paper presents DOC concentrations derived from remote sensing, we chose to use LOADEST modeled CDOM as calibration data for remote sensing models because of this decrease in explanatory power, in addition to CDOM being a more direct measure of water bodies' spectral characteristics [*Brezonik et al.*, 2014].

3.2 Landsat Regression Models of CDOM and DOC

Our results indicate that CDOM, and subsequently DOC, can be estimated using Landsat TM and ETM+ data (Figure 3), given certain conditions. Using river-specific regressions from Table 2, CDOM a_{375} from Landsat data correlates with LOADEST-derived CDOM a_{375} with $R^2 = 85\%$ across all rivers. DOC estimates from Landsat correlate with LOADEST-derived DOC with $R^2 = 74\%$. These models are built from 424 Landsat scenes from 2000 – 2013, with scenes from spring (May-June), summer (July-August), and fall (September-October) (Table 3). However, when we tested whether a single, universal regression could explain CDOM across all rivers using Landsat, R^2 decreased to 52%.

Although our overall ability to predict CDOM in large Arctic rivers is good, regression models vary widely between each river in terms of formulation and

19

performance (Table 2). The Yenisey performs best, with R^2 of 84% and root mean square error (RMSE) of 1.17. CDOM models for the Yenisey and the Kolyma are the only two cases that share the same band variables, a combination of the log-transformed green and red bands with a ratio of green to red (Table 2). The Ob' regression also uses a ratio of green to red, in combination with the blue band, although R^2 is only 33%, although RMSE is comparable to other rivers at 1.21. This green-to-red ratio is commonly used in other studies of remote sensing of CDOM with multispectral data. The Yukon River model uses the blue band, green band, and a ratio of the blue and NIR bands and explains 75% of the variance in CDOM and RMSE of 2.33. The Lena model uses natural log-transformed red and NIR bands with a natural-log of the green to NIR band ratio, resulting in an R^2 of 68% and RMSE of 2.96. The Mackenzie River model is the only model that does not include a band ratio, instead using the NIR and natural log of the green band for an R^2 of 53% and RMSE of 1.45. The universal model, that includes all rivers, used a combination of the red, NIR, and ratio of green to red bands, for an R^2 of 52% and RMSE of 3.23.

3.3 Spatial Evaluation

CDOM in the Kolyma main stem samples fall close to the one-to-one line, despite spanning almost 300 km along the river (Figure 4 and 5). CDOM estimates from tributaries of the Kolyma were less consistent, although three observations were within 1 m^{-1} of measured values (Figure 4). When converted to DOC, seven out of nine Landsat-derived estimates were within 1.1 mg/L C of measured DOC concentrations. The Mackenzie remote sensing model, however, did not yield reliable estimates of CDOM or DOC. Although measured CDOM concentrations range by nearly 20 m^{-1} in the Mackenzie, our remote sensing model could not capture that variability. Landsat-derived

estimates from the main stem of the Mackenzie and two major tributaries (the Arctic Red and Peel rivers) are relatively close to measured CDOM. However, the much more variable sites throughout the Mackenzie delta could not be accurately estimated.

3.4 Comparing measured, LOADEST, and Landsat DOM concentrations

For more comparable assessment against Landsat-derived estimates, we subsampled both Arctic-GRO measurements and LOADEST estimates to solely the ice-free season. Cross-sectional river sampling is dangerous while ice floats during spring break-up and freeze, so all field-collected samples from May to mid-October are assumed to be ice-free. Unfortunately, there are not consistent data on the timing of river ice-out and freeze-up for most of the discharge records used in LOADEST modeling. We assumed that rivers would be ice-free from three days after peak discharge until October 15th. Average concentrations for seasonal and total ice-free periods were calculated for 2004 – 2006 and 2009 – 2012, the common years between all three methods (measured, LOADEST, and Landsat; Table 4). Mean seasonal concentrations were averaged together for the total ice-free period, so that seasons were given equal weight despite differences in coverage between methods.

Remotely sensed estimates of seasonal CDOM and DOC show little significant difference from either measured or LOADEST values, in most rivers (Table 4). During freshet (May-June), average measured CDOM and DOC are significantly higher than Landsat estimates for the Lena and Kolyma rivers. Average LOADEST DOC during freshet on the Kolyma also significantly exceeds Landsat estimated DOC. Freshet in the Lena exhibits the largest divergence between methods for any season on any river, with average measured concentrations exceeding Landsat estimates by 6.61 m^{-1} and 3.55 mg/L for CDOM and DOC, respectively. In the Ob' River, average Landsat DOC

concentrations in summer are significantly lower than measured or LOADEST values. Measured CDOM in the Ob' River during fall is significantly less than Landsat CDOM. However, LOADEST DOC is significantly higher than Landsat DOC for the same season in the Ob. During summer in the Yukon River, average CDOM from Landsat is significantly higher than LOADEST values, and Landsat-derived DOC is significantly than both measured or LOADEST values. Overall, only in four cases did average seasonal CDOM differ significantly from measured or LOADEST values, while DOC differed significantly in six cases (Welch's t-test, p-value > 0.05). In no instance did CDOM or DOC values for the entire ice-free period differ significantly between methods.

3.5 DOM during the ice-free season from Landsat data

All rivers display clear seasonal variation during the ice-free period, with the exception of the Ob' River (Figure 6). The Lena River varies the most, with average DOC concentration of 12.3 mg/L C during spring and 7.5 mg/L C in the fall. The Lena is also the only river where fall and summer DOM concentrations differ significantly. In the Kolyma, Mackenzie, Yenisey, and Yukon rivers, spring DOM always substantially exceeds summer and fall concentrations. Although not always statistically significant, DOM consistently decreases from spring to summer, and again through fall across all rivers. These relationships hold true for CDOM and DOC. The seasonal signal in these results is strongly linked to discharge. Rivers with tight coupling between discharge and CDOM, such as the Lena and Yenisey, show more robust LOADEST modeling, and a greater variability in DOM across seasons. CDOM in the Mackenzie and Ob' rivers, in contrast, cannot be modeled as successfully using LOADEST, and show the least variation across the ice-free season. The lowest values in each season come from the Mackenzie River, which also has the lowest average CDOM concentration of 5.14 m^{-1}.

Although the Ob' shows little variation across seasons, it does have the highest average DOM concentrations in summer and fall (Figure 6).

4. DISCUSSION

Remote sensing of CDOM in inland and coastal waters remains a challenging exercise, particularly at high latitudes where high seasonality, limited datasets, and complex optical properties conspire to limit the applicability of satellites. Complicating matters, up to 90% of the radiance over water can be attributed less to the inherent optical properties of water, and more so to the atmospheric conditions [*Gordon and Wang*, 1994; *Kutser et al.*, 2015]. This sensitivity to characteristics such as haze, aerosols, and humidity, necessitates reliable atmospheric correction, particularly when using multi-spectral sensors with relatively low radiometric sensitivity like Landsat 5 TM and 7 ETM+, [*Lobo et al.*, 2014; *Palmer et al.*, 2015]. Despite these limitations, we were able to build successful remote sensing models to estimate CDOM concentration for the major Arctic rivers using the USGS LEDAPS product. Ultimately, watershed characteristics such as suspended sediment concentrations and discharge seasonality are linked to the relative success in estimating CDOM from remote sensing. This remote sensing approach more than doubles the number of ice-free observations of CDOM and DOC per river of those available from field measurements, and extend the time series back to 2000. The capability to estimate DOM from remote sensing enhances our ability to observe spatial patterns across on a landscape-scale in regions known for high costs and logistical challenges associated with field campaigns. Furthermore, the Landsat TM/ETM+ record extends from 1984-present, allowing for future studies to analyze variations and potential trends in DOM concentration and flux associated with anthropogenic climate change or large-scale climate patterns such as the Arctic Oscillation.

23

4.1 Comparing measured, LOADEST-derived, and Landsat-derived DOM

CDOM concentrations in Arctic rivers can change rapidly over the course of the ice-free season [*Mann et al.*, 2016]. The targeted sampling of Arctic-GRO was designed to address this seasonality, as capturing the biogeochemical character of the spring is essential for accurate flux calculations [*Raymond et al.*, 2007; *McClelland et al.*, 2008]. Our Landsat data is likewise somewhat skewed towards the spring, as there are more scenes included in our analyses from May-June than September-October owing to the vagaries of cloud cover and the timing of satellite overpasses (Table 3). However, within spring freshet, our remote sensing approach cannot target peak flow conditions as closely as field programs can. For instance, only 10% of the Landsat scenes observe May through the first week of June, when discharge peaks on most rivers (Figure 7). Early freshet samples contribute 22% of the Arctic-GRO dataset during the ice-free season. Thus, particularly on the Kolyma and Lena rivers, average CDOM and DOC concentrations for spring tend to be lower than from measured samples. LOADEST lacks this bias towards peak flow, and Landsat results match LOADEST more closely, with only DOC from the Kolyma significantly different between the two methods in spring.

The Ob' and Yukon are the only rivers where remote sensing estimates routinely differ significantly from measured or LOADEST results in summer or fall (Table 4). DOM concentrations in the Ob' do not vary seasonally or annually as much as other rivers considered here – thus, despite the statistical significance, mean seasonal DOC in the Ob' never differs between methods more than 1.25 mg/L. The elevated DOM concentrations from Landsat on the Yukon, in relation to measured or LOADEST values, may be tied to suspended sediment concentrations as discussed in more detail below. Despite these anomalies, average Landsat-derived CDOM and DOC for most seasons and

across the ice-free period for all rivers consistently reflect both measured and LOADEST datasets.

4.2 Watershed characteristics as controls on remote sensing of CDOM

The six Arctic-GRO rivers represent 67% of the Arctic Ocean watershed [*Holmes et al.*, 2012], and vary widely in watershed characteristics that influence riverine organic matter and our ability to remotely sense CDOM. Figure 3 shows that across all rivers, we can predict riverine DOM quite well, with R^2 of 85% and 74% for CDOM and DOC, respectively. However, a closer examination of individual river models reveals more variability in the strength of the relationship between measured and estimated CDOM (Table 2). CDOM remote sensing models are most robust when measured and LOADEST modeled values vary widely across seasons. CDOM concentrations from LOADEST range the widest in the Yenisey, which also features the strongest relationship between remotely sensed CDOM and calibration data (Table 2). The Mackenzie and Ob' rivers vary relatively little in CDOM throughout the ice-free season compared to other rivers (Table 4). In consequence of the relatively stable CDOM, the regressions lack the power to explain the variance seen in these rivers. Despite this limitation, RMSE for the Mackenzie and Ob' are comparable to other rivers (Table 2). When plotted with all other data, Mackenzie and Ob' rivers do not stand out from other rivers as being biased or more scattered from the one-to-one line (Figure 3). One possible source of error in the Mackenzie River originates from the use of frozen CDOM samples. Cryopreservation effects can be large in a portion of samples – particularly when CDOM concentrations are low [*Griffin et al.,* in preparation (see Chapter 3 of dissertation)].

Using LOADEST to model daily CDOM concentrations expanded the amount of calibration data available by nearly 500%. Most riverine CDOM concentrations could be

predicted with R^2 of 70 – 89%. Many Arctic rivers are hydrologically "flashy" during the spring freshet, with a peak in discharge followed by lower flow during the summer, such as in the Yenisey River (Figure 7). DOM concentrations correlate positively with discharge, and shift in source and composition across the hydrograph. However, discharge fails to explain DOM concentrations in the Mackenzie or Ob' as it does in the other rivers. Both the Mackenzie and Ob' have a less distinctive peak in spring discharge (Figure 7), and measured DOM concentrations change less over the course of the ice-free season than in other large Arctic rivers (Table 4). Several watershed features may contribute to these characteristics. The Mackenzie contains Great Slave Lake, Great Bear Lake, and the inland Peace-Athabasca delta. These large lake systems mediate seasonal discharge, and place a strong lake storage effect upon the Mackenzie River [*Woo and Thorne*, 2003]. The extensive non-permafrost peatlands in the Ob' watershed retain large amounts of water, and may have a similar effect on attenuating streamflow as the extensive lakes found in the Mackenzie [*Smith et al.*, 2012].

In addition to the inherent lack of CDOM variability in the Mackenzie River, other optical properties of natural waters may obscure the CDOM signal. Chlorophyll is low in many large Arctic rivers [*Meon and Amon*, 2004; *Emmerton et al.*, 2008]. Suspended sediment loads in Arctic rivers, on the other hand, can be high depending on location and time of year. Concentrations are particularly high during spring in the North American rivers (Figure 8). Total suspended solids (TSS) can exceed 400 mg/L on the Mackenzie and Yukon during spring freshet. Since Arctic-GRO sampling is depth-integrated, these TSS values are higher than the surface concentrations observed by satellite imagery (particle concentrations increase with depth due to sinking). Nonetheless, TSS concentrations at the surface may still be high enough to mask CDOM. Few studies have addressed remote sensing of both CDOM and sediments in waters

where both are high, and teasing apart the two signals is difficult [*Pavelsky and Smith*, 2009]. However, in the case of large Arctic rivers, TSS and CDOM generally increase with discharge (Figure 8). Where these two variables are tightly and consistently coupled, it is possible to estimate CDOM concentrations from satellite remote sensing even when backscatter from sediments obscures the organic matter absorbance signal.

The results presented in Table 2 are purely empirical, and only the Kolyma and Yenisey rivers share common band combinations. However, these differences may further inform the theoretical underpinnings of using satellite remote sensing to monitor CDOM, for which we still have limited understanding [*Brezonik et al.*, 2014]. Green and red bands appeared most frequently in our models, including a "universal" regression based on all rivers grouped together (Table 2). The ratio of green to red commonly is used in other empirical approaches to remote sensing of CDOM in complex waters [*Kutser et al.*, 2005; *Menken et al.*, 2006; *Ficek et al.*, 2011; *Brezonik et al.*, 2014]. Although CDOM absorbance decreases exponentially with increasing wavelength, the functional light-paths of inland waters measured from space are much longer than lab techniques. Thus, there is a greater CDOM signal at longer wavelengths than might otherwise be measured through laboratory techniques. This may explain partially why longer wavelengths (e.g., Landsat TM and ETM+ bands 2 and 3) can still strongly relate to CDOM absorbance in UV or blue wavelengths (350 – 440 nm). Furthermore, because atmospheric effects tend to be largest in the blue region (400 – 500 nm), reflectance from green and red wavelengths may be preferred in regression-based approaches [*Kutser et al.*, 2005]. Although it has been suggested that reflectance near 670 nm in many CDOM remote sensing is linked to a chlorophyll-*a* correction, the low chlorophyll concentrations in many Arctic rivers indicate this may not be the sole explanation for the inclusion of these longer wavelengths. Reflectance in NIR wavelengths appears in empirical models

from the Lena, Mackenzie, and Yukon rivers. NIR reflectance has long been used to estimate TSS or suspended sediment concentrations (SSC) in inland and coastal waters, with some indication that models may be transferrable between systems [*Novo et al.*, 1989; *Quibell*, 1991; *Long and Pavelsky*, 2013]. Although TSS concentrations in the Lena are similar to other Siberian rivers, it is noteworthy that the sediment-laden North American rivers both utilize the NIR band in regression models.

We applied the models from the Mackenzie and Kolyma rivers to Landsat imagery that captured spatially distributed field samples from 2011 and 2013, to assess whether temporal variability could be used to evaluate spatial patterns in CDOM (Figures 4 and 5). While CDOM in major tributaries and the main stem of the Mackenzie River were largely consistent with expected results, CDOM throughout the delta could not be reliably estimated from Landsat data, possibly owing to interference from sediment. The Mackenzie is the single largest exporter of sediment to the Arctic Ocean [*Holmes et al.*, 2002], and surface TSS concentrations can exceed 1000 mg/L in the delta during spring freshet (*Griffin and Vonk, unpublished data*). In early June, the Mackenzie floods lakes and inundates wetlands throughout the delta [*Marsh and Hey*, 1989]. Particulate matter may settle out or become resuspended, depending on water levels and velocities [*Emmerton et al.*, 2007]. The inability of our remote sensing approach to accurately estimate CDOM at delta sites in the Mackenzie suggest that the model for this river may be more tightly coupled to suspended sediment concentrations than CDOM concentrations. Kolyma CDOM, on the other hand, can be estimated more reliably at different locations within the river network. Even CDOM from tributaries in the Kolyma watershed are estimated with better accuracy than any of the Mackenzie delta samples. Without a larger dataset, extrapolating the Kolyma remote sensing model to include

major tributaries must be done conservatively. However, this dataset adds to our confidence in mapping CDOM throughout the lower main stem of the Kolyma.

4.3 Remotely sensed CDOM as a proxy for other DOM characteristics

CDOM concentrations vary widely in each river system, corroborating previous studies on Arctic rivers that DOM is tightly coupled with discharge [*Finlay et al.*, 2006; *Townsend-Small et al.*, 2010]. DOC falls over the course of the ice-free season, in tandem with CDOM. Many previous studies also show strong correlations between DOC and CDOM absorbance in Arctic rivers [*Spencer et al.*, 2008; *Frey et al.*, 2016]. Indeed, CDOM can predict DOC across a wide range of river and stream types, although these relationships falter when photobleaching and autochtonous DOM production become major factors [*Spencer et al.*, 2012]. While strong relationships between CDOM and DOC concentrations have been leveraged in a variety of recent studies, it is noteworthy that DOC and dissolved organic nitrogen (DON) are also strongly correlated in Arctic rivers [*Frey et al.*, 2007; *Holmes et al.*, 2012; *McClelland et al.*, 2014]. Riverine DON may be particularly important to coastal ecosystems, as it greatly exceeds dissolved inorganic nitrogen (DIN) in these six Arctic rivers [*Tank et al.*, 2012b; *Le Fouest et al.*, 2013]. Both bacterial and photochemical remineralization of DON could contribute to production in Arctic coastal waters [*Bélanger et al.*, 2006; *Le Fouest et al.*, 2013]. Although beyond the scope of this study, it might be possible to use relationships between CDOM, DOC, and DON to calculate satellite-derived estimates of DON concentrations.

Remotely sensed CDOM may be a useful proxy for other DOM characteristics as well. Stubbins et al [2015] proposed using absorbance at 254 nm or 412 nm to predict dissolved black carbon (DBC) from the Arctic-GRO rivers, with $R^2 > 97\%$. The aromatic

compounds that make up DBC strongly absorb light, providing a mechanistic link between DBC and CDOM. Similarly, CDOM commonly is used to assess relative molecular weights and DOM source. For instance, Walker et al [2013] showed that lignin phenol concentrations in the Kolyma, Lena, and Yenisey rivers could be estimated from a_{350}. Lignin phenols, derived from plant matter, have been widely used as terrestrial biomarkers in aquatic and marine systems. Likewise, spectral slopes derived from CDOM absorbance scans have proven to be good indicators of terrestrial DOM. Indeed, Fichot et al. [2013] used $S_{275-295}$ to track riverine DOM in the Arctic Ocean from MODIS imagery. In all of these cases, CDOM spectra offer inexpensive, fast alternatives to complex lab analyses for terrestrial tracers. Future studies can thus link remotely sensed CDOM to these important indicators of organic matter source. Particularly in this era of rapid climate change, tracing inputs of allochthonous carbon from vegetation and permafrost soils will enhance our understanding of carbon cycling in the Arctic.

5. IMPLICATIONS AND CONCLUSIONS

Estimation of CDOM in the major Arctic rivers from Landsat data provides a new tool to synoptically monitor river biogeochemistry on a Pan-Arctic scale. We built river-specific empirical models between satellite reflectance and LOADEST-modeled CDOM over six Arctic rivers, using 424 separate observations from 2000 – 2013. In the Kolyma, Lena, Yenisey, and Yukon rivers, this regression-based approached predicted CDOM with R^2 of 67 – 84%, with RMSE of 1.17 – 2.96. CDOM in the Mackenzie and Ob' rivers could not be explained through these methods as well (R^2 of 53% and 33%, RMSE of 1.45 and 1.21, respectively), likely owing to a relative lack in inherent CDOM variability for the regression models to explain. Sediment may also have been a confounding factor, particularly in the Mackenzie River. Satellite-derived CDOM will

allow assessment of climate change impacts on riverine DOM fluxes to the Arctic Ocean, and extend time series to the 1980s in some rivers. These riverine endmembers complement other efforts to trace terrestrial DOM into the Arctic Ocean with ocean-color remote sensing. The remotely-sensed data products may be further used to extrapolate across space, and estimate CDOM losses or transformations throughout the lower watershed. Riverine CDOM has been strongly tied to many terrestrial biomarkers, such as lignin, humics, and molecular weight. These Landsat results are an inexpensive alternative to laboratory-intensive analyses.

Table 1.1 LOADEST model coefficients and R^2 values from Model 6 (see methods), used to develop daily DOM concentration estimates, ± standard error. Statistically significant coefficients are marked with an asterisk (*).

River	Coefficients ± 1 Standard Deviation					R^2 (%)
CDOM	a_0	a_1	a_2	a_3	a_4	
Kolyma	1.56 ± 0.20*	0.50 ± 0.09*	-0.003 ± 0.05	-0.55 ± 0.26*	0.28 ± 0.14*	73
Lena	2.56 ± 0.11*	0.45 ± 0.05*	-0.02 ± 0.05	-0.53 ± 0.13 *	0.40 ± 0.09*	89
Mackenzie	1.47 ± 0.31*	1.58 ± 0.43*	0.06 ± 0.45	1.00 ± 0.31*	-0.77 ± 0.37*	53
Ob	2.62 ± 0. 24*	0.53 ± 0.13*	-0.17 ± 0.28	-0.30 ± 0.21	-0.16 ± 0.18	45
Yenisey	1.83 ± 0.19*	0.59 ± 0.13*	0.25 ± 0.14	0.37 ± 0.20	-0.29 ± 0.13*	72
Yukon	1.66 ± 0.23*	1.01 ± 0.17*	-0.15 ± 0.18	-0.57 ± 0.27*	0.58 ± 0.19*	70
DOC	a0	a1	a2	a3	a4	
Kolyma	1.82 ± 0.16*	0.41 ± 0.07*	-0.03 ± 0.04*	-0.67 ± 0.20*	-0.07 ± 0.10*	64
Lena	2.38 ± 0.12*	0.33 ± 0.06*	-0.03 ± 0.05	-0.57 ± 0.14 *	-0.42 ± 0.08	74
Mackenzie	1.43 ± 0.12*	0.18 ± 0.15*	0.17 ± 0.17*	0.08 ± 0.16	-0.04 ± 0.08	31
Ob	2.33 ± 0. 13*	0.18 ± 0.07*	-0.17 ± 0.15*	-0.03 ± 0.12	-0.07 ± 0.09*	43
Yenisey	1.74 ± 0.10*	0.39 ± 0.08*	0.06 ± 0.08*	0.29 ± 0.11*	-0.07 ± 0.08*	75
Yukon	1.63 ± 0.13*	0.78 ± 0.09*	-0.08 ± 0.10*	-0.50 ± 0.15*	0.37 ± 0.10*	80

Table 1.2   Landsat multispectral bands used to develop regressions between CDOM and reflectance for each river, and the respective R^2 and root mean square error (RMSE). Also included are results from a regression utilizing data across all rivers.

River	Landsat Bands and Band Ratios			R^2 (%)	RMSE
Kolyma	ln(B2)	ln(B3)	B2/B3	73	1.48
Lena	ln(B3)	ln(B4)	ln(B2/B4)	67	2.96
Mackenzie	ln(B2)	B4		53	1.45
Ob	B1	B2B3		33	1.21
Yenisey	ln(B2)	ln(B3)	B2/B3	84	1.17
Yukon	B1	B2	B1/B4	75	2.33
All Rivers	B3	B4	B2/B3	52	3.23

Table 1.3   Number of Landsat scenes used to develop regression equations between CDOM absorbance and remote sensing reflectance data. Scenes are from 2000 – 2013.

River	Landsat Scenes used			
	Freshet	Summer	Fall	Total
Kolyma	25	35	8	68
Lena	19	38	14	71
Mackenzie	50	47	14	111
Ob	23	33	19	75
Yenisey	10	38	7	55
Yukon	14	19	11	44
Total	141	210	73	424

Table 1.4　Average CDOM and DOM concentrations for the ice-free period from three data sources, for 2004 – 2006 and 2009 - 2012. Seasonal averages were calculated for the entire time period, ± standard error. Total ice-free period concentrations are averages of the seasonal values, so that equal weight is given to each season. Landsat-derived seasonal means were compared to measured and LOADEST values using Tukey's post hoc test (p = 0.05). Italics indicates significant difference from measured data and bold indicates significant difference from LOADEST results. CDOM units are a_{375} m^{-1}. DOC is in mg/L C.

| | Freshet | | | Summer | | | Fall | | | Total Ice-free Period | |
	CDOM	DOC	n	CDOM	DOC	n	CDOM	DOC	n	CDOM	DOC
Kolyma											
Measured	12.1 ±1.54	9.65 ±0.99	14	5.70 ± 0.83	5.51 ± 0.62	6	4.00 ± 0.32	4.42 ± 0.44	7	7.25 ± 2.45	6.53 ± 1.59
LOADEST	9.42 ±0.2	8.46 ±0.13	172	4.95 ± 0.07	5.06 ± 0.05	434	5.21 ± 0.06	5.59 ± 0.05	280	6.53 ± 1.45	6.37 ± 1.06
Landsat	*8.75 ±0.61*	***7.1 ±0.34***	15	5.89 ± 0.44	5.53 ± 0.24	17	6.59 ± 0.57	5.92 ± 0.32	4	7.08 ± 0.86	6.18 ± 0.47
Lena											
Measured	25.6 ±0.87	16.3 ±0.77	14	9.23 ± 0.76	7.41 ± 0.46	5	8.23 ± 0.31	7.26 ± 0.26	7	14.4 ± 5.62	10.3 ± 2.98
LOADEST	20.1 ±0.29	13.2 ±0.12	178	10.6 ± 0.11	8.46 ± 0.06	434	9.55 ± 0.07	8.18 ± 0.04	280	13.4 ± 3.34	9.93 ± 1.61
Landsat	*18.97 ±1.12*	*12.7 ±0.61*	10	11.3 ± 0.64	8.49 ± 0.35	23	9.77 ± 0.66	7.67 ± 0.36	12	13.3 ± 2.85	9.63 ± 1.57
Mackenzie											
Measured	6.08 ±0.94	5.47 ±0.35	12	3.51 ± 0.51	4.57 ± 0.36	11	3.80 ± 1.17	4.10 ± 0.43	4	4.46 ± 0.81	4.71 ± 0.40
LOADEST	6.86 ±0.15	5.66 ±0.04	237	3.64 ±0.05	4.61 ± 0.02	434	5.13 ± 0.08	4.25 ± 0.01	280	5.21 ± 0.93	4.84 ± 0.42
Landsat	6.01 ±0.12	5.6 ±0.12	31	4.22 ±0.22	4.61 ± 0.12	25	3.8 ± 0.29	4.38 ± 0.16	6	4.68 ± 0.68	4.86 ± 0.37
Ob											
Measured	14.5 ±0.58	9.88 ±0.37	15	14.0 ± 0.68	11.2 ± 0.55	7	9.18 ± 1.15	9.36 ± 0.49	4	12.6 ± 1.69	10.1 ± 0.54
LOADEST	14.3 ±0.05	9.94 ±0.01	211	13.0 ± 0.09	10.3 ± 0.02	434	12.4 ± 0.06	10.3 ± 0.02	280	13.3 ± 0.56	10.2 ± 0.12
Landsat	14.2 ±0.11	10.1 ±0.06	14	13.9 ± 0.16	***9.93 ± 0.09***	19	*13.1± 0.21*	***9.49 ± 0.12***	14	13.7 ± 0.33	9.84 ± 0.18

Yenisey

Measured	17.4 ±0.65	10.2 ±0.31	15	6.14 ± 1.05	5.72 ± 0.59	6	9.01 ± 1.17	6.70 ± 0.72	5	10.9 ± 3.39	7.52 ± 1.34
LOADEST	16.8 ±0.48	9.72 ±0.14	172	8.58 ± 0.04	6.74 ± 0.02	434	8.52 ± 0.05	6.46 ± 0.03	280	11.3 ± 2.75	7.64 ± 1.04
Landsat	14.7 ±1.25	10.4 ±0.69	7	9.04± 0.26	*7.26 ± 0.14*	23	9.34 ± 0.55	7.43 ± 0.30	4	11.0 ± 1.83	8.35 ± 1.01

Yukon

Measured	14.2 ±1.64	10.5 ±0.91	15	5.25 ± 1.36	4.61 ± 0.66	8	6.55 ± 1.70	5.65 ± 1.12	4	8.66 ± 2.79	6.92 ± 1.82
LOADEST	12.6 ±0.19	9.28 ±0.12	254	6.01 ± 0.07	5.37 ± 0.04	434	4.75 ± 0.06	4.8 ± 0.08	280	7.78 ± 2.43	6.48 ± 1.41
Landsat	12.7 ±9.27	9.27 ±0.31	10	**8.15 ± 0.54**	***6.77 ± 0.3***	9	5.70 ± 0.66	5.42 ± 0.36	5	8.85 ± 2.05	7.15 ± 1.13

Figure 1.1   Map of the Arctic Ocean drainage basin, with the watersheds of the six rivers included in this study. Red points are sampling locations on each river: Ob' at Salekhard, Yenisey at Dudinka, Lena at Zhigansk, Kolyma at Cherskiy, Yukon at Pilot Station, and Mackenzie at Tsiigehtchic.
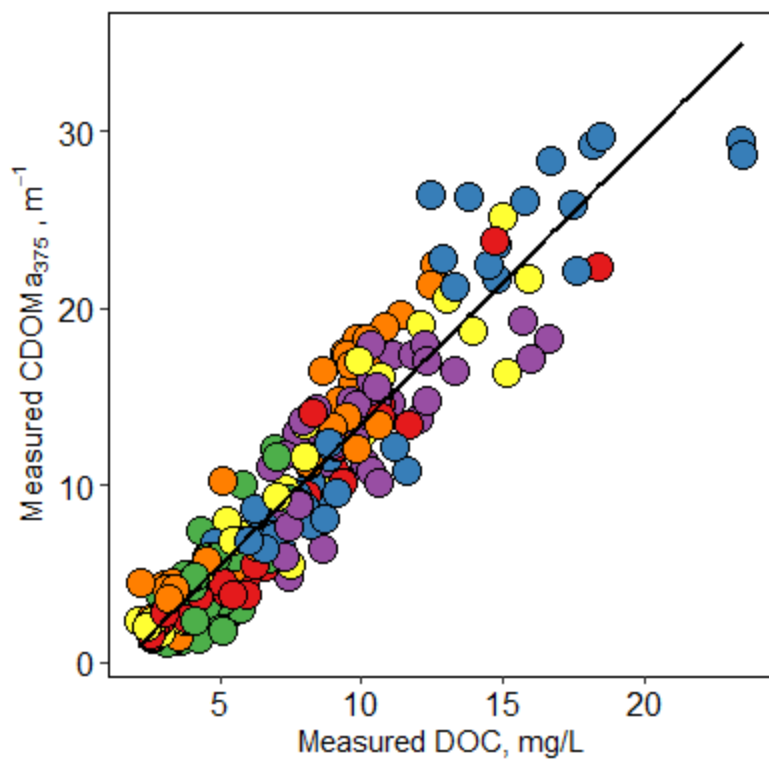
Figure 1.2   Regression between measured DOC and CDOM a_{375}, from the complete
Arctic-GRO dataset from 2004-2014. Red = Kolyma, Green = Mackenzie,
Orange = Yenisey, Blue= Lena, Purple = Ob', Yellow = Yukon.
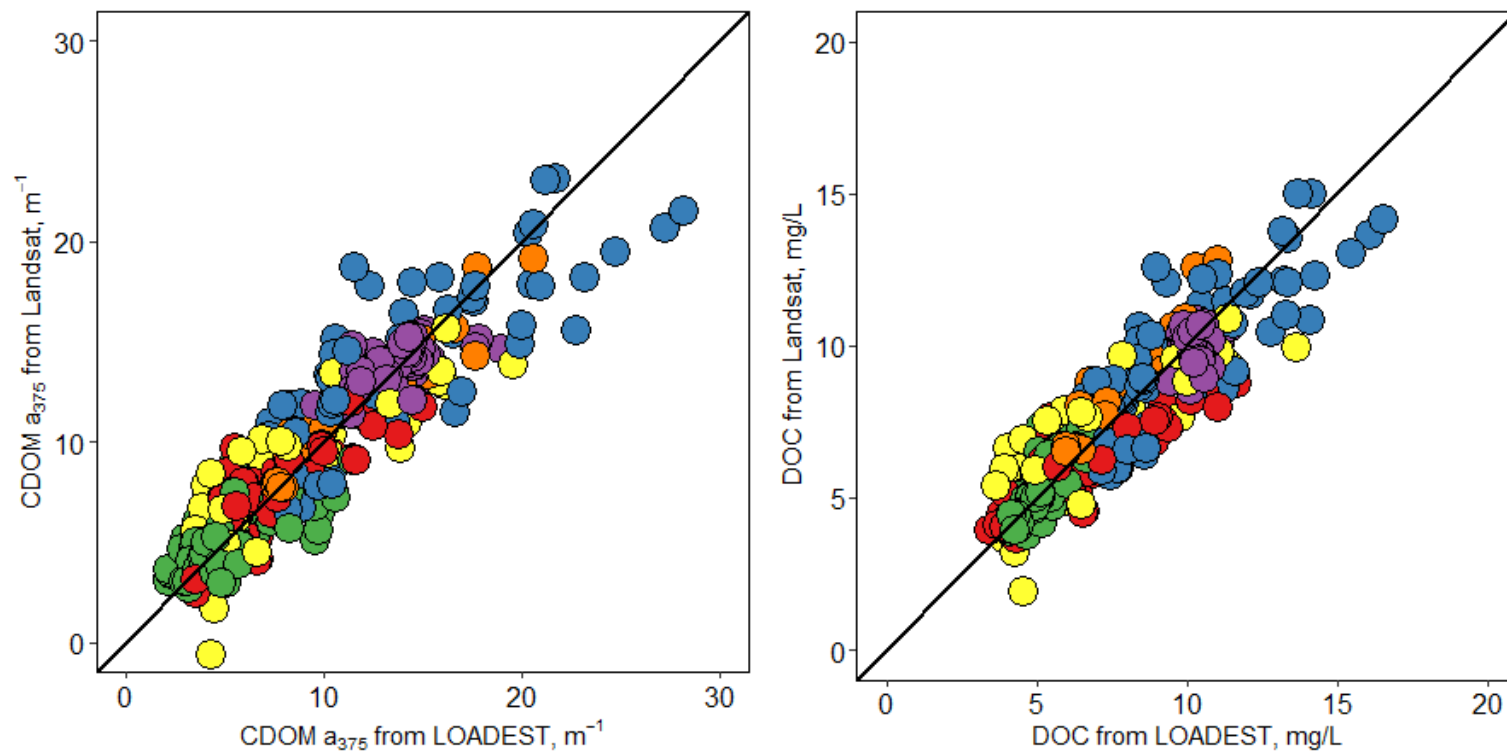
Figure 1.3 Scatterplots of CDOM and DOC from LOADEST compared to remote sensing estimates. The line in both plots is one-to-one. Individual river regressions vary, but overall CDOM is predicted with $R^2 = 85\%$, DOC with $R^2 = 74\%$. Red = Kolyma, Green = Mackenzie, Orange = Yenisey, Blue = Lena, Purple = Ob', Yellow = Yukon.
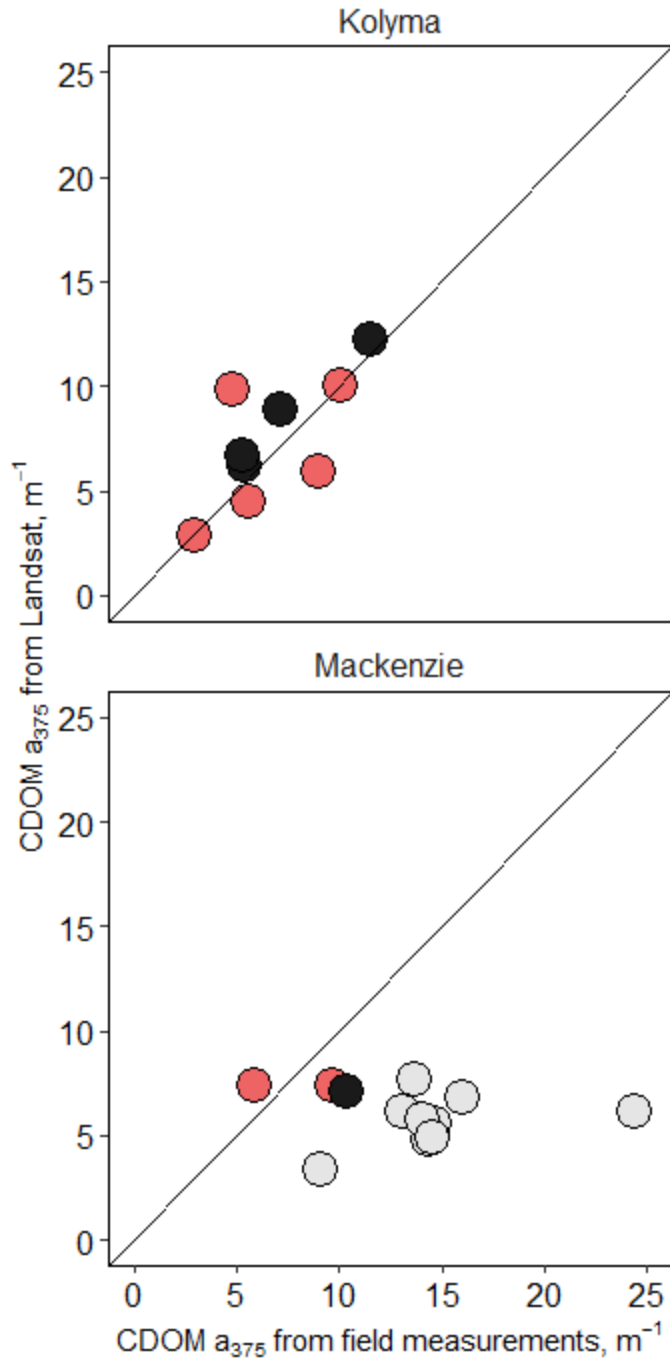
Figure 1.4   Comparison of field collected CDOM measurements and Landsat-derived
estimates, from samples distributed across the lower watersheds of the
Kolyma and Mackenzie rivers. Line is 1:1, Grey points = delta, Black
points = main stem, Pink points = tributary.
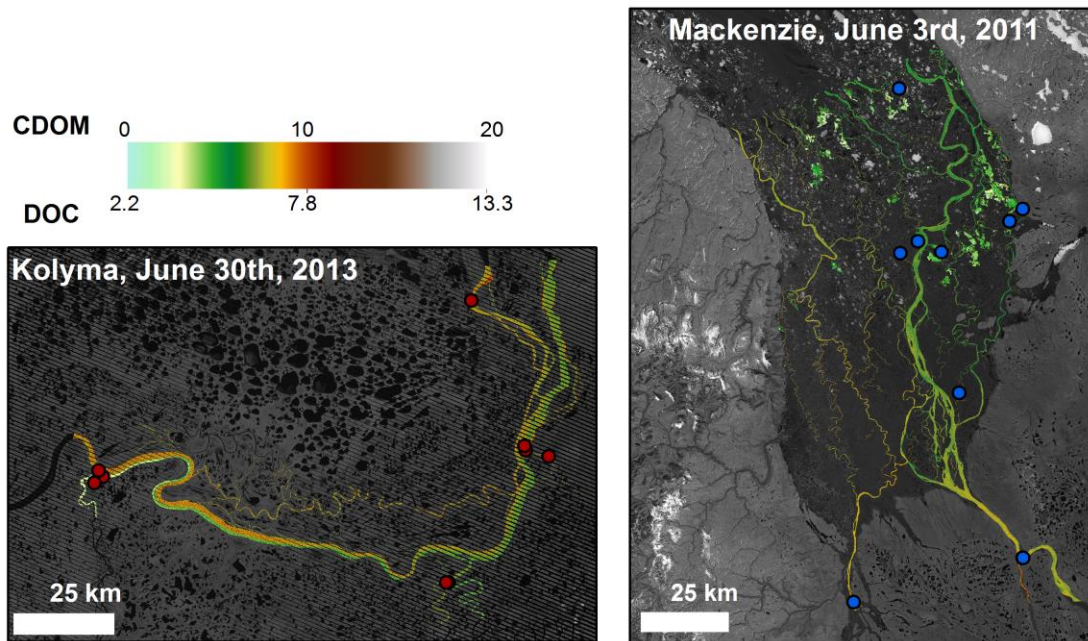
Figure 1.5   Map of CDOM and DOC from remote sensing for the Kolyma and
              Mackenzie rivers, with sampling sites used for spatial evaluation included.
              Imagery corresponds to field campaigns (Mackenzie in June 2011, Kolyma
              in June-July 2013). Red points = Kolyma, Blue points = Mackenzie.
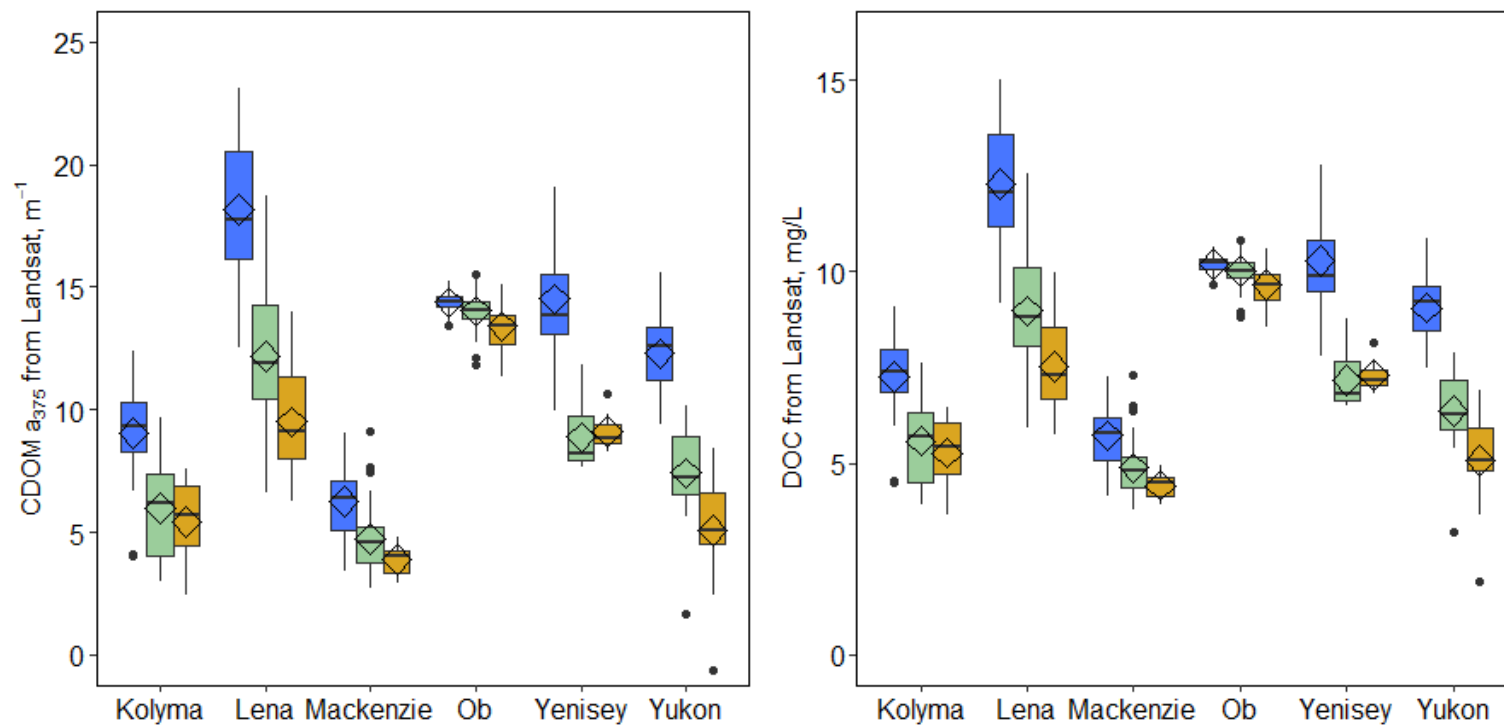
Figure 1.6   Seasonal variation in DOM from remote sensing, from 2000 – 2013. Boxes are 25th to 75th percentile. Whiskers are 1.5* interquartile range. Lines through boxes are median, diamonds are mean. Points are outliers. Blue = Freshet (May-June), Green = Summer (July-August), Yellow = Fall (September-October).
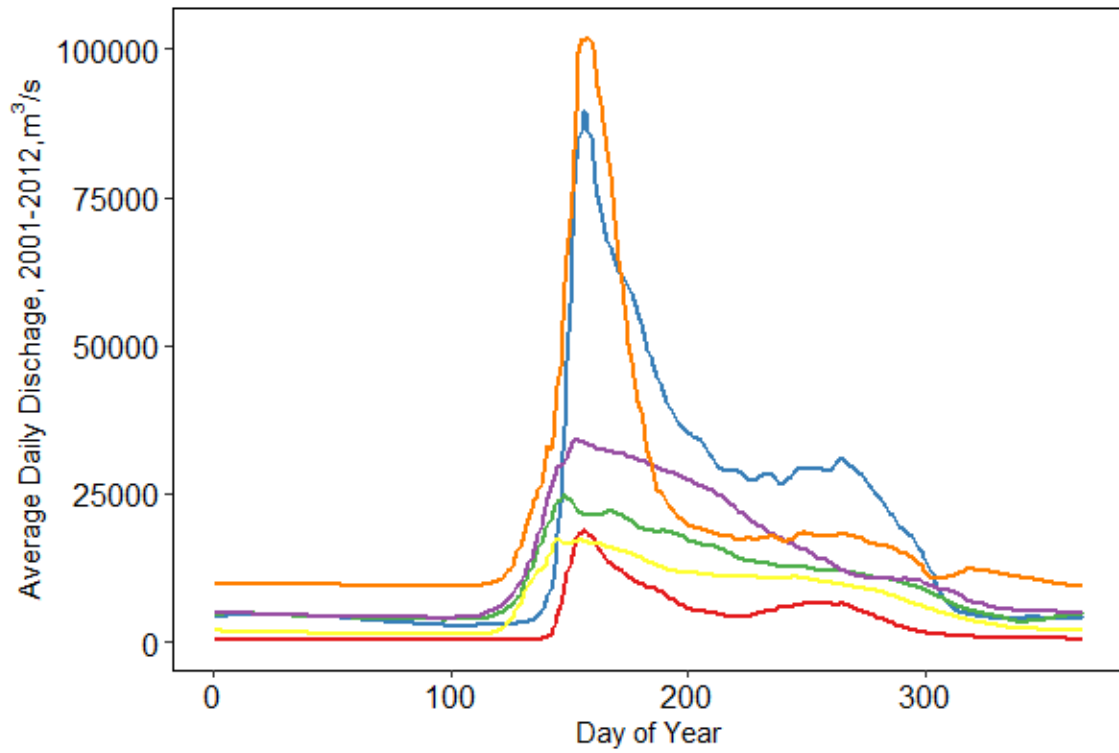
Figure 1.7　Average daily discharge for each river, 2001 – 2012. Red = Kolyma, Green = Mackenzie, Orange = Yenisey, Blue= Lena, Purple = Ob', Yellow = Yukon.
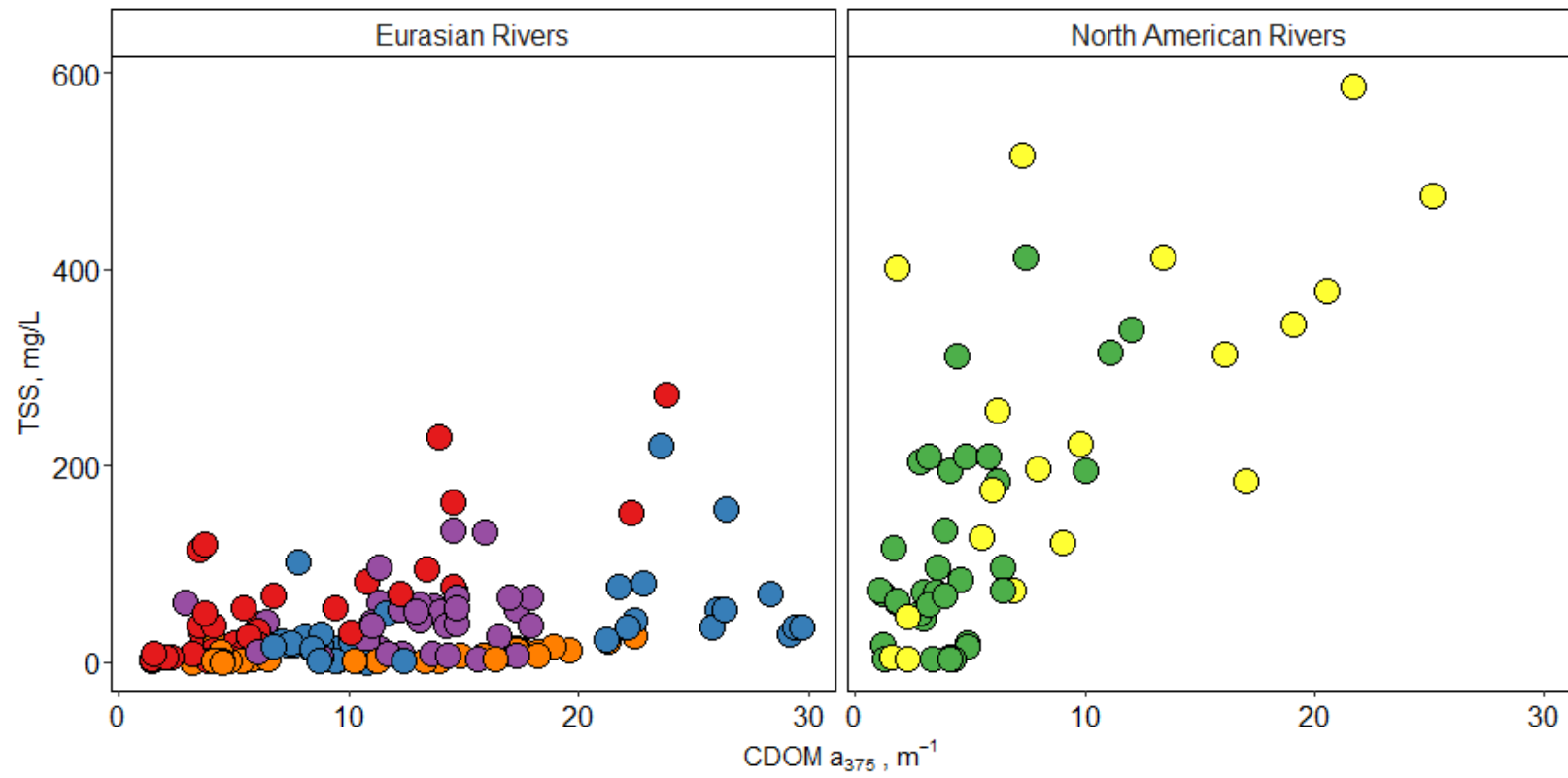
Figure 1.8   CDOM versus TSS for the Eurasian (left) and North American (right) rivers. Red = Kolyma, Green = Mackenzie, Orange = Yenisey, Blue = Lena, Purple = Ob', Yellow = Yukon.

Chapter Two: Decadal-scale Dissolved Organic Matter Concentrations and Fluxes Across the Pan-Arctic from Remote Sensing

ABSTRACT

Climate change in the Arctic is significantly impacting land-ocean linkages. Climate-driven changes in river discharge have been particularly well documented. However, other impacts of regional warming – such as thawing permafrost and potential changes in microbial processing – mean it is unclear how these increases in discharge ultimately impact fluxes of water-borne materials to the Arctic Ocean. We used a satellite remote sensing approach to estimate dissolved organic matter (DOM) concentrations and fluxes from the six largest Arctic rivers (Yenisey, Ob', Lena, Kolyma, Yukon, Mackenzie) and evaluate potential changes beginning as far back as the 1980s. Landsat TM and ETM+ reflectance data were used to quantify chromophoric dissolved organic matter (CDOM) and associated dissolved organic carbon (DOC) concentrations. These results were then coupled with long-term records of river discharge to estimate fluxes. During 2001 – 2013, all six rivers showed high seasonality in both CDOM and DOC concentrations and export, corroborating previous work from field-based measurements. Inter-annual to inter-decadal variations linked to the Arctic Oscillation Index were also evident in most of the rivers. Landsat data extends back to 1985 for the Mackenzie, Ob', and Yenisey rivers. CDOM concentrations in the Mackenzie River increased over a 30 year period, however this was not matched by increased CDOM flux. Discharge-normalize CDOM in the Yenisey River decreased from the 1980s to 2000s, although trends in flux and concentration were not significant. The Ob' River showed no long-term changes in export, but there was a potential increase in CDOM concentrations

relative to discharge over the past ~30 years. While remote sensing results must be interpreted cautiously, such long-term biogeochemical datasets are rare. The patterns that we observed may be linked to changes in permafrost and hydrology in major Arctic watersheds over recent decades.

INTRODUCTION

The Arctic has experienced regional warming at approximately twice the rate of the global average over the past half-century, resulting in widespread changes to Arctic systems [*Bekryaev et al.*, 2010; *Pithan and Mauritsen*, 2014]. Impacts of climate change include an accelerating hydrological cycle [*Peterson et al.*, 2006], permafrost thaw and carbon release [*Koven et al.*, 2011; *Schuur et al.*, 2015], and shifting vegetation patterns [*Berner et al.*, 2011; *Pearson et al.*, 2013]. Such processes have the potential to alter the transportation and transformation of organic matter in inland waters throughout high latitudes, and ultimately impact organic matter fluxes from land to sea [*Guo et al.*, 2007; *Walvoord and Striegl*, 2007; *Beaulieu et al.*, 2011; *Spence et al.*, 2015; *Vonk et al.*, 2015].

Rivers deliver approximately 35 Tg of dissolved organic carbon (DOC) to the Arctic Ocean each year [*Raymond et al.*, 2007; *Holmes et al.*, 2012]. Riverine organic matter delivered to the Arctic Ocean may be mineralized by biological [*Cooper et al.*, 2005; *Alling et al.*, 2010; *Karlsson et al.*, 2011] or photochemical processes [*Bélanger et al.*, 2006; *Osburn et al.*, 2009], incorporated into food webs [*Dunton et al.*, 2012], or stored in deep waters and sediments [*Benner et al.*, 2004]. Particularly in nearshore environments, riverine organic carbon can contribute substantially to food webs, and remineralized organic nitrogen may fuel primary production [*Manizza et al.*, 2009; *Tank et al.*, 2012b; *Le Fouest et al.*, 2013]. Chromophoric (colored) dissolved organic matter (CDOM), which is often high in Arctic rivers [*Spencer and Aiken*, 2009; *Griffin et al.*, 2011; *Mann et al.*, 2016], also influences light attenuation in coastal environments and is integral to photochemistry [*Hu et al.*, 2002; *Helms et al.*, 2008; *Manizza et al.*, 2011]. Climate-driven changes in export of DOM from land to sea will thus have multiple ramifications for carbon cycling and ocean ecosystem functioning.

There have been well-documented increases in riverine discharge, particularly in Eurasian rivers, attributable to increased transport of atmospheric moisture from low to high latitudes [*Peterson et al.*, 2006]. Given the tight, positive relationship between discharge and organic matter concentration observed in many high-latitude rivers [*Peterson et al.*, 1986; *Holmes et al.*, 2012], we might expect an even greater flux of organic matter from Arctic rivers as a result of climate change. However, relationships between hydrology and biogeochemistry are unlikely to remain constant as the Arctic warms, and organic matter export responses are unlikely to be uniform throughout the pan-Arctic domain. In the Yukon River basin, researchers have suggested that there may be a decrease in the export of DOC as permafrost thaws and flow paths deepen [*Striegl et al.*, 2005; *Walvoord and Striegl*, 2007]. In this case, it is hypothesized that greater flow through organic-poor mineral soils and increased path lengths that allow for enhanced microbial decomposition will promote DOC losses. In contrast, there may be a temperature-dependent increase in DOC export from peat-dominated catchments in the West Siberian lowlands as permafrost thaws [*Frey and Smith*, 2005]. Thus, landscape characteristics may control changes in the linkage between discharge and DOM concentrations as permafrost thaws [*Tank et al.*, 2012a].

Despite the vulnerability of riverine DOM to regional climate change, there are few long-term records available. The Kuparuk River, in the foothills of Alaska's Brooks Range, has been intensively sampled during summer months since the 1970s [*McClelland et al.*, 2007]. The Water Survey of Canada has also routinely measured DOC in the Mackenzie River for several decades [*Tank et al.,* in review]. However, reliable records of nutrients or organic matter are lacking from Russian rivers [*Holmes et al.*, 2001]. Neither is there consistently-collected data available from major Alaskan rivers prior to roughly the past 15 years [*Striegl et al.*, 2005]. Process-based models have the potential

to address some of these concerns, by linking DOC leaching and export to hydrology, vegetation and soil types [*McGuire et al.*, 2010]. Indeed, such an approach estimated an increase in DOC flux from Arctic rivers of 0.037 Tg C/yr over the course of the 20th century [Kicklighter et al., 2013]. However, there are few decadal-scale datasets to calibrate or validate such modelling approaches.

Growing concern about potential impacts of climate change on organic matter stocks and fluxes in the Arctic has prompted a sharp increase in studies of DOM in high-latitude rivers during the past 10-15 years. Along with numerous short-term studies, the Arctic Great Rivers Observatory (Arctic-GRO; originally established as the Pan Arctic River Transport of Nutrients, organic mattER, and suspended Sediments or PARTNERS project) began monitoring biogeochemical characteristics of the six largest Arctic rivers in 2003 [*McClelland et al.*, 2008]. The Kolyma, Lena, Mackenzie, Ob', Yenisey, and Yukon rivers together represent approximately half of annual discharge to the Arctic Ocean (Figure 1). The Yukon is included, despite not emptying directly into the Arctic Ocean, as a contributor to low-salinity Pacific waters transported northward through the Bering Strait. Arctic-GRO has explicitly targeted the highly seasonal nature of Arctic rivers, with an emphasis on sampling during high-flow conditions shortly after spring freshet. However, this biogeochemical database does not yet extend through a long enough time period to assess whether climate change has influenced DOM export from these large Arctic rivers.

Satellite remote sensing offers an opportunity to fill gaps in the available records of DOM concentrations from Arctic rivers. CDOM is a good proxy for riverine DOC in the Arctic [*Spencer and Aiken*, 2009; *Griffin et al.*, 2011; *Mann et al.*, 2016], and a variety of satellite-based approaches have been used to estimate CDOM in lakes, rivers, and estuaries at northern latitudes [*Morel and Bélanger*, 2006; Kuster, 2012; *Fichot et al.*,

2013; *Heim et al.*, 2014]. Of particular relevance to this study, Landsat Thematic Mapper and Enhanced Thematic Mapper Plus (Landsat TM and ETM+) sensors have been used to quantify CDOM in a Siberian river [*Griffin et al.*, 2011] and in boreal lakes [*Kutser et al.*, 2005; *Kallio et al.*, 2008] . The length of the Landsat record (~30 years) makes it especially attractive for retrospective studies. For example, CDOM was estimated throughout the thirty-year Landsat record in a Swedish boreal lake [*Kutser*, 2012], and was used in a 20+ year analysis of lake clarity (of which CDOM was a major determinant) in the Midwest region of the United States [*Olmanson et al.*, 2008]. Nonetheless, long-term studies using Landsat to estimate CDOM remain relatively rare. This is, in part, because Landsat TM and ETM+ lack sensitivity to monitor CDOM effectively in some CDOM-rich, low-sediment systems where the water-leaving radiance can be very low [*Gordon and Wang*, 1994; *Kutser et al.*, 2005, 2009]. Newer sensors, such as Landsat Operational Land Imager (OLI) and Sentinel-2, hold great potential to monitor CDOM even in very dark waters [*Palmer et al.*, 2015; *Olmanson et al.*, 2016]. Other sensors, such as the MODerate resolution Imaging Spectroradiometer (MODIS) and MEdium Resolution Imaging Spectrometer (MERIS) have also been used to map CDOM in Arctic estuaries [*Morel and Bélanger*, 2006; *Fichot et al.*, 2013; *Heim et al.*, 2014]. Despite these advances, however, Landsat TM and ETM+ data remain the best historical archive available for estimating CDOM in inland waters. No other sensors have both the high spatial resolution (30m) and data archive extending to the 1980s needed to develop time series of inland water quality [*Kloiber et al.*, 2002; *Kutser*, 2012; *Lobo et al.*, 2014; *Olmanson et al.*, 2014].

In this study, we use a previously developed set of empirical remote sensing models [*Griffin et al.*, in preparation (Chapter 2 of dissertation)] to assess decadal-scale concentrations and fluxes of CDOM from the six largest Arctic rivers. Time series of

seasonal and annual CDOM concentrations from each river are developed, extending to 1985 for the Mackenzie, Ob', and Yenisey rivers. We used historical data to assess whether the relationship between discharge and CDOM concentration has changed substantially. Fluxes of CDOM, based on seasonally-averaged concentrations, are presented. These represent the first known empirically-based assessments of DOM flux from multiple major Arctic rivers spanning several decades.

2. METHODS

A complete description of data acquisition and processing, algorithm development, and evaluation of the remote sensing approach used in this study can be found in Griffin et al [in preparation (Chapter 2 of dissertation)]. A brief description of model development follows, with additional details of the decades-long Landsat time series and methods used to calculate CDOM and DOC flux estimates.

2.1 Biogeochemistry, discharge, and climate data

DOM data from field sampling comes from the Arctic Great Rivers Observatory (Arctic-GRO; www.arcticgreatrivers.org). Arctic-GRO monitors biogeochemistry of the six largest rivers draining the pan-Arctic watershed (Kolyma, Lena, Mackenzie, Ob', Yenisey, and Yukon rivers), from 2003 – present. Field expeditions to collect biogeochemical information target seasonal variability, with depth-integrated cross-sectional sampling near river mouths [*Holmes et al.*, 2012]. Previous publications from Arctic-GRO contain more details on methods and sampling design [*Raymond et al.*, 2007; *Holmes et al.*, 2012; *Walker et al.*, 2013]. Arctic-GRO and PARTNERS DOM samples were filtered through 0.45 μm capsule filters into pre-cleaned, pre-rinsed HDPE bottles and frozen until analysis. DOC samples from 2003 – 2006 were sent to the

National Ocean Sciences Atomic Mass Spectrometry (AMS) facility at Woods Hole Oceanographic Institute or the AMS facility at University of Arizona for analysis [*Raymond et al.*, 2007; *Holmes et al.*, 2012]. All Arctic-GRO (2008–present) DOC samples were measured at the Woods Hole Research Center (WHRC) using a Shimadzu (TOC-V) organic carbon analyzer. CDOM absorbance was measured with a Shimadzu UV-1800 with a 1 cm quartz cuvette, from wavelengths 200 – 800 nm at 1 nm intervals at the WHRC. Absorption coefficients calculated using Equation 1:

$$a(\lambda) = 2.303 A(\lambda)/l \ (1)$$

where $a(\lambda)$ is the absorption coefficient at a given wavelength, $A(\lambda)$ is the absorbance at a given wavelength and l is the path length in meters [*Hu et al.*, 2002]. Absorbance at 375 nm (a_{375}) was used for subsequent data analysis, owing to limited data availability at longer wavelengths from PARTNERS data (2003 – 2006).

To obtain adequate ground-truthing data for remote sensing analyses, we modeled CDOM concentrations discharge for 2000 – 2013 using the US Geological Survey (USGS) Load Estimator (LOADEST) [*Runkel et al.*, 2004]. Full details are available in [*Griffin et al.*, in preparation (Chapter 1 of dissertation)]. LoadRunner version 2.1 (http://environment.yale.edu/loadrunner) was used to automate LOADEST runs. LOADEST contains multiple models, some of which include variables to account for seasonality. We used Model 6 (Equation 2) to predict CDOM concentrations on each river.

$$\text{Ln (Conc)} = a_0 + a_1 \, \text{LnQ} + a_2 \, \text{LnQ}^2 + a_3 \, \text{Sin} \, (2 \, \pi \, d_{time}) + a_4 \, \text{Cos} \, (2 \, \pi \, d_{time}) \qquad (2)$$

Where concentration is calculated in mg/L, Q is water discharge in ft³/s, LnQ equals Ln (Q) minus center of Ln (Q), and d_{time} is decimal time minus center of decimal

time. The resulting concentration estimates are from the adjusted maximum likelihood output.

Discharge from Russian rivers was downloaded from the ArcticRIMS website (http://rims.unh.edu/data.shtml). Yukon River discharge was obtained from US Geological Survey and Mackenzie discharge from Environment Canada. Arctic Oscillation Index January-February-March data (used for comparison with flux estimates derived in this paper) were retrieved from the National Oceanic and Atmospheric Administration's National Centers for Environmental Information website (http://www.ncdc.noaa.gov/teleconnections/ao/), from 1985 – 2013.

2.3 CDOM retrieval from Landsat TM and ETM+ imagery

Previous work has established strong relationships between remote sensing reflectance and CDOM concentration for most of the Arctic-GRO rivers [*Griffin et al.*, in preparation (Chapter 1 of dissertation)]. Image processing occurred in Google Earth Engine (GEE), which allows for cloud-based remote sensing analyses of datasets stored on Google servers. We used the Landsat Ecosystem Disturbance Adaptive Processing System (LEDAPS) surface reflectance data product for Landsat 5 TM and 7 ETM+ scenes [*Masek et al.*, 2006]. LEDAPS, also a data product from USGS EROS Data Center, applies the Moderate Resolution Imaging Spectroradiometer (MODIS) atmospheric correction routines to Level 1 Landsat data, with auxiliary ozone, water vapor, aerosol optical thickness, and geopotential height data from NASA sensors [*Masek et al.*, 2006; *Schmidt et al.*, 2013].

For the time period 2000-2013, we created image collections from Landsat TM and ETM+, using scenes with 30% or less cloud cover, and clear-sky conditions over sampling locations. Because floating ice may interfere with the reflectance signal from

53

CDOM, only scenes from May 15th – October 15th were included in collections. Scenes from near ice break-up and formation were visually inspected, as on-the-ground observation of ice conditions are rarely available. At each river's monitoring site, a 3-pixel-wide cross-section region-of-interest (ROI) was digitized, from which reflectance was extracted. Landsat 7 experienced a failure of the Scan Line Correcter (SLC) in 2003, which causes striping in each scene, with about 25% of data lost. In these large, rivers, however, ROIs are hundreds of meters wide and contain dozens of pixels even with SLC-off data. River networks were masked using the Hansen et al (2013) dataset within Google Earth Engine. We used a simple cloud score method based on the thermal band to differentiate clouds from bright surfaces, and subsequently remove clouds [*Hansen et al.*, 2013].

Reflectances extracted from ROIs 2000 – 2013 were compared with CDOM a_{375} output from LOADEST models for each river in an exhaustive series of linear and multiple linear regression. All statistical analyses, unless stated otherwise, were performed in R software. For a detailed model evaluation, please see Griffin et al [in preparation (Chapter 1 of dissertation)]. Reflectance from blue, green, red and near infrared (B1, B2, B3, and B4, respectively) bands were included in regressions [*Griffin et al.*, in preparation (Chapter 1 of dissertation)]. Individual river regressions varied in ability to explain CDOM, with R^2 ranging from 33% in the Ob' and 53% in the Mackenzie, to 67%-84% for the Kolyma, Lena, Yenisey, and Yukon rivers. Although our regression models were not able to catch the full range of variability in the Mackenzie or Ob' rivers, root mean square error (RMSE) was comparable to other regressions (1.21-1.45 for the Mackenzie and Ob' versus 1.17 – 2.96 for other rivers). The lower R^2 for these specific rivers may be driven by the relative stability CDOM across seasons and years, resulting in less overall variation for the regression to explain.

These empirical models were then applied to all available Landsat TM and ETM+ imagery from 1985-2013.

DOM estimates from remote sensing during 2000 – 2013 include 424 scenes from all rivers, with multiple scenes from almost every year, which were used for remote sensing model development (Figure 2). Throughout 2003 – 2011 both Landsat 5 and Landsat 7 operated, increasing the data density greatly. Seasonal coverage varies, with more scenes from summer than either freshet or fall (Figure 2). Image availability for the Yukon River was relatively low compared to the others owing to the greater cloudiness over the Yukon Delta region during May – October. Furthermore, the paths of the polar-orbiting Landsat satellites overlap at high latitudes. As such, the Yukon (which is at a lower latitude than any of the other rivers) only has two paths that overlap at our sampling site, rather than three as is the case for all other rivers considered here. The Mackenzie has more than twice as many observations than the Yenisey or Yukon rivers.

Prior to the launch of Landsat 7 ETM+ in 1999, data coverage in most Arctic rivers was spotty, as scenes were not always automatically collected and stored for most of the 1990s. However, historical imagery covering the Mackenzie River extends to 1985, and include multiple dates per year in most cases (Figure 2). Images from the Ob' and Yenisey were captured regularly 1985 – 1990, with additional observations in 1994. The Mackenzie, Ob', and Yenisey rivers were expanded to include an additional 84, 28, and 53 scenes, respectively, from 1985 – 1999. The Ob' and Yenisey data are dominated by summer observations, but do include multiple dates from freshet and fall from 1985 – 1990. The Mackenzie River dataset also has more observations during summer, with more than twice as many additional scenes from July-August than September-October.

2.4 Fluxes of CDOM and DOC

We used a binned approach for DOM flux calculations, in order to account for the seasonal differences in DOM loading across the ice-free hydrograph. Average concentrations for spring freshet (May-June), summer (July-August), and fall (September-October) were calculated for 3-year periods from remote sensing data (Figure 3). These breaks were chosen to correspond to hydrology of most major Arctic rivers, where peak flow lasts through June, discharge continues to decrease through summer and fall. Fall roughly corresponds to when active layers have thawed to their deepest before beginning to re-freeze [*Spencer et al.*, 2015]. Unfortunately, not every season in every year was observed with clear-sky conditions by Landsat TM or ETM+, even during recent years when two satellites doubled the number of overpasses at any given site (Figure 2). Thus, we calculated 3-year seasonal means for each river. These aggregated seasonal values were then averaged together to establish mean CDOM values for the entire ice-free period (Figure 3). These 3-year averages across the ice-free period are only presented when there are data from all seasons (freshet, summer, and fall) for that time period.

These 3-year seasonal averages were used with daily discharge to calculate flux during the ice-free season from each river. This seasonally binned approach captured the increased CDOM concentrations associated with high flow conditions, and subsequent decline throughout the summer and fall. Annual fluxes were not calculated, as it is impossible estimate CDOM concentrations under-ice from remote sensing. However, winter export of DOC only accounts for ~11% of annual fluxes from these rivers [*Holmes et al.*, 2012]. Given the strong relationship between CDOM and DOC in most Arctic rivers, we can assume that our approach captures most of the annual export of CDOM [*Spencer and Aiken*, 2009; *Frey et al.*, 2016]. All CDOM flux values presented here for

56

the ice-free season are calculated for May 15 – October 15 for each river. Although this often includes under-ice conditions in mid to late May, discharge remains low until ice-break up and over-estimating concentration during this time period does not substantially alter flux calculations on a seasonal or annual basis.

Fluxes were only calculated when seasonal averages for all three seasons were available. For example, fluxes for 2012 – 2013 are not presented for the Yenisey, as clouds obscured all available imagery during fall for this time period. Nonetheless, fluxes of CDOM throughout the ice-free period could be constructed for each river in time series extending 13 – 27 years. The Mackenzie includes the longest and most complete time series, extending 1985 – 2011. The Yenisey and Ob' rivers also include annual fluxes from the 1980s. However, a lack of clear-sky imagery during the 1990s and early 2000s divide these data into two sections. Discharge data are missing from the Yukon River from 1995 – 2000, limiting flux calculations to 2001 – 2013. Fluxes from the Kolyma and Lena rivers were calculated for 2000 – 2013. We used the regression developed in Griffin et al. [in preparation (Chapter 2 of dissertation)] to convert remote sensing derived CDOM to DOC concentrations, prior to calculating fluxes for 2001-2013.

3. RESULTS

In the following sections, we present concentration and flux estimates derived from remote sensing. Three-year averages of CDOM for the ice-free period and on a seasonal basis can be assessed for each river in time series extending to the 1980s for the Mackenzie, Ob', and Yenisey rivers (Figure 3). Satellite-derived CDOM concentrations were also compared to daily discharge through time (Figure 4). In recent years (2001 – 2013) when all rivers have adequate discharge and remote sensing data, we calculated

57

average fluxes of CDOM and DOC on a seasonal basis and covering the entire ice-free period (Table 1). Finally, we present time series of CDOM fluxes for the ice-free season, based upon remote sensing observations from 1985 – 2013.

3.1 Remote sensing estimates of CDOM and DOC concentrations

Three-year seasonal averages show that CDOM concentrations are almost universally highest during freshet (Figure 3). The Ob' is the main exception, with summer or fall CDOM concentrations exceeding freshet for the 1997-1999, 2000-2002, and 2006-2008 periods. In some rivers, fall varies more widely in 3-year seasonal averages of CDOM concentration than other seasons. For instance, in the Kolyma, fall 3-year averages range from 3.1 to 8.6 m^{-1}, while freshet only varies from 8.2 to 11.1. Rivers that include data extending to the 1980s follow this pattern as well. In the Ob', average seasonal CDOM concentrations vary the most during fall, ranging by 2.6 m^{-1} in contrast to freshet which only ranges by 0.8 m^{-1}. In the Yukon, mean summer concentrations vary more widely than fall, and both seasons range more than the relatively steady freshet CDOM concentrations. The Yenisey is the only case where fall is the most stable, varying only 2.1 m^{-1}, while freshet and summer vary 4.8 and 5.0 m^{-1}, respectively.

There are few significant trends in CDOM concentration from 1985 - 2013, examining 3 year averages across the ice-free period (Figure 3). The Mackenzie River shows a significant increase in CDOM concentrations from 1985 – 2013 (Mann-Kendall, $\tau = 0.33$, p-value = 0.01). Although not significant to the 95% confidence, mean concentrations of Yenisey CDOM decreased during ice-free conditions from the 1980s to the 2000s (Mann-Kendall, $\tau = 0.-2$, p-value = 0.08). However, seasonal gaps in the time series mean there are only 5 points to include in any analysis of trends throughout the ice-

free period (Figure 3). A similar problem exists in the Ob' River, where ice-free averages only vary by 1.1 m^{-1} and there is no obvious trend. On a shorter time scale, the Yukon River increased CDOM concentrations from 2000 – 2013 (Mann-Kendall, τ = 0.67, p-value = 0.03).

On a seasonal basis, fall and summer concentrations of CDOM tend to rise in the Mackenzie River from the 1980s to 2000s. Mackenzie River freshet concentrations do not appear to follow the same trend, however. Although concentrations during fall can vary widely in the Ob', there are no obvious trends in CDOM concentration for any particular season. Freshet concentrations in the Yenisey River reveal no apparent trends through time. Spring and summer concentrations of CDOM in the Yenisey are lower in the 2000s than in the 1980s and 1990s, although given data gaps in the 1990s it is difficult to determine whether this is a trend.

Given the strong correlation between water discharge and CDOM concentration in these rivers, changes in CDOM concentration within rivers could be driven by interannual differences in discharge. Alternatively, the relationship between discharge and concentration may change through time as vegetation shifts, permafrost thaws, and microbial activity is stimulated at higher temperatures. Figure 4 displays all available CDOM concentrations from remote sensing against daily discharge. A handful of observations were excluded (5 from the Kolyma, 2 from the Yenisey, and 1 from the Yukon) owing to a lack of daily discharge. The Kolyma, Lena, Mackenzie, and Yukon rivers show clear linear relationships between discharge and CDOM concentration. CDOM in the Yenisey and Ob' rivers tends to vary at relatively low flow levels, with concentrations increasing at higher flow before flattening which suggests a logarithmic relationship. Discharge-specific CDOM concentrations in the Yenisey were higher during the 1980s and 1990s than in the 2000s and 2010s, although the four maximum

concentrations are observed in 2005 − 2013 (Figure 4; Welch's t-test, p-value < 0.01). Confidence in this decrease increases when freshet CDOM data is excluded (p-value = 0.0001). In contrast, discharge-specific CDOM concentrations in the Ob' tend to be lower in the 1980s than 2000s, suggesting an increase in CDOM loading through time (Welch's t-test, p-value = 0.03). However, removing spring freshet data from the Ob' results in a non-significant difference between the two time periods (p-value = 0.19). CDOM does not appear to change in relation to discharge in the Mackenzie River over the course of nearly 30 years. Other rivers lack long enough time series to evaluate whether there have been shifts in the relation between CDOM and discharge.

3.2 Fluxes of CDOM and DOC

Remote sensing based estimates of annual CDOM and DOC fluxes over the 2001 − 2013 time period average $19,600 \times 10^9$ m^2 and $14,600$ g C $\times 10^9$, respectively, for the ice-free period (Table 1). Fluxes of CDOM and DOC are dominated by spring freshet in most rivers. These satellite-based fluxes tend to underestimate CDOM flux during spring freshet compared to LOADEST estimates. In contrast, summer estimates of CDOM export from remote sensing methods mostly exceed LOADEST results with the exception of the Ob' River. Fall estimates of CDOM flux match closely between the two methods, with the exception of the Mackenzie where our remote sensing approach substantially underestimates flux. For the entire ice-free period, the Yenisey River differs the most between remote sensing and LOADEST approaches, mostly owing to underestimates during spring freshet. Total CDOM fluxes from the two methods are very close for the Ob' and Yukon rivers, while the Kolyma, Lena, and Mackenzie rivers are within 15% of LOADEST estimates. DOC export differs less between remote sensing and LOADEST methods. Only the Kolyma underestimates DOC flux by more than 10%. Over all, ice-

free fluxes of CDOM are below LOADEST estimates by ~10% and DOC is underestimated by ~3% from 2001-2013.

Percentage anomalies of ice-free flux estimates relative to 2001 – 2013 averages (Table 1) are shown in Figure 5. Annual fluxes can vary by as much as 40% relative to the 2001 – 2013 average. The Ob' shows the most inter-annual variability. The Yenisey and Yukon rivers, in contrast, stay within 20% of the baseline. Variations over intermediate timeframes are also evident, with higher average concentrations in some decades than others. Evidence of long-term trends, on the other hand, is scarce. . Only the Yenisey River showed an indication of change through time, although – as with concentration – this decrease in CDOM flux was not significant to 95% confidence (Mann-Kendall, τ = -0.324, p-value = 0.07).

4. DISCUSSION

Using remotely-sensed concentration estimates, we modeled CDOM and DOC export from major Arctic rivers, and achieved results consistent with previously published methods. Additionally, we were able to extend time series of CDOM concentration and flux to the 1980s in the Mackenzie, Ob', and Yenisey rivers. These results corroborate previous studies highlighting the importance of seasonality to organic matter fluxes from large Arctic rivers [*Finlay et al.*, 2006; *Guo et al.*, 2010; *Holmes et al.*, 2012; *Mann et al.*, 2016] and build upon sporadic existing data from some of these systems [*Striegl et al.*, 2005]. Seasonal patterns in CDOM concentration and export were apparent in all rivers throughout the available record. Few trends in CDOM concentration or export are apparent over a roughly 30-year period. However, CDOM fluxes from most of the rivers does appear to be associated with global teleconnections such as the Arctic Oscillation (Figure 5). Possible changes in the relationship between

CDOM concentration and discharge (Figure 4) suggest changing organic matter dynamics throughout the Arctic as hydrology, climate, and permafrost alter. Future work may refine these time series as new satellite platforms such as Sentinel-2 and Landsat 8 gather new, more sensitive optical data. Although we focus here on CDOM absorbance, with some discussion of DOC, remote sensing of CDOM may also be related to other geochemical characteristics such as black carbon, spectral slopes, and lignins [*Fichot and Benner*, 2011; *Osburn and Stedmon*, 2011; *Fichot et al.*, 2013; *Stubbins et al.*, 2015]. Ultimately, remote sensing proved a useful tool for investigating organic matter dynamics in high-latitude rivers over a longer timeframe than allowed by field sampling alone.

4.1 Remote sensing fluxes of CDOM and DOC

The highly seasonal nature of DOM in Arctic rivers has long been recognized [*Peterson et al.*, 1986; *Lobbes and Fitznar*, 2000], although it is only relatively recently that concerted efforts to monitor major rivers across the entire hydrograph have been made [*McClelland et al.*, 2008; *Holmes et al.*, 2012]. Landsat imagery can only observe during ice-free conditions, so assessments of seasonality are limited to freshet (mid-May – June), summer (July – August), and fall (September – mid-October). Our results support the paradigm of seasonally-driven changes in CDOM and DOC concentration and export, with the exception of the Ob' River (Figure 3, Table 1). Capturing the dynamic and rapid changes in DOM concentration during peak flow is essential for accurate assessments of export from these rivers [*Raymond et al.*, 2007; *Kicklighter et al.*, 2013], when the largest fraction of DOM flux occurs. Remote sensing using high spatial resolution sensors with longer return intervals cannot target this dynamic time period as explicitly as field campaigns designed for such a purpose. Nevertheless, Landsat has observed high-flow conditions on a regular basis over the course of the past ~15 years

(Figure 2). Given the potentially high inter-annual variability in DOM concentrations and fluxes from year-to-year (Figure 3 and 5, Table 1), this expanded database for the recent decade-and-half increases confidence in baseline conditions from which to measure future change.

In most rivers, our estimates of CDOM and DOC flux during the ice-free season are within 15% of LOADEST models, a method that has been used extensively to model DOM flux from discharge in Arctic rivers [*Spencer and Aiken*, 2009; *Holmes et al.*, 2012; *Tank et al.*, 2012b; *Spencer et al.*, 2013]. Our seasonal binning approach from Landsat-derived CDOM and DOC underestimates flux during freshet for two possible reasons. First, as mentioned previously, Landsat does not target the highest flow conditions shortly after spring freshet, when DOM concentrations are highest. Our averages of freshet DOM concentration thus tend to be slightly lower than measured data from Arctic-GRO which has focused on such peak conditions [*Griffin et al.* in preparation, see dissertation Chapter 2]. Secondly, while seasonal bins have been used successfully in other studies of Arctic rivers [*McClelland et al.*, 2014], this approach does miss the tightly-coupled increase in both DOM and discharge at the highest flow conditions. Despite these limitations, summer and fall fluxes of DOC and CDOM closely match LOADEST estimates. DOC flux estimates correspond more closely between the two methods across all seasons than CDOM fluxes. The largest difference is seen in the Yenisey River, which may be explained by the calibration data used in the separate LOADEST models for CDOM and DOC. CDOM concentrations measured by the Arctic-GRO correlate with discharge from the Yenisey more strongly than DOC does (R^2 = 78% versus 68%, for CDOM and DOC respectively).

Although freshet most often accounts for the largest fraction of CDOM and DOC export, the Ob' is an exception. We designate freshet as mid-May – June. However,

flow and DOM export remain very low until ice-break-up in late May or early June, in many years. Thus, the freshet season may be slightly shorter than either summer or fall. In most rivers considered here, the flashy nature of their hydrology means freshet still dominates export. However, the falling limb of seasonal discharge in the Ob' is much shallower than in most other rivers, resulting in roughly equal export from spring and summer before tapering dramatically in fall. The Ob' is also a unique case in that concentrations of CDOM do not show as consistent seasonality (Figure 3), despite some association between high discharge and high concentrations (Figure 4). Partially this may be driven by limitations in our remote sensing model, as we could only predict 33% of variation in CDOM calibration data from satellite reflectance. Additionally, the Ob' River contains the least permafrost of any river considered in this study [*Brown et al.,* 1998] as well as extensive peatlands storing water [*Smith et al.*, 2012] which temper the highly seasonal hydrograph that we might otherwise expect. Despite these possible issues, our model performs well against LOADEST in the Ob. Across all rivers, we were able to characterize the highly variable concentrations and fluxes of CDOM and DOC on multiple time scales.

4.2 Potential linkages between riverine CDOM and climate over a 30-year period

Recent studies have demonstrated that Arctic rivers transport ~35 Tg DOC annually, over roughly the past decade [*Raymond et al.*, 2007; *Holmes et al.*, 2012; *Kicklighter et al.*, 2013]. However, a lack of decadal scale biogeochemical data has limited our ability to detect whether regional warming has resulted in changes to organic matter export from rivers [*Macdonald et al.*, 2015]. Our results do not show consistent, widespread evidence of long-term changes in CDOM export, but do demonstrate some interesting climate-linked patterns over intermediate timeframes. CDOM flux in most of

the rivers is associated with extremes in the JFM Arctic Oscillation (AO) index (Figure 5). For instance, a strongly negative phase of the AO in 2010 is associated with low CDOM flux in the Kolyma, Lena, Mackenzie, and Yukon rivers, while a positive peak in the AO in 2002 corresponds to increased CDOM flux from the Kolyma, Mackenzie, and Ob' rivers. General increases in both CDOM export and AO from circa 2005 to 2007 are also apparent, consistent with previous studies [*Fichot et al.*, 2013]. As annual variations in discharge are a key driver in these calculations of flux, these associations corroborate existing literature linking Arctic river flow to global teleconnections such as the Pacific Decadal Oscillation [*Brabets and Walvoord*, 2009], the Arctic Oscillation, and the North Atlantic Oscillation [*Peterson et al.*, 2002].

Such variations in CDOM flux may be largely driven by discharge, but a key question remains: has the relationship between discharge and DOM loading changed through time, as a consequence of climate change? Such a change would indicate a fundamental shift in hydrological and biogeochemical cycling throughout the Arctic, likely as a consequence of ongoing climate change. What's more, any such changes in these major Arctic rivers would likely be associated with additional, possibly more dramatic, changes in headwaters streams and high-order rivers [*Spencer et al.*, 2015, *Tank et al.,* in review], as these smaller systems can be sensitive to local climatic changes and hotspots for organic matter processing [*Larouche et al.*, 2015; *Mann et al.*, 2015]. In the Ob' River, there is a potential increase in discharge-specific CDOM concentrations from the 1980s to 2000s (Figure 5). The vast West Siberian peatlands, which the Ob' River partially drains, are projected to export more DOM as temperatures warm and permafrost peatlands thaw [*Frey and Smith*, 2005]. In contrast, the nearby Yenisey River watershed encapsulates fewer and shallower peatlands [*Kremenetski et al.*, 2003; *Lehner and Doll*, 2004; *Vonk et al.*, 2015], and discharge-specific CDOM has decreased over

time (Figure 5). Such results are analogous to previous work in the Yukon River, where discharge-normalized DOC concentrations decreased from the 1970s to 2000s as a likely consequence of a deepening active layer allowing for groundwater to flow through mineral soils [*Striegl et al.*, 2005]. Indeed, Pokrovsky et al. [2015] predicted such a mechanism would become important even in permafrost peatlands in West Siberia. This previous work in Siberia has been dependent upon space-for-time substitutions, rather than direct measurements of organic matter through time [*Frey and Smith*, 2005; *Frey et al.*, 2007; *Pokrovsky et al.*, 2015], however, making ours the first empirical results that potentially verify such predictions.

No rivers presented here have shown statistically significant increases in CDOM flux over a thirty year period, despite rising discharge in many of these same systems[*Holmes et al.*, 2015]. Few studies have been able to demonstrate empirically changes in organic matter export over several decades in the Arctic. The Kuparuk River, on the North Slope of Alaska, is one of the most thoroughly studied Arctic rivers and one of the few sites with long-term, high quality biogeochemical data. Despite an increase in nitrate export, there has been little directional change in DOC export from the Kuparuk over the past 35+ years [*McClelland et al.*, 2007]. The Mackenzie River has also been routinely monitored since the 1970s, and is the most consistently observed by Landsat of any of our rivers since the 1980s. Tank et al. [in review] demonstrate a substantial increase in DOC concentration and flux over the course of several decades. Landsat-derived data do show increases through time of CDOM concentration in the Mackenzie River(Figure 3), although not as clearly as seen in measured data [*Tank et al.*, in review]. The limitations in using our binned-approached, as described in section 4.1, may be part of this. As well, our remote sensing model in the Mackenzie does not capture the full range of variability in CDOM concentration [*Griffin et al.,* in preparation].

5. SUMMARY AND IMPLICATIONS

Consistent, long-term monitoring of organic matter in rivers is essential for our understanding of the role climatic change will play in nutrient and organic matter cycling in the rapidly warming Arctic regions [*McClelland et al.*, 2008; *Macdonald et al.*, 2015]. Not only could changes in organic matter concentration and export reflect widespread functional changes to carbon balances on land, but fluxes of riverine organic matter may be important nutrient and energy subsidies to coastal food webs, linking terrestrial and marine ecosystems. In this study, we have demonstrated that satellite-derived CDOM concentrations can be used with discharge data to successfully estimate CDOM and DOC export across the Arctic. Over recent years, the highly seasonal nature of CDOM concentrations and fluxes corroborated previous research showing the importance of spring freshet for annual export from most rivers studied here. For the Mackenzie, Ob', and Yenisey rivers, we developed longer time series of CDOM concentration and fluxes, extending to the 1980s. CDOM concentrations increased through time in the Mackenzie River, but there is no evidence of a change in discharge-specific concentrations in this river. The Yenisey decreased in discharge-specific CDOM concentrations that may reflect an increase in proportional groundwater flow through mineral soils relative to organic-rich surface soils as a result of permafrost thaw [*Striegl et al.*, 2005; *Pokrovsky et al.*, 2015]. Such changes in organic matter concentration may have led to a decrease in CDOM export from the Yenisey, although these results must be interpreted conservatively given gaps in remote sensing data from the 1990s. In contrast, discharge-specific CDOM concentrations in the Ob' River may have increased, potentially reflecting organic matter release from thawing permafrost in peatlands [*Frey and Smith*, 2005; *Pokrovsky et al.*, 2015].

Remote sensing has proven to be a useful tool for monitoring of organic matter concentrations and fluxes in these major Arctic rivers. Given the high costs and difficult logistics of sampling these remote locations, spread across multiple continents, such an approach may become increasingly important. Furthermore, CDOM absorbance may be related to other biomarkers such as black carbon, spectral slope, or lignins [*Helms et al.*, 2008; *Fichot and Benner*, 2011; *Walker et al.*, 2013; *Stubbins et al.*, 2015; *Mann et al.*, 2016]. With the onset of new, more sensitive satellite sensors such as Landsat 8 and Sentinel 2, our confidence in such methods will increase, as will the frequency that these rivers may be observed. Future work may also more explicitly link land-sea couplings using remote sensing, as other researchers have been able to trace terrestrial organic matter within the Arctic Ocean using MODIS [*Belanger et al.*, 2008; *Fichot et al.*, 2013]. Our understanding of Arctic riverine DOM fluxes has improved a great deal over the past decade, however many questions still remain about the fate of this organic material as it moves through watersheds to the Arctic Ocean. Remote sensing offers a unique tool tracing riverine DOM through both space and time, particularly if future work explicitly links satellite data to on-the-ground measurements of DOM transformations.

Table 2.1. Average seasonal fluxes of CDOM and DOC for the six Arctic-GRO rivers, derived from remote sensing for 2001 – 2013. The ice-free season extends from May 15 – October 15. CDOM is in 10^9 m^2; DOC is in 10^9 g. Percentage of remote sensing derived estimates compared to LOADEST for the same time period are included in parentheses. Average seasonal concentration from 3 year intervals was combined with daily discharge data to calculate fluxes.

	Freshet		Summer		Fall		Ice Free Season	
CDOM								
Kolyma	415	(81)	188	(105)	111	(102)	714	(89)
Lena	3790	(77)	2170	(112)	1010	(100)	6970	(89)
Mackenzie	531	(78)	394	(109)	164	(69)	1090	(85)
Ob	1720	(99)	1800	(99)	662	(95)	4180	(98)
Yenisey	3660	(77)	968	(103)	609	(102)	5240	(83)
Yukon	753	(89)	450	(118)	223	(123)	1430	(101)
Sum	10900	(81)	5960	(106)	2780	(98)	19600	(90)
DOC								
Kolyma	329	(76)	175	(99)	108	(93)	613	(84)
Lena	2580	(85)	1590	(105)	797	(92)	4960	(92)
Mackenzie	486	(98)	410	(101)	191	(101)	1090	(100)
Ob	1220	(104)	1280	(98)	474	(93)	2980	(100)
Yenisey	2580	(102)	767	(105)	490	(109)	3840	(103)
Yukon	557	(90)	388	(115)	205	(113)	1150	(101)
Sum	7750	(93)	4610	(103)	2270	(98)	14630	(97)

Figure 2.1. The Arctic Ocean watershed, with each of the Arctic-GRO rivers delineated separately. Red dots are sampling locations.
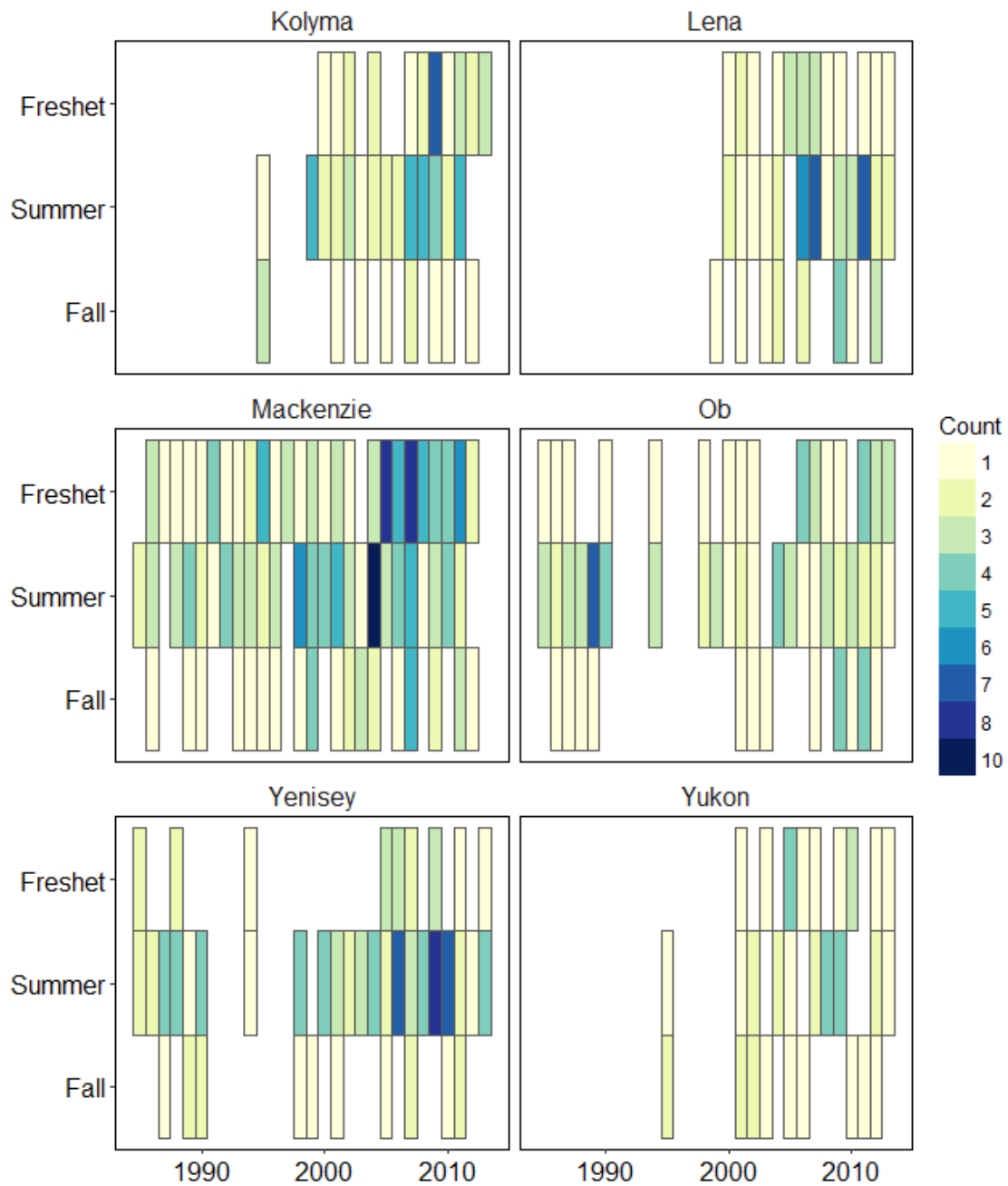
Figure 2.2. Heatmap of the Landsat imagery database used to develop time series of CDOM concentration and flux for each river. Rivers are split between freshet (May – June), summer (July – August), Fall (September – October).
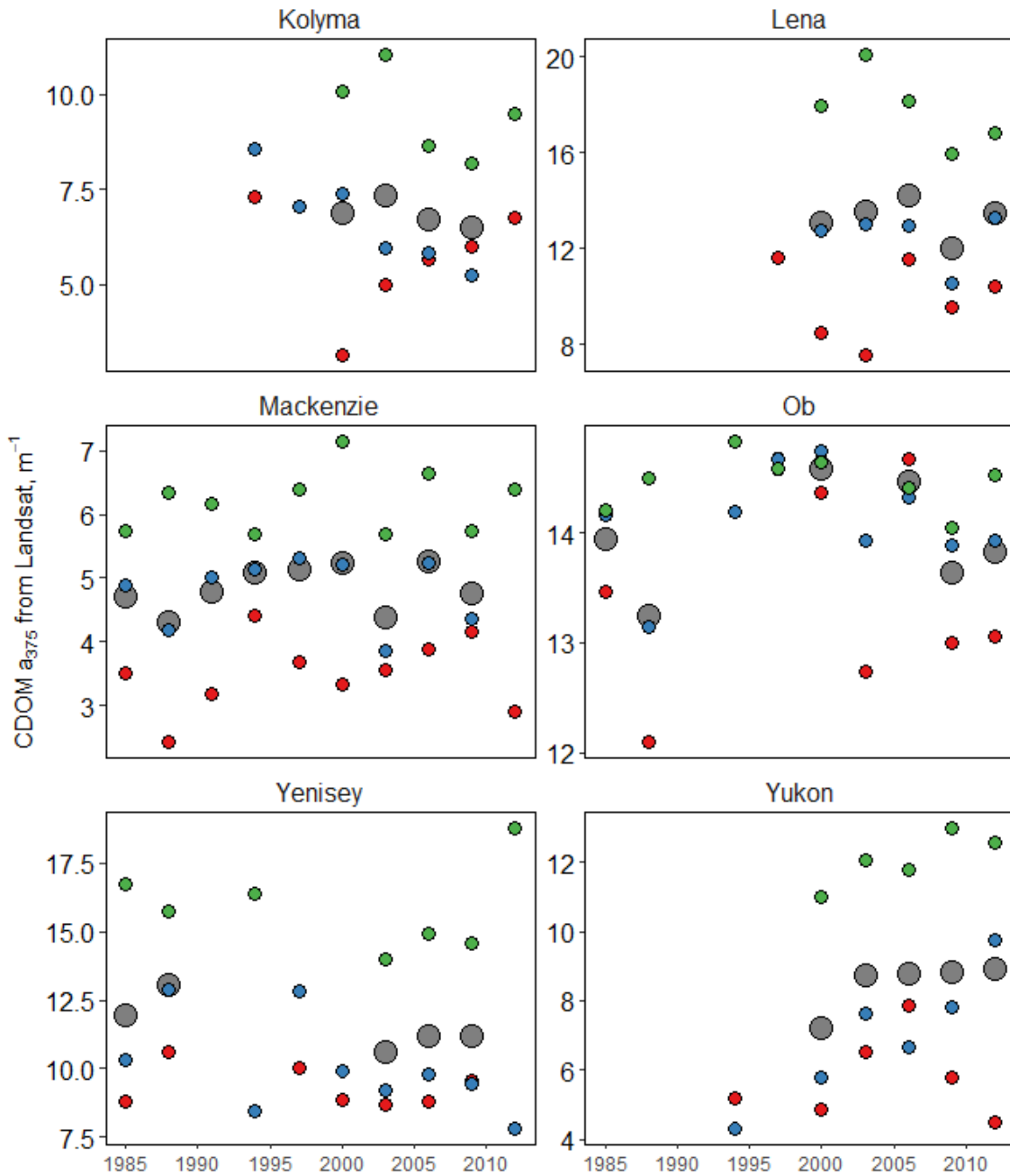
Figure 2.3.   Three-year average CDOM concentrations from Landsat for each river.
Seasonal means over each three year interval were averaged together to
calculate a mean concentration for the ice-free period. Points are plotted on
the first year of each 3-year period. Grey = ice-free average, Green =
freshet, Blue = summer, Red = fall.
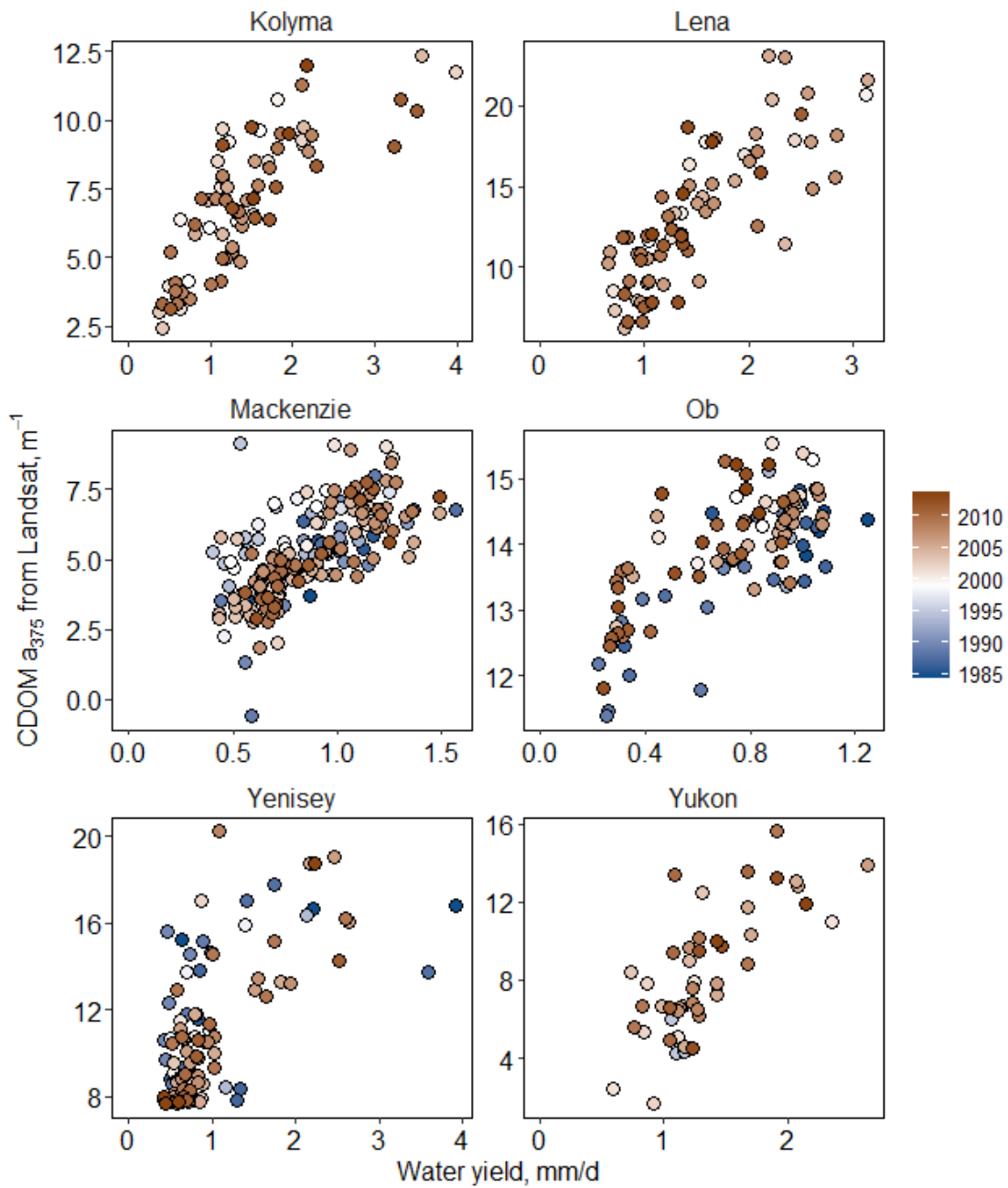
Figure 2.4.   All available concentrations of CDOM (m^{-1}) from Landsat versus water yield (mm/d).
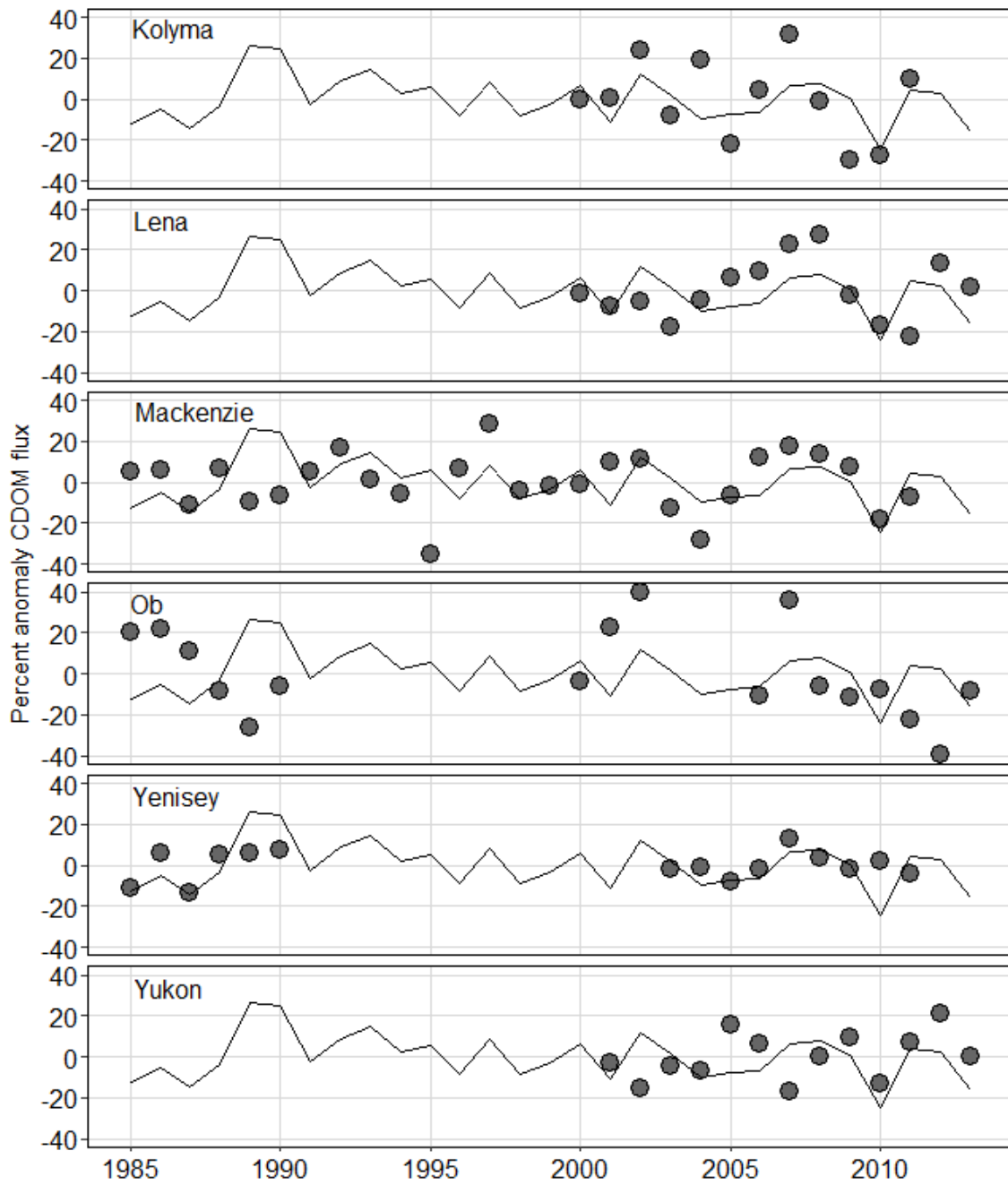
Figure 2.5. Time series of the percent anomaly in CDOM flux throughout the ice-free period for each year, relative to the 2001 – 2013 average for each river. The black line is the January-February-March average of the Arctic Oscillation Index.

74

Chapter Three: Chromophoric Dissolved Organic Matter in Cryopreserved Samples: Quantifying Changes after a Freeze-Thaw Cycle and Methods to Ameliorate Freezing Effects

ABSTRACT

Chromophoric dissolved organic matter (CDOM) absorbance has become a widely used measurement in studying natural waters as an inexpensive and analytically simple method to assess organic matter concentrations and composition. While generally it is acknowledged that CDOM samples should be analyzed as soon as possible after collection, remote field locations and a need to archive samples mean sometimes preservation is required. Filtered water is commonly stored frozen, and thawed at a later date for analyses. Using water samples collected from rivers in the Arctic and Texas, we assessed the impacts of a freeze/thaw cycle on CDOM measurements. Additionally, we tested whether sonifying, filtering, or a combination of the two could correct the effects of freezing on CDOM. We found that absorption at low wavelengths (e.g., 254 nm) changed relatively little after freezing for preservation, although some portion of samples may be notably more impacted. At longer wavelengths, such as absorption at 400 nm, freezing had a much larger impact. SUVA, a common proxy for aromaticity, remained relatively stable while a_{250}:a_{365} was more variable as it is dependent on absorption at a wavelength near the visible spectrum. Sonifying samples led to increases in percent difference relative to initial in the Mackenzie, Yukon, and Texas rivers. However, statistical corrections after sonifying performed better than simply freezing samples. The effects of both freezing and sonifying samples were more pronounced for samples with lower CDOM concentrations (e.g., $a_{400} < 5$ m^{-1}). Filtration had deleterious effects on CDOM after freezing. Overall, sonifying appears to improve the relationship between

fresh and preserved samples in some rivers but large differences between the rivers indicate that the approaches tested here do not universally improve results.

1. INTRODUCTION

Dissolved organic matter (DOM) is abundant throughout natural waters, coming from both allochthonous and autochthonous sources [*Morris et al.*, 1995; *Hedges et al.*, 1997]. The use of chromophic dissolved organic matter (CDOM), the light absorbing fraction of the DOM pool, to monitor DOM quantity and quality has proliferated in recent years, as an inexpensive and analytically simple alternative to more complex molecular techniques [*Dilling and Kaiser*, 2002; *Helms et al.*, 2008; *Murphy et al.*, 2010; *Spencer et al.*, 2012]. This is particularly useful in waters influenced by terrestrial inputs because DOM leached from vegetation and soils is often rich in CDOM [*Bertilsson and Tranvik*, 2000; *Murphy et al.*, 2008; *Osburn and Stedmon*, 2011]. Organic matter absorbance at specific wavelengths (e.g., 250, 350, and 400 nm) has proven to be a useful proxy for dissolved organic carbon (DOC) in many systems [*Del Castillo and Miller*, 2008; *Spencer et al.*, 2012; *Frey et al.*, 2016]. Additionally, ratios of specific wavelengths and spectral slopes have been used to approximate molecular qualities of DOM such as lignins, black carbon, and relative molecular weight [*Peuravuori and Pihlaja*, 1997; *Spencer and Aiken*, 2009; *Stubbins et al.*, 2012; *Walker et al.*, 2013; *Mann et al.*, 2016]. Specific ultraviolet absorbance (SUVA), often reported as absorbance at 254 nm normalized by DOC concentration, is widely used to approximate aromaticity and trace terrestrial materials [*Weishaar et al.*, 2003]. Water treatment plants have used CDOM to monitor DOC and the aromatic compounds that contribute to the formation of halogenated disinfectant byproducts (DBPs) [*Reckhow et al.*, 1990]. Furthermore, CDOM may be related to remote sensing reflectance, allowing for the mapping of CDOM and DOC across space and time where comprehensive field sampling may be difficult and expensive [*Mannino et al.*, 2008; *Matsuoka et al.*, 2012; *Brezonik et al.*, 2014; *Slonecker et al.*, 2016].

Despite its utility, storage of CDOM samples prior to analysis continues to pose problems. When possible, samples should be analyzed shortly after collection [*Spencer and Coble,* 2014]. However, it is not always feasible to analyze samples quickly when studying natural waters in remote locations. Preservations techniques include simply keeping samples cool, freezing samples, or acidifying samples [*Spencer et al.*, 2007; *Hudson et al.*, 2009; *Santos et al.*, 2010; *Tfaily et al.*, 2011]. Freezing DOM-rich samples can result in significant changes in both the quantity and quality of DOM [*Giesy and Briese*, 1978; *Fellman et al.*, 2008; *Yu et al.*, 2010; *Peacock et al.*, 2015; *Xue et al.*, 2015]. For instance, Fellman et al. [2008] reported as much as a 35% decrease in DOC concentrations after freezing samples from Alaskan streams. In contrast, CDOM in Venezuelan streams showed little change after freezing, with only 2.5% ± 6.9% change in absorbance at 350 nm (a_{350}) and -0.4% ± 1.5% in the spectral slope ratio S_r [*Yamashita et al.*, 2010]. Such results are supported by similar small changes through a freeze/thaw cycle from samples in a Congolese river which showed less than 2% change in a_{350}, SUVA, or S_r [*Spencer et al.*, 2010]. A few other studies support that optical properties of DOM may be preserved through freeze/thaw cycles, but the impacts of freezing can vary greatly [*Gao et al.*, 2010; *Spencer and Coble*, 2014]. Freeze/thaw cycles have caused statistically significant changes in a_{340} and SUVA from UK streams [*Spencer et al.*, 2007], fluorescent intensity of rainwater [*Santos et al.*, 2010], and unpredictable changes in DOM absorbance and fluorescence from peatlands that at times exceeded 233% for a_{365} [*Peacock et al.*, 2015]. Such changes may be attributable to flocculation and precipitation of humic material during the freezing process, which skew size-distributions of colloidal DOM and create particulates [*Giesy and Briese*, 1978; *Xue et al.*, 2015]. These changes in particle size may interfere with absorbance measurements by increasing backscatter [*Vodacek et al.*, 1994; *Ferrari and Dowell*, 1998; *Coble*, 2007]. Removing or

re-solubilizing particulates formed during freezing for bulk DOC analyses was shown to be at least partially effective in the 1970s [*Giesy and Briese*, 1978]. However, such practices have not been evaluated for optical properties that relate to DOM amount or composition. Here, we performed experiments to quantify the changes in CDOM absorbance through a freeze/thaw cycle using samples from river systems in the Arctic and Texas. Additionally, we assessed whether sonicating samples or additional filtration to correct flocculation could improve results, relative to initial measurements.

2. METHODS

We aimed to determine the impacts of freezing and subsequent processing of samples on CDOM absorbance across a broad range of freshwater streams and rivers. Samples were collected from multiple sites associated with concurrent projects in the Arctic and Texas. More specifically, experiments on the impacts of freezing and subsequent processing were performed on waters from three Arctic rivers (Mackenzie, Yukon, Kolyma) and four Texas rivers (Colorado, Guadalupe, Nueces, San Antonio). Further tests were done to examine the difference between frozen and sonified CDOM from archival samples collected as part of the Arctic Great Rivers Observatory (Arctic-GRO). These included additional samples from the Mackenzie, Yukon, and Kolyma as well as samples from the Yenisey, Ob', and Lena rivers. Collection and analysis of CDOM and DOC samples for each region are described below (Section 2.1). Experiments (described in section 2.2) determined the extent of freezing impacts on CDOM, and whether sonication, filtration, or a combination of the two could correct for changes post-thaw.

2.1 Data Collection and Analysis

2.1.1 Mackenzie and Yukon rivers

Surface water samples were collected from the lower Mackenzie and Yukon rivers in 2011 (May-June) and 2012 (June), respectively. Samples were collected on a daily basis from the main stem of each river, during and shortly after spring freshet when concentrations of CDOM and DOC change dramatically in conjunction with discharge [*Raymond et al.*, 2007; *Mann et al.*, 2016]. Additional samples were collected from large tributaries and other locations along the main stem of each river. From the Mackenzie, we also collected samples from smaller rivers and streams, and throughout the extensive delta.

Samples were collected in 1 or 2 L polycarbonate or HDPE bottles from ~0.5 meters depth, at least 2 meters away from shore. All samples were kept in the dark until processing within a few hours of collection. Water was filtered through 0.45 μm polyethersulfone filters into pre-cleaned, pre-rinsed 125 mL and 60 mL polycarbonate bottles. For DOC analyses, 60 mL bottles were frozen shipped to the Woods Hole Research Center (WHRC). 125 mL bottles were shipped frozen to the University of Texas at Austin Marine Science Institute (UTMSI) for experimental analyses. Additional water was filtered at 0.45 μm for immediate CDOM analysis. DOC was analyzed using a Shimadzu TOC-V organic carbon analyzer at WHRC. All CDOM analyses were performed using an Ocean Optics ChemUSB 4000 at room temperature with a 1 cm quartz cuvette. Absorbance was converted to absorption coefficients using Equation 1:

$$a(\lambda) = 2.303 A(\lambda)/l \ (1)$$

where $a(\lambda)$ is the absorption coefficient at a given wavelength, $A(\lambda)$ is the absorbance at a given wavelength and l is the path length in meters [*Hu et al.*, 2002].

2.1.2 Texas Rivers

Water samples were collected from the Colorado, Guadalupe, Nueces, and San Antonio rivers in summer of 2012. Sampling included baseflow and flood conditions. Water was collected using a Van Dorn sampler lowered from a bridge into the mid-points of each river, to a depth of ~0.5 meters. Water was stored in the dark on ice in 2 L polycarbonate bottles until processing within 12 hours. Water was filtered through 0.7 GF/F µm Whatman filters, and stored frozen in 125 mL and 60 mL polycarbonate bottles. Additional water was filtered for immediate CDOM analyses. CDOM from Texas rivers were analyzed at UTMSI with a Cary50 UV-VIS spectrometer at room temperature using a 1 cm quartz cuvette. DOC was analyzed using a Shimadzu TOC-V organic carbon analyzer, also at UTMSI. Absorbance was converted to absorption coefficients with Equation 1.

2.1.3 Kolyma River

Water samples from the lower Kolyma River basin in Northeastern Siberia were collected in June and July 2013. We sampled the main stem at multiple locations at different times, with additional samples from both major tributaries and smaller streams. Water was collected in 1-2 L polycarbonate bottles at ~0.5 m depth or less. Some streams were less than 0.5 meters deep, in which case water was collected from approximately mid-depth of the stream. Samples were stored in the dark until processing. Water was filtered using GeoTech 0.45 µm polyethersulfone capsule filters. Samples for CDOM analyses were frozen in 125 mL polycarbonate bottles for experiments, or analyzed immediately. DOC samples were stored at 4°C in ashed 20 mL glass vials and acidified to pH 2 until analyzed. CDOM samples were analyzed at the Northeast Science Science Station (NESS) with a Shimadzu UV-Vis spectrometer using a

1 cm quartz cuvette. Absorbance was converted to absorption coefficients with Equation 1. DOC was analyzed at NESS with a Shimadzu TOC-V organic carbon analyzer.

2.1.4 Arctic Great Rivers Observatory

Previous publications provide details about Arctic-GRO sampling of the Yenisey, Ob', Lena, Kolyma, Yukon, and Mackenzie rivers [*Holmes et al.*, 2012]. Briefly, cross-sectional, depth-integrated samples were collected across the seasonal hydrograph of each river. Water was filtered using 0.45 µm GeoTech capsule filters, and shipped frozen to the WHRC. CDOM was analyzed using a Shimadzu UV-Vis spectrometer with a 1 cm quartz cuvette and DOC with a Shimadzu TOC-V organic carbon analyzer, both at WHRC. Full absorbance scans from samples from 2009 – 2014 are available from the Arctic-GRO website (www.arcticgreatrivers.org). We also re-analyzed CDOM from a subsample of the Arctic-GRO dataset, including samples from each river collected during spring and summer 2009 - 2011, after the samples had been sonicated.

2.2 Experimental Design

Although literature exists describing the impacts freezing water for preservation has on CDOM absorbance, we aimed to test methods for correcting these effects through either sonication or additional filtration after one freeze/thaw cycle (Table 1). Unless otherwise specified, references to Mackenzie, Yukon, and Kolyma samples denote samples collected in 2011, 2012, and 2013 (respectively) for the full suite of freeze/thaw experiments. Arctic-GRO samples refer to the archived frozen samples, as described in section 2.1.4. Samples from the Mackenzie, Yukon, and Texas rivers were stored frozen for 3-4 months. Kolyma River samples were frozen for one week before thawing. Arctic-GRO samples were stored frozen for 2-4 years before being thawed, sonified, and

re-analyzed. Frozen samples (stored in 125 mL polycarbonate bottles) were thawed slowly in a refrigerator over the course of 2-3 days, then allowed to warm to room temperature before further analysis. Experimental design is summarized in Table 1. We measured each sample after thawing (T1), then tested whether sonication with a sonifying probe (T2a) or sonic bath (T2b), filtration (T3), filtration followed by sonication with a probe or bath (T4a and T4b, respectively), and sonication with a probe or bath followed by filtration (T5a and T5b). Aliquots were separated into 15 mL polypropylene conical centrifuge tubes. Samples from the Mackenzie, Yukon, and Texas rivers were sonified with a Branson 250 Sonifier at 10% amplitude for 20 seconds with a 1/8 inch microtip at UTMSI. Arctic-GRO samples were sonified with a Misonix Microson XL 2000, also at 10% amplitude for 20 seconds with a 1/8 inch microtip, at the Marine Biological Laboratory in Woods Hole, MA in 2013. Owing to logistical restraints, we used a Elmasonic S40 sonic bath rather than a sonifying probe at NESS for Kolyma samples. We submerged 15 mL tubes with sample water into the sonic bath at 40 kHz for 3 minutes. We re-filtered samples using handheld syringes and filter holder tips. Kolyma, Mackenzie, and Yukon samples were re-filtered with 0.45 µm polyethersulfone filters, to correspond with original filter size and type. Texas river samples were re-filtered through 0.7 µm Whatman GF/F filters.

Statistics were performed using R software. We assessed absorption coefficients at 254 nm and 400 nm as common indicators for bulk DOM concentrations in natural waters [*Spencer et al.*, 2012; *Frey et al.*, 2016]. In particular, wavelengths in the UV-A and visible spectrum (350-440 nm) are frequently used to calibrate remote sensing models [*Menken et al.*, 2006; *Belanger et al.*, 2008; *Matsuoka et al.*, 2012; *Xie et al.*, 2012]. Thus, even though absorbance in the UV-C spectrum (200-280 nm) often correlates more strongly with DOC concentrations, it is important to understand

preservation effects on these longer wavelengths. We also calculated $a_{250}:a_{365}$ and SUVA, as indicators of molecular weight and aromaticity [*Peuravuori and Pihlaja*, 1997; *Weishaar et al.*, 2003]. SUVA was calculated as absorbance, A(254), normalized by DOC concentration. It should be noted that although we evaluated the impacts of freezing on CDOM concentrations, all DOC analyses were performed on frozen samples with no further treatment.

3. RESULTS AND DISCUSSION

Results by river are summarized in Table 2 and 3, showing the percent differences and regression statistics for each treatment relative to initial for a_{254}, a_{400}, $a_{250}:a_{365}$, and SUVA$_{254}$. Average percent differences were calculated using the absolute difference between initial and post-treatment CDOM measurements. Data from the Kolyma, Mackenzie, Yukon, and Texas rivers are also presented by treatment as scatterplots in Figures 1-4, and percent difference for T1 and T2 relative to initial CDOM measurement in Figures 5-6. Results from the Arctic-GRO data showing the difference between frozen and sonicated CDOM are shown in Figure 7.

3.1. Impacts of freezing on CDOM

Absorption at 254 nm (a_{254}) remained the most stable over the course a freeze/thaw cycle, of any parameter presented here. In the Mackenzie and Yukon rivers, a_{254} changes relatively little between initial measurements and freezing, only 6-7% on average (Figure 1a; Table 2). Indeed, there was no significant difference in a_{254} post-freezing in the Mackenzie River samples. The largest absolute difference for an individual sample came from a small, DOC-rich stream in the Mackenzie basin, which decreased from 156 m^{-1} to 129 m^{-1} (Figure 5a). A sample collected from a channel in the Mackenzie basin while still ice-covered showed the largest percentage change, with a_{254}

84

increasing 41% from 18 m^{-1} to 26 m^{-1} (Table 2; Figure 5). Absorbance in such samples with relatively little color may be particularly sensitive to backscatter from flocculants formed during freezing, or prone to error being near the limits of detection. All but 5 samples from the Mackenzie and Yukon rivers were within 15% of initial a_{254} after a freeze-thaw cycle (Table 2; Figure 5a). Samples from Texas rivers differed the most between pre- and post- freezing in terms of percent difference (Figure 1a and 5a; Table 2). The samples with highest a_{254} from Texas rivers tend to be the most underestimated after freezing, with up to 43% loss from one sample collected during a flood event on the Guadalupe River, while low DOM samples tended to be overestimated (Figure 5a). The Kolyma River samples, which were stored frozen for only one week, showed almost no change overall to a_{254}, although two samples increased by 10-12 m^{-1} and another showed loss of 15 m^{-1}(Figure 1a). These divergent samples were from separate rivers or streams within the Kolyma basin, and none were amongst the highest or lowest concentrations from the dataset. Initial and T1 (Table 1) a_{254} were generally very tightly correlated overall, with little loss from the Mackenzie, Yukon or Kolyma rivers (Table 3). In Texas rivers, however, while a_{254} were tightly correlated, there was significant bias of greater loss from samples with higher a_{254} (Figure 5a).

Variability increased markedly for a_{400} relative to a_{254} in all rivers. In the Mackenzie River, average difference increased to 70%, with some samples increasing as much as six-fold (Table 2; Figure 5b). However, the most dramatic increases post-freeze were associated with under-ice samples, which are characterized by low DOC (1-2.5 mg/L C) and absorbance. The highest percent differences tended to be at low concentrations in the Mackenzie. Average difference after freezing for samples less than 10 m^{-1} initially was 115%, while samples above 10 m^{1} were 46% different after preservation (Figure 5b). Indeed, there was an overall offset of 7 m^{-1} between initial and

85

frozen a_{400} in the Mackenzie, causing a disproportionate impact on low CDOM samples (Figure 1b). Yukon River samples did not change as dramatically in a_{400} as in the Mackenzie River, with an average difference of 21% (Table 2). Also in contrast, a_{400} was underestimated in all but two samples, and there was no relation between CDOM concentration and percent difference (Figure 5b). The Yukon River showed an R^2 of 60% between initial and post-freeze samples (Table 3). In Texas Rivers, samples with CDOM absorbance initially over 10 m^{-1} were underestimated by 26% – 45% (Table 2). This underestimation of absorbance at high wavelengths in Texas rivers is common at both 254 and 400 nm. Texas samples with initial a_{400} below 3 m^{-1} were overestimated by 128 – 188% after freezing. Similar to Mackenzie samples with a_{400} below 10 m^{-1}, these samples with initial low absorbance may undergo the most relative impacts from particulates created during a freeze-thaw cycle. In all three of these river systems, R^2 between initial and frozen samples decreased to 59-76% for absorbance 400 nm, respectively, more variable impacts of freezing at longer wavelengths (Table 3). In contrast, absorbance at visible wavelengths did not vary as dramatically in the Kolyma as in these other, systems (Table 3; Figure 1b). Only three samples were significantly different in a_{400} after freezing, the same samples that also showed the greatest difference in a_{254}.

The spectral ratio $a_{250}:a_{365}$ is altered by freezing more so than a_{254}, reflecting the increased variability in CDOM absorption at longer wavelengths post-thaw (Figure 1c; Table 2). In the Mackenzie, $a_{250}:a_{365}$ is underestimated in nearly all samples, with average difference of 28% between pre- and post- preservation and decreasing percent difference as $a_{250}:a_{365}$ increases. Under-ice samples again prove to be the most variable between initial and frozen treatments in the Mackenzie. Yukon and Texas $a_{250}:a_{365}$ tend to be overestimated with average differences of 9% and 30 %, respectively. Average

percent difference was low from the Yukon River, and ranged from 21.9% to -4.4%. Although there is a significant relationship between initial and thawed a_{250}:a_{365} in the Kolyma and Yukon, R^2 is 31% - 39% and slopes are both 0.56 (Table 2; Figure 1b). In Mackenzie and Texas samples, there is no significant relationship between original and frozen spectral ratios (Table 2). The weak relationship in regressions between initial and thawed samples is driven by the relative lack of variability within the spectral ratio, in part. Across rivers, a_{250}:a_{365} only ranged from 3.1 to 7.5, with only two under-ice Mackenzie samples exceeding 6.5. In the Mackenzie, Texas, and Yukon rivers, percent difference decreased with increasing a_{250}:a_{365}. SUVA, a good proxy for aromaticity, shows more robust preservation after freezing than a_{250}:a_{365}, when anomalously high samples are excluded. Very high SUVA values, in excess of 5.5 L mg-C^{-1} m^{-1}, are uncommon in natural waters, and often more indicative of other dissolved material such as Iron(III) and nitrate [*Weishaar et al.*, 2003; *Poulin et al.*, 2014]. Only one under-ice sample in the Mackenzie exceeds this threshold. In Texas rivers, several SUVA samples collected during flood conditions and one during baseflow from the Guadalupe and San Antonio rivers also exceed 5.5 (Figure 1d). A Guadalupe sample collected at baseflow has the lowest absorption of any Texas sample and low nitrate concentrations, indicating either influence from iron or possible issues measuring CDOM near detection limits. Other Texas samples with anomalously high SUVA values are characterized by high CDOM and low nitrate, raising the likelihood of iron interfering with CDOM measurements. These excessively high values also deviate the most from initial measurements after a freeze-thaw cycle. Samples with initial values ranging from 6.0 to 12.7 L mg-C^{-1} m^{-1} are thus excluded from regression statistics (Table 3).

We did not test changes in DOC concentrations through a freeze-thaw cycle, instead using the same DOC data to calculate SUVA$_{254}$ for all treatments. Thus, percent

differences are the same for SUVA and a_{254} (Table 2). While regression statistics show SUVA in the Mackenzie has the greatest change (Table 3), each individual sample does not vary greatly post-preservation, with an average percent difference of 7.3%, excluding under-ice samples. Initial SUVA only varies between 2.4 and 4.0 L mg-C^{-1} m^{-1}, with most samples clustered between 2.9 and 3.2 L mg-C^{-1} m^{-1} in the Mackenzie (Figure 1d). Yukon River samples differ between initial and frozen samples by 6% on average, with no samples exceeding 5.5 L mg-C^{-1} m^{-1}. SUVA in the Yukon initially measured between 3.9 – 5.0 L mg-C^{-1} m^{-1}, while post-freezing samples were underestimated with a range of 3.6 – 4.8 L mg-C^{-1} m^{-1}, showing a slight decrease in concentrations. Texas river samples varied by 21% on average, with samples above initial 6.0 L mg-C^{-1} m^{-1} excluded. When high-SUVA samples were included, variance increased to 31%. Kolyma SUVA values varied the least, on average only by 5.0% (Table 2; Figure 1d). It seems to be common for aromatic-rich samples to be relatively more stable throughout a freeze-thaw cycle than other types of DOM [*Hudson et al.*, 2009; *Peacock et al.*, 2015], although Spencer et al. [2007] found no such pattern. It is difficult to determine whether our own data support this conclusion, as many samples with SUVA above 4.5 mg-C^{-1} m^{-1} were possibly influenced by high Fe(III) concentrations.

The unpredictable differences we observed in absorbance over the course of a freeze-thaw cycle are consistent with other recent studies [*Otero et al.*, 2007; *Spencer et al.*, 2007; *Hudson et al.*, 2009; *Peacock et al.*, 2015]. The increases in absorbance at 400nm in the Mackenzie River are particularly striking in our study, but are corroborated by work in peatlands that also show consistent increases in absorbance at wavelengths greater than 365 nm [*Peacock et al.*, 2015]. CDOM in UK streams also showed occasional increases in a_{340} after freezing, although loss was more common [*Spencer et al.*, 2007]. DOC and CDOM are partitioned during the freezing process, as humic

material is preferentially excluded from ice during the freezing process [*Xue et al.*, 2015]. As such, the original composition of the DOM is likely a determining factor in how much and in what way DOM is lost or transformed during the freezing process.

Our data cover a broad range of systems, using multiple analytical techniques based on what equipment was available in sometimes-remote locations. Thus, the impacts of freeze-thaw presented here may be in part attributable to differences in equipment, as inter-laboratory comparisons have shown substantial differences in optical measurements even using the same methods [*Murphy et al.*, 2010]. A more careful assessment of the same CDOM samples on multiple different instruments would be needed to fully address this possibility, however.

Time frozen may also be a consideration, as samples from Mackenzie, Texas, and Yukon systems were stored for 3-4 months while Kolyma samples were in the freezer for one week. Using water from the Kolyma river, we measured CDOM in three samples after one week, two weeks, three weeks, 1 month and 2 months frozen. This was a small dataset, of three samples, however, and change was low and random – less than 10%, with no clear indication of a time effect. Santos et al. [2010] found that storage time had an impact of the fluorescence of rainwater, however, as fluorescence intensity dropped at wavelengths less than 300 nm on a weekly basis up to four weeks after initial freeze. Aromatic DOM fractions and SUVA also changed as a function of freezer time in a study by Chen at al [2015], although these measurements were more stable than fluorescence peaks.

Other factors may also be important in determining whether CDOM alters significantly after freezing. For instance, our samples from Texas rivers tended to have less predictable responses to freezing than Arctic samples (Figure 1; Table 3). Although DOM within Arctic rivers may only have recently been leached out of terrestrial soils and

vegetation, it is likely that the source organic matter has undergone natural freeze-thaw cycles of long duration, and possibly multiple times. Cell lysis, one proposed mechanism for changes in CDOM during freezing [*Hudson et al.*, 2009; *Xue et al.*, 2015], would thus already have occurred in much of the Arctic DOM. CDOM exclusion and transformation during ice formation has been demonstrated in both lake ice and sea ice, indicating that some of the processes seen during preservation may also occur in natural waters [*Belzile et al.*, 2002; *Müller et al.*, 2011, 2013]. Organic matter in Texas, even before becoming mobilized and solubilized, most likely rarely experienced freezing conditions [*Jiang and Yang*, 2012]. However, several studies at tropical latitudes saw little change in CDOM after freezing, indicating that processes driven by freezing in natural environments is not a consistent factor in preservation effects [*Spencer et al.*, 2010; *Yamashita et al.*, 2010].

3.2. Correcting CDOM absorbance after freezing through sonication and filtering

Of the treatments we tested to determine whether the impacts of freezing samples could be corrected, no method consistently resulted in a stronger relationship between initial and post-treatment CDOM measurements across all rivers (Figures 2-4, Table 3). Sonication resulted in roughly equal or higher R^2 between initial and treatment values for a_{254} and a_{400} in all river systems (Table 3), indicating that with sufficient testing sonication may be an effective way to correct for freezing at specific wavelengths. However, this did not consistently hold true for spectral ratio or SUVA, and was accompanied by offsets that would require a statistical correction post-treatment. Although in a few cases, filtration improved results (e.g., a_{400} in Texas rivers), more often R^2 declined and CDOM parameters were underestimated when filtration was included at any step post-thaw (Figure 3 and 4).

90

After sonifying, a_{254} remained largely unchanged or improved in R^2, with average difference decreasing to 6% in Mackenzie watershed samples (Table 2). However, Mackenzie a_{400} remained well above initial measurements (Figure 6b). Yukon samples were somewhat more adversely affected by sonication, as percent difference increased at both a_{254} and a_{400}. Samples with initially low CDOM in the Yukon tended to be more greatly impacted by sonication. These samples, originating from the Andreafsky River within the Yukon watershed, are also characterized by low initial SUVA and high sprectral slope. Such measurements indicate DOM from this tributary is relatively low in both aromaticity and molecular weight. Other studies have demonstrated that low aromatic DOM is less consistently preserved through the freezing process. It may also be that these low-aromaticity DOM samples are more greatly impacted by sonication, as high energy sonication may lead to dispersion of the original organic molecules [*Kaiser and Asefaw Berhe*, 2014]. Indeed, while a_{254} differed by 22 – 29% from these three low-DOM samples in the Yukon, all other samples varied within 0.3 – 15% after sonication (Figure 2a). Within Texas rivers, sonifying samples resulted in no significant difference between initial and post-treatment measurements for all CDOM parameters examined here (Table 2). Sonified Texas samples differed in percent from initial samples by 15% for a_{254}, although one sample also associated with very high SUVA increased by 76% after sonifying (Figure 6b). Average difference in SUVA dropped from 8% to 6% in the Mackenzie, and from 21% to 15% in Texas rivers after sonifying. Yukon basin samples increased in average difference from 6% to 16%, with the increase once again driven by low DOM samples from the Andreafsky River. However, a_{250}:a_{365} did not improve consistently in most cases after sonifying (Figure 2c). Although results from Texas rivers shift from being over-estimated to underestimated relative to initial a_{250}:a_{365}, most systems show no noticeable improvement in a_{250}:a_{365} after sonifying (Table 2; Table 3).

Within Mackenzie and Texas river samples, the inverse relationship between initial $a_{250}{:}a_{365}$ and percent difference after freezing was removed post-sonication (Figure 6c). Within both the Mackenzie and Yukon river systems, sonifying samples resulted in significant differences between initial and post-treatment CDOM, likely as an effect from the offsets seen across all wavelengths (Table 2). Kolyma samples were sonicated in a bath, rather than with a sonifying probe. Kolyma river samples showed very little difference in a_{254} or a_{400} after freezing, except in three samples. Overall, sonication resulted in no significant differences between initial and post-treatment CDOM in the Kolyma, improving results over simply using thawed samples without any further manipulation (Table 2). Although sonifying did not change a_{254} for one of these samples, the other two samples significantly improved from $10 - 15\%$ different, to $1 - 2.5\%$ different from initial measurements (Figure 6a). Similarly, a_{400} improved in five samples differing from initial by 15-35%, to $2.8 - 12\%$ within the Kolyma. SUVA also improved marginally in Kolyma samples, from 5.1% to 3.7%.

Although sonifying (Figure 2) resulted in some improvements in the relationship between initial and post-treatment CDOM, we also present results from filtration (Figure 3), filtration followed by sonifying (Figure 4), and sonifying followed by filtration (not shown; Table 2 and 3). We did not perform sonifying followed by filtration on Mackenzie samples. In most cases, including a filtration step at any point led to further underestimations of CDOM absorbance, spectral ratio, and SUVA (Figures 3 and 4; Table 3). While filtration did correct for some of the elevated a_{400} values in Mackenzie samples, R^2 decreased, as did slope (Table 3). The spectral ratio $a_{250}{:}a_{365}$ remained unpredictable after freezing, no matter which treatment was applied, in Mackenzie, Yukon, and Texas samples (Table 3). In the Kolyma, filtration increased variance slightly for a_{254}, a_{400}, and SUVA, compared to sonified samples (Figure 3; Table 2). Of

92

these treatments that included filtration, sonifying followed by filtration yielded the most improved results relative to initial measurements (Table 2).

Although many samples remained within 15% of original measurements after freezing, particularly at lower wavelengths, sonifying samples improved or had little impact on the relationship between initial and post-treatment CDOM at specific wavelengths (e.g., 254 and 400 nm) for all rivers (Figure 2). However, these were accompanied by offsets in absorption in the Mackenzie, and Yukon rivers that increased percent difference. Few studies address the exact impacts of sonication on DOM at a molecular level, but it has been used to break organic aggregates in soils and improve bulk DOC analyses after freezing [*Giesy and Briese*, 1978; *Kaiser and Asefaw Berhe*, 2014]. Assuming that aggregation and flocculation is a major contributor to the changes in CDOM seen after freezing, sonication would thus help to disrupt these new particles. The Mackenzie is however, shows the largest increases in percent differences after sonifying in the majority of samples. Sonifying made results more predictable. In cases like the Mackenzie, it may be possible to develop a statistical correction, as a_{400} was offset from initial measurements by a more uniform amount after being sonified than either post-thaw or when filtration was included. It is also possible that longer sonication times would improve results further. We limited sonifying with a probe to only 20 seconds, as experiments were performed with small volumes of water. High power or long exposure to a sonifying probe may result in the disruption of organic molecules that were originally within DOM before freezing, in addition to newly formed aggregates [*Kaiser and Asefaw Berhe*, 2014]. Thus more work is required to determine the optimum length of sonication for differing DOM samples.

Filtration after freezing, on the other hand, may remove newly formed particulates. While this would correct for backscatter issues, as seen in Mackenzie

samples where average percent difference in a_{400} decreased after filtration (Table 2; Figure 3), possibly substantial portions of CDOM may be removed through this process. Indeed, while conducting these experiments, filters often appeared yellow and clogged after filtration of just 20 – 30 mL from Mackenzie and Yukon samples. Although we did not test bulk DOC concentrations after filtration, we may presume that such removal led to a decrease in total organic carbon within samples. Given that transformations during freezing are likely tied to the original composition of DOM [*Hudson et al.*, 2009; *Xue et al.*, 2015], this may mean not only a loss in total organic matter, but a preferential loss of certain types of material.

3.3. Sonification impacts on CDOM from archival data in major Arctic rivers

Having found that sonifying frozen CDOM samples can improve results for specific wavelengths when DOM concentrations are relatively high, as in above experiments from the Kolyma and Texas rivers, we applied this method to archived water samples from the Arctic-GRO (Figure 7, Table 4 and 5). Unfortunately, owing to the remote locations these samples were collected from, no data exists on initial CDOM spectra. In general, a_{254} decreased after sonifying, SUVA increased, and a_{400} showed no consistent pattern. Despite a few samples that did shift drastically after sonifying, only six samples out of 34 showed more than 20% change between the two treatments for a_{254} and SUVA. These more variable samples came from the Kolyma, Mackenzie, and Yukon rivers. Average percentage differences between frozen and frozen/sonified samples for a_{254}, a_{400}, and SUVA were all ~17%, while $a_{250}{:}a_{365}$ differed by 11% (Table 4; Figure 7). Siberian rivers (Kolyma, Lena, Ob', and Yenisey) tended to be less effected by sonication than North American rivers (Mackenzie and Yukon). Sonifying had the largest relative impacts on samples with low-CDOM (Figure 7). For instance, a_{254} for

samples below 50 m^{-1} after freezing averaged a 30% difference between frozen and sonifying treatments (T1 versus T2). However, this average difference was only 9% for samples above 50 m^{-1} at 254 nm. Most of these low CDOM samples originated from the Mackenzie and Yukon rivers within the Arctic-GRO database. Absorption at 400 nm confirms these results, with sonication resulting in a 32% average change in samples with a_{400} less than 5 m^{-1} after freezing versus 10% difference in higher CDOM concentration samples (Figure 5b). These results are similar to above experiments comparing initial versus sonified absorption from Mackenzie and Yukon samples (section 3.2), where sonication had the most varied impacts in samples with low CDOM concentrations. However, the Arctic-GRO data differs in that these more variable results after sonication were not necessarily associated with low SUVA. Indeed, the three samples which showed the lowest CDOM concentrations after freezing were also associated with the highest SUVA values (5.9 – 8.5 mg-C^{-1} m^{-1}) of any Arctic-GRO samples analyzed for this study. Sonication reduced SUVA in these samples to 3.6 – 4.8 mg-C^{-1} m^{-1}. While it is impossible to say whether these results are more realistic, given the lack of available data from samples that were not impacted by freezing, these lower SUVA results post-sonication more closely match previous studies of SUVA in Mackenzie and Yukon watersheds [*Spencer et al.*, 2008; *Spencer and Aiken*, 2009; *Tank et al.*, 2011]. Despite these results in samples with low CDOM concentrations, Arctic-GRO samples are typically only altered by 10-15% as a result of sonication.

4. CONCLUSIONS: HOW SHOULD CDOM SAMPLES BE TREATED?

When at all possible, CDOM samples should be analyzed immediately. Previous work has shown that even in DOM-rich porewaters, it may be preferable to store samples cool, in the dark for a number of days rather than freeze samples [*Peacock et al.*, 2015].

The freezing process preferentially concentrates material in un-frozen water as ice forms, possibly leading to interactions between molecules and even formation of additional humic material [*Xue et al.*, 2015]. Our results show that this process is unpredictable. While CDOM may often remain stable through a freeze/thaw cycle, some percentage of samples will be significantly impacted. CDOM absorbance may increase or decrease by a large margin within a given sample, although most samples show a small amount of CDOM loss in the UV wavelengths. Absorption tends to be most resilient to freezing at short UV wavelengths, which may be why studies relating $S_{275-295}$ and SUVA to other environmental variables still show significant patterns despite samples being stored frozen [*Yamashita et al.*, 2010; *Stedmon et al.*, 2011; *Walker et al.*, 2013]. At longer, visible wavelengths CDOM appears more prone to variation from initial measurements, possibly as a consequence of new flocculants creating backscatter. However, this is an unpredictable pattern, with CDOM from the Kolyma watershed changing relatively little at 400 nm, while Mackenzie samples are notably overestimated compared to initial values. Thus, researchers must anticipate that their results will be accompanied by added uncertainty when using frozen samples to quantify optical properties at longer wavelengths. Although filtration did sometimes improve results, a substantial portion of the organic matter that had precipitated may have been removed. Sonifying, in contrast, either improved results or made little change in most samples, where a_{400} exceeded 5 m^{-1}. However, in samples containing lower amounts of CDOM, both freezing and sonication often resulted in large percentage errors that could not be corrected through statistics. Sonifying samples likely broke apart conglomerations or flocculants that formed during freezing, leaving the sample a closer approximation of its original composition. If freezing samples is unavoidable, sonifying before CDOM analyses may be effective at correcting at least a portion of the impacts of freezing. These results are highly river-

96

specific, however. If cryopreservation is unavoidable, researchers must carefully test the effects of both freezing and sonication to have confidence in CDOM measurements.

Table 3.1. Treatments using frozen waters samples were applied to Kolyma, Mackenzie, Texas, and Yukon datasets for comparison against initial measurements. We also compared T1 (frozen) samples with T2a (frozen and sonicated with a probe) to Arctic-GRO samples.

Treatment	Description	Datasets
I	Measured within hours of sample collection	Kolyma, Mackenzie, Yukon, and Texas
T1	Frozen and later thawed	Arctic-GRO, Kolyma, Mackenzie, Yukon, and Texas
T2a	Frozen, then thawed and sonicated with a probe	Arctic-GRO, Mackenzie, Yukon, and Texas
T2b	Frozen, then thawed and sonicated in a bath	Kolyma
T3	Frozen, then thawed and re-filtered	Kolyma, Mackenzie, Yukon, Texas
T4a	Frozen, thawed, re-filtered and sonicated with a probe	Mackenzie, Yukon, and Texas
T4b	Frozen, thawed, re-filtered and sonicated in a bath	Kolyma
T5a	Frozen, thawed, sonicated with a probe, and re-filtered	Mackenzie, Yukon, and Texas
T5b	Frozen, thawed, sonicated in a bath, and re-filtered	Kolyma

Table 3.2. Average, minimum, and maximum percent differences between treatments and initial CDOM. Average percent differences are calculated using absolute values of differences. P-values are for a paired t-test between initial and treated CDOM measurements before calculation of percentages.

River System		Treatment	p-value	Average (%)	Min (%)	Max (%)
Mackenzie	a_{254}	T1	0.061	7.3	-17.6	40.8
		T2a	0.001	6.5	-14.3	35.3
		T3	<0.001	12.0	-82.0	36.2
		T4a	<0.001	8.0	-29.0	35.8
	a_{400}	T1	<0.001	69.6	-6.5	643.4
		T2a	<0.001	93.5	11.6	525.5
		T3	<0.001	62.4	-68.7	526.8
		T4a	<0.001	58.6	-42.7	480.2
	$a_{250}{:}a_{365}$	T1	<0.001	28.0	-71.1	-2.9
		T2a	<0.001	29.3	-69.0	-9.3
		T3	<0.001	22.5	-90.2	41.6
		T4a	<0.001	21.9	-67.3	27.0
	SUVA	T1	0.353	7.3	-17.6	40.8
		T2a	<0.001	6.4	-14.3	35.3
		T3	<0.001	10.7	-43.2	36.2
		T4a	<0.001	8.0	-29.0	35.8
Yukon	a_{254}	T1	0.001	6.1	-14.8	3.3
		T2a	<0.001	13.7	-29.3	0.3
		T3	<0.001	18.5	-36.8	-3.7
		T4a	<0.001	16.9	-38.0	1.6
		T5a	<0.001	15.5	-35.9	-4.5
	a_{400}	T1	0.001	21.1	-52.1	7.0
		T2a	<0.001	32.9	-56.0	-5.4
		T3	<0.001	43.4	-77.4	-12.7
		T4a	<0.001	39.9	-74.7	-0.7
		T5a	<0.001	36.1	-76.6	-4.9
	$a_{250}{:}a_{365}$	T1	0.003	8.1	-4.4	21.9
		T2a	<0.001	14.6	2.1	34.2
		T3	<0.001	26.2	4.9	78.7
		T4a	0.001	21.3	-3.8	73.9
		T5a	<0.001	23.3	0.0	66.4
	SUVA	T1	0.002	6.1	-14.8	3.3
		T2a	<0.001	16.3	-33.9	-8.0
		T3	<0.001	18.5	-36.8	-3.7
		T4a	<0.001	17.0	-32.1	-10.0
		T5a	<0.001	15.5	-35.9	-4.5

Table 3.2, continued

River System		Treatment	p-value	Average (%)	Min (%)	Max (%)
Texas	a_{254}	T1	0.008	20.5	-43.2	14.2
		T2a	0.429	15.7	-24.8	72.5
		T3	0.001	31.8	-54.3	-6.6
		T4a	0.002	31.5	-54.5	28.9
		T5a	0.001	25.2	-47.8	1.9
	a_{400}	T1	0.414	59.8	-43.5	188.1
		T2a	0.074	129.1	-28.1	859.3
		T3	0.003	56.8	-74.4	48.5
		T4a	0.009	64.1	-74.8	195.7
		T5a	0.005	51.9	-68.5	123.8
	$a_{250}{:}a_{365}$	T1	0.441	30.0	-39.9	69.9
		T2a	0.153	23.3	-68.0	3.0
		T3	0.007	32.8	-23.8	55.0
		T4a	0.002	32.6	-44.0	58.0
		T5a	0.006	24.8	-37.6	36.3
	SUVA	T1	<0.001	20.5	-43.2	14.2
		T2a	0.290	15.7	-24.8	72.5
		T3	<0.001	31.8	-54.3	-6.6
		T4a	<0.001	31.5	-54.5	28.9
		T5a	<0.001	25.2	-47.8	1.9
Kolyma	a_{254}	T1	0.152	5.1	-11.5	25.4
		T2b	0.770	3.7	-7.6	29.0
		T3	0.004	5.9	-12.6	27.6
		T4b	0.007	5.0	-13.1	24.0
		T5b	0.001	4.7	-12.9	6.5
	a_{400}	T1	0.161	10.3	-32.8	35.6
		T2b	0.882	7.8	-19.9	60.6
		T3	0.005	11.1	-29.6	24.0
		T4b	0.005	11.7	-36.0	3.9
		T5b	0.102	15.6	-59.5	31.8
	$a_{250}{:}a_{365}$	T1	0.031	5.7	-15.5	21.8
		T2b	0.768	3.1	-15.7	13.1
		T3	0.001	5.8	-6.0	18.2
		T4b	0.001	6.9	-2.6	22.7
		T5b	0.022	8.1	-8.6	40.9
	SUVA	T1	0.117	5.1	-11.5	25.4
		T2b	0.754	3.7	-7.6	29.0
		T3	0.019	5.9	-12.6	27.6
		T4b	0.600	5.0	-13.1	24.0
		T5b	<0.001	4.7	-12.9	6.5

Table 3.3.   Regression statistics for treatments plotted as a function of initial CDOM measurements, separated by river system. R^2 (%), slope, and lower and upper 95% confidence intervals are reported.

River System		Treatment	R^2 (%)	Slope	Lower CI	Upper CI
Mackenzie	a_{254}	T1	97	0.90	0.86	0.95
		T2a	98	0.93	0.89	0.97
		T3	86	0.83	0.75	0.92
		T4a	96	0.83	0.79	0.87
	a_{400}	T1	59	0.87	0.68	1.06
		T2a	71	0.97	0.81	1.14
		T3	32	0.66	0.41	0.91
		T4a	51	0.58	0.43	0.73
	$a_{250}{:}a_{365}$	T1	3.0	-0.14	-0.34	0.07
		T2a	0.7	0.06	-0.14	0.27
		T3	4.5	0.35	-0.07	0.76
		T4a	4.2	-0.16	-0.37	0.04
	SUVA	T1	23	0.53	0.26	0.79
		T2a	46	0.68	0.47	0.88
		T3	13	0.43	0.11	0.74
		T4a	19	0.34	0.14	0.54
Yukon	a_{254}	T1	98	0.96	0.87	1.04
		T2a	98	0.95	0.87	1.04
		T3	98	0.91	0.82	1.00
		T4a	97	0.93	0.83	1.03
		T5a	98	0.95	0.86	1.03
	a_{400}	T1	60	0.67	0.32	1.01
		T2a	82	0.78	0.53	1.02
		T3	80	0.72	0.50	0.93
		T4a	76	0.74	0.50	0.99
		T5a	86	0.87	0.65	1.10
	$a_{250}{:}a_{365}$	T1	39	0.56	0.12	1.00
		T2a	34	0.27	0.02	0.51
		T3	48	-0.65	-1.08	-0.22
		T4a	46	-0.81	-1.37	-0.26
		T5a	45	-0.51	-0.87	-0.15
	SUVA	T1	65	0.86	0.44	1.27
		T2a	13	0.38	-0.28	1.04
		T3	34	-0.33	-0.63	-0.04
		T4a	3.2	0.11	-0.27	0.50
		T5a	12	-0.22	-0.61	0.16

Table 3.3, continued

River System		Treatment	R^2 (%)	Slope	Lower CI	Upper CI
Texas	a_{254}	T1	91	0.53	0.41	0.65
		T2a	96	0.81	0.70	0.91
		T3	85	0.42	0.31	0.54
		T4a	84	0.42	0.30	0.53
		T5a	94	0.54	0.45	0.62
	a_{400}	T1	76	0.43	0.26	0.60
		T2a	76	0.64	0.41	0.88
		T3	85	0.22	0.16	0.28
		T4a	31	0.19	0.01	0.36
		T5a	87	0.33	0.24	0.41
	a_{250}:a_{365}	T1	10	0.37	-0.43	1.16
		T2a	5.1	0.16	-0.31	0.64
		T3	30	0.56	0.05	-0.01
		T4a	56	1.07	0.48	1.66
		T5a	24	0.47	-0.06	1.00
	SUVA	T1	98	0.76	0.65	0.86
		T2a	96	0.84	0.68	1.00
		T3	64	0.95	0.50	0.78
		T4a	89	0.60	0.41	0.80
		T5a	98	0.67	0.59	0.74
Kolyma	a_{254}	T1	99	0.99	0.95	1.03
		T2b	100	0.99	0.96	1.01
		T3	99	0.99	0.96	1.02
		T4b	99	0.99	0.96	1.03
		T5b	100	1.01	0.98	1.03
	a_{400}	T1	94	1.00	0.89	1.12
		T2b	99	1.01	0.96	1.07
		T3	98	1.04	0.98	1.10
		T4b	97	1.05	0.97	1.13
		T5b	96	1.09	0.99	1.20
	a_{250}:a_{365}	T1	31	0.56	0.18	0.94
		T2b	61	0.81	0.52	1.09
		T3	51	0.70	0.40	1.00
		T4b	44	0.78	0.39	1.17
		T5b	33	1.06	0.37	1.75
	SUVA	T1	69	0.81	0.56	1.05
		T2b	71	0.85	0.61	1.09
		T3	69	0.84	0.60	1.08
		T4b	74	0.85	0.63	1.07
		T5b	87	1.01	0.83	1.19

Table 3.4.   Percent differences between T1 and T2 CDOM samples from archived
              Arctic-GRO samples, separated by river and for the entire dataset. Average,
              minimum, and maximum differences are included.

River		Average (%)	Min (%)	Max (%)
Kolyma	a_{254}	12.8	-28.2	-4.5
	a_{400}	15.1	-32.3	10.0
	a_{250}:a_{365}	6.4	-4.1	15.3
	SUVA	12.8	-28.2	-4.5
Lena	a_{254}	9.5	-11.8	-5.8
	a_{400}	3.2	-4.2	6.5
	a_{250}:a_{365}	2.6	-5.2	4.7
	SUVA	9.5	-11.8	-5.8
Mackenzie	a_{254}	17.3	-19.5	37.8
	a_{400}	29.0	-51.1	51.0
	a_{250}:a_{365}	29.4	-18.2	41.8
	SUVA	17.3	-19.5	37.8
Ob'	a_{254}	9.9	-12.9	-6.7
	a_{400}	12.0	-14.5	28.4
	a_{250}:a_{365}	7.1	-15.3	7.7
	SUVA	9.9	-12.9	-6.7
Yenisey	a_{254}	7.4	-10.6	-3.7
	a_{400}	13.5	-7.2	30.5
	a_{250}:a_{365}	5.4	-12.1	3.2
	SUVA	7.4	-10.6	-3.7
Yukon	a_{254}	40.4	-69.2	133.0
	a_{400}	26.9	-73.1	30.8
	a_{250}:a_{365}	17.3	-8.9	50.3
	SUVA	40.4	-69.2	133.0
Arctic-GRO	a254	16.8	-69.2	133.0
	a400	16.9	-73.1	51.0
	a250:a365	11.3	11.7	-18.2
	SUVA	16.8	-69.2	133.0

Table 3.5.   Regression statistics between T1 and T2 CDOM samples from archived
Arctic-GRO samples. R^2 (%), slope, 95% confidence intervals. Regression
statistics are not reported for individual rivers, as there were only 4 – 8
samples per river.

	R^2 (%)	Slope	2.50%	97.50%
a_{254}	97	0.88	0.82	0.94
a_{400}	93	0.95	0.85	1.04
$a_{250}{:}a_{365}$	19	0.70	0.18	1.23
SUVA	14	0.18	0.02	0.35

Figure 3.1. CDOM from frozen samples (T1) versus initial (I) measurements of a) a_{254}, b) a_{400}, c) $a_{250:365}$, and d) $SUVA_{254}$. Mackenzie, Texas, and Yukon samples were stored frozen for 3-4 months. Kolyma samples were stored frozen for 1 week. Colors of points indicate river system: Red = Kolyma, Green = Mackenzie, Brown = Texas, Yellow = Yukon.
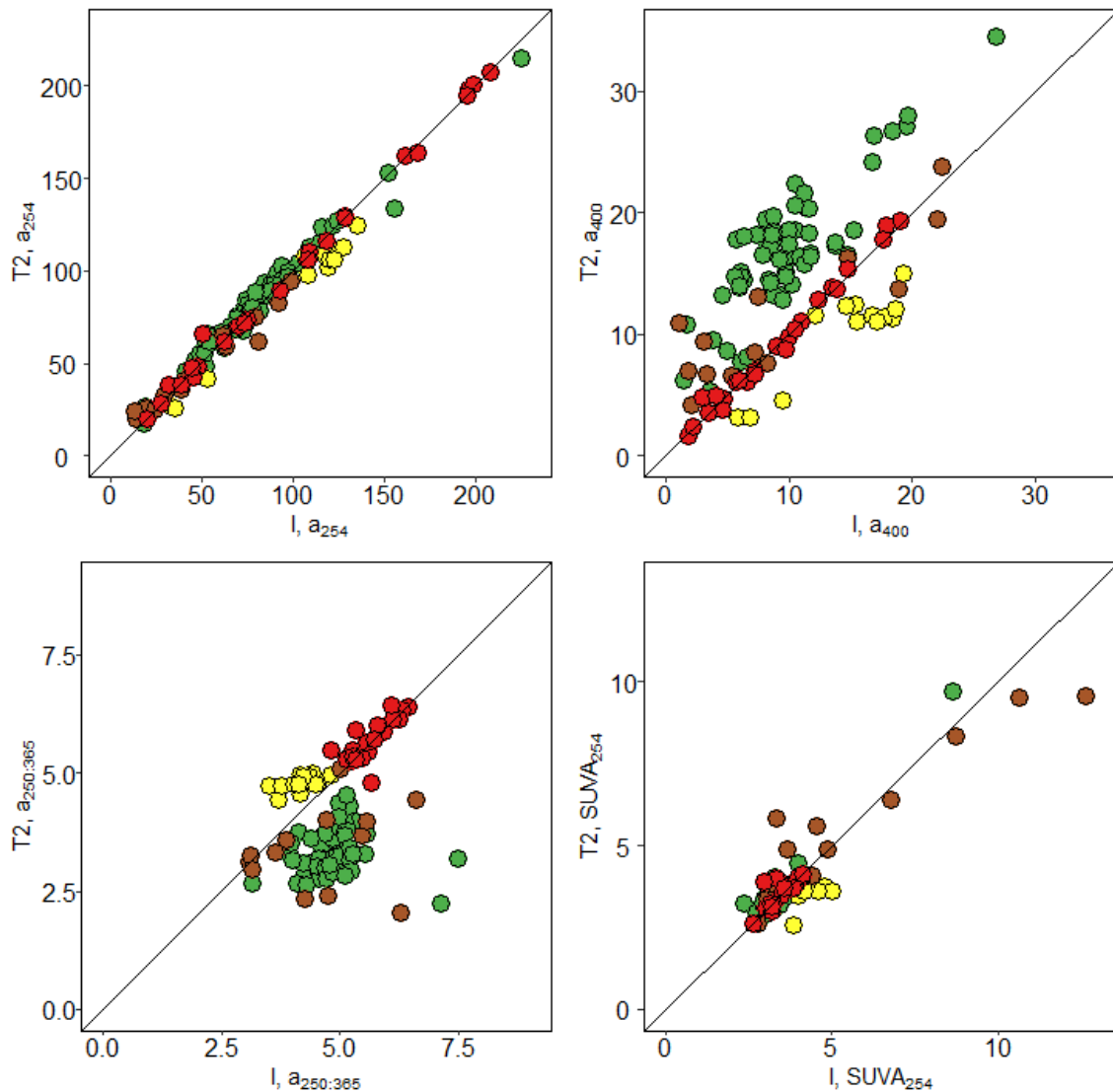
Figure 3.2. CDOM from frozen sonified samples (T2) versus initial (I) measurements of a) a_{254}, b) a_{400}, c) $a_{250:365}$, and d) $SUVA_{254}$. Mackenzie, Texas, and Yukon samples were stored frozen for 3-4 months and sonified using microtip probe. Kolyma samples were stored frozen for 1 week, and sonified in a bath. Colors of points indicate river system: Red = Kolyma, Green = Mackenzie, Brown = Texas, Yellow = Yukon.
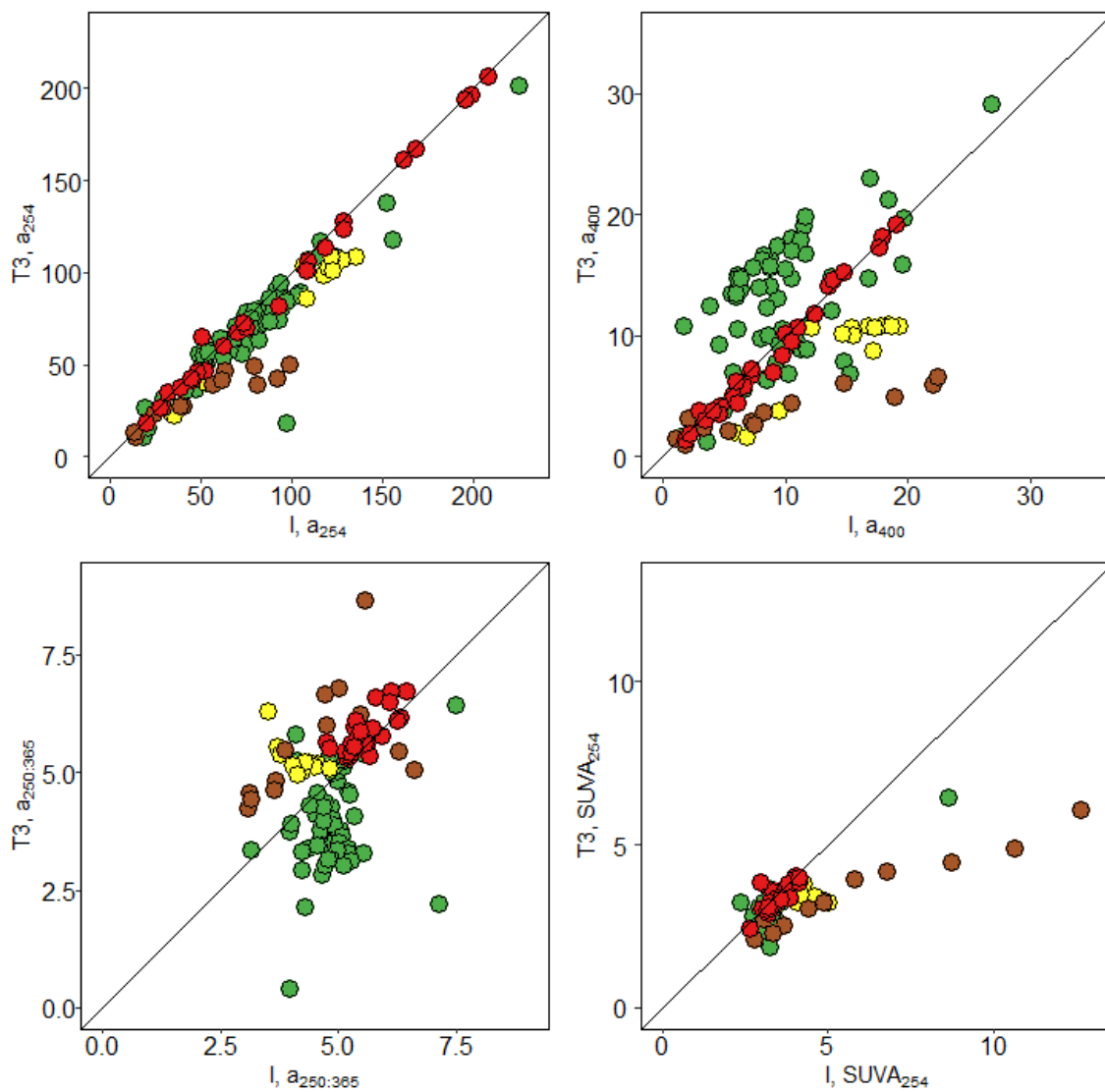
Figure 3.3. CDOM from frozen re-filtered samples (T3) versus initial (I) measurements of a) a_{254}, b) a_{400}, c) $a_{250:365}$, and d) $SUVA_{254}$. Mackenzie, Texas, and Yukon samples were stored frozen for 3-4 months. Kolyma samples were stored frozen for 1 week. Colors of points indicate river system: Red = Kolyma, Green = Mackenzie, Brown = Texas, Yellow = Yukon.
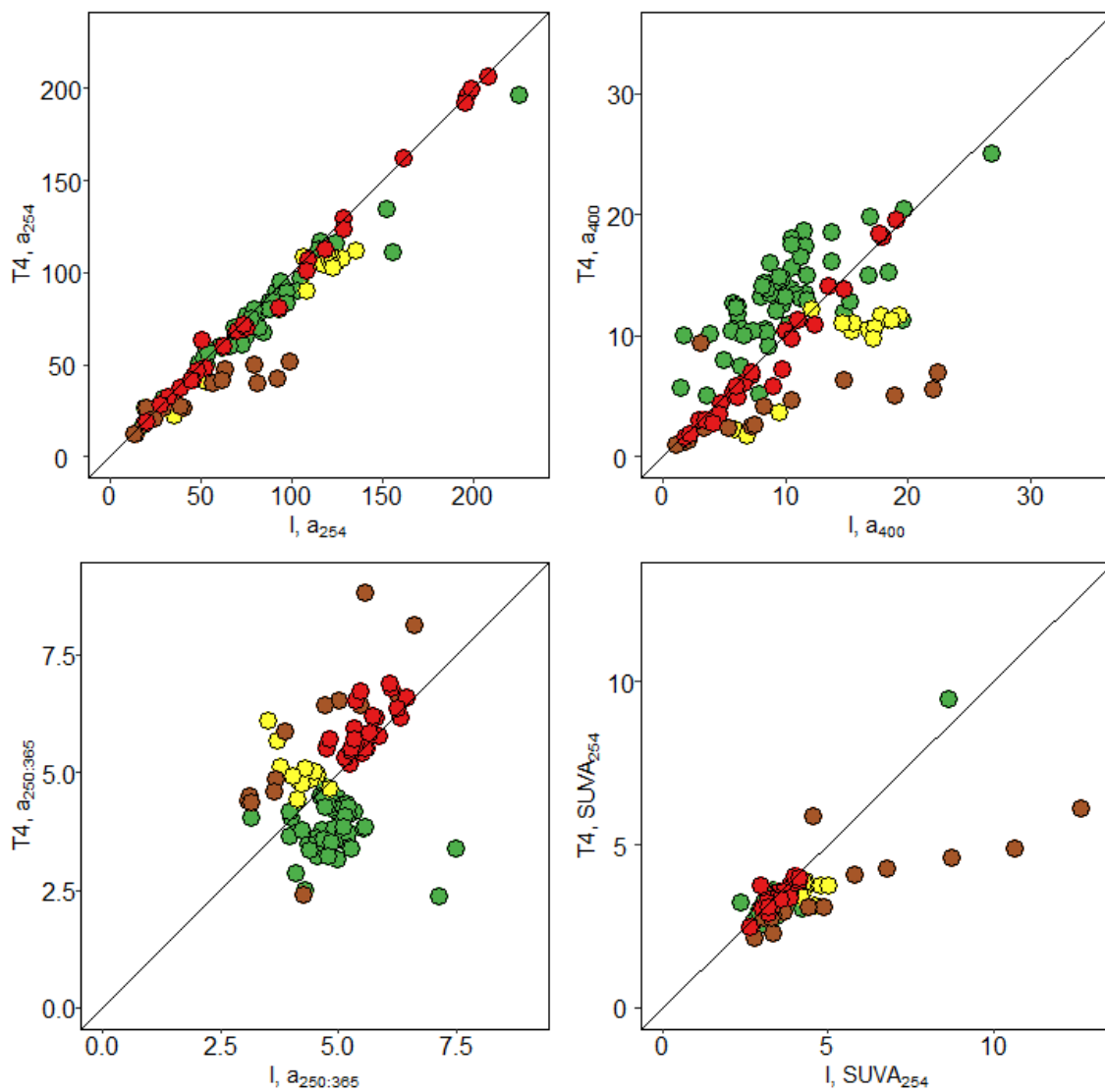
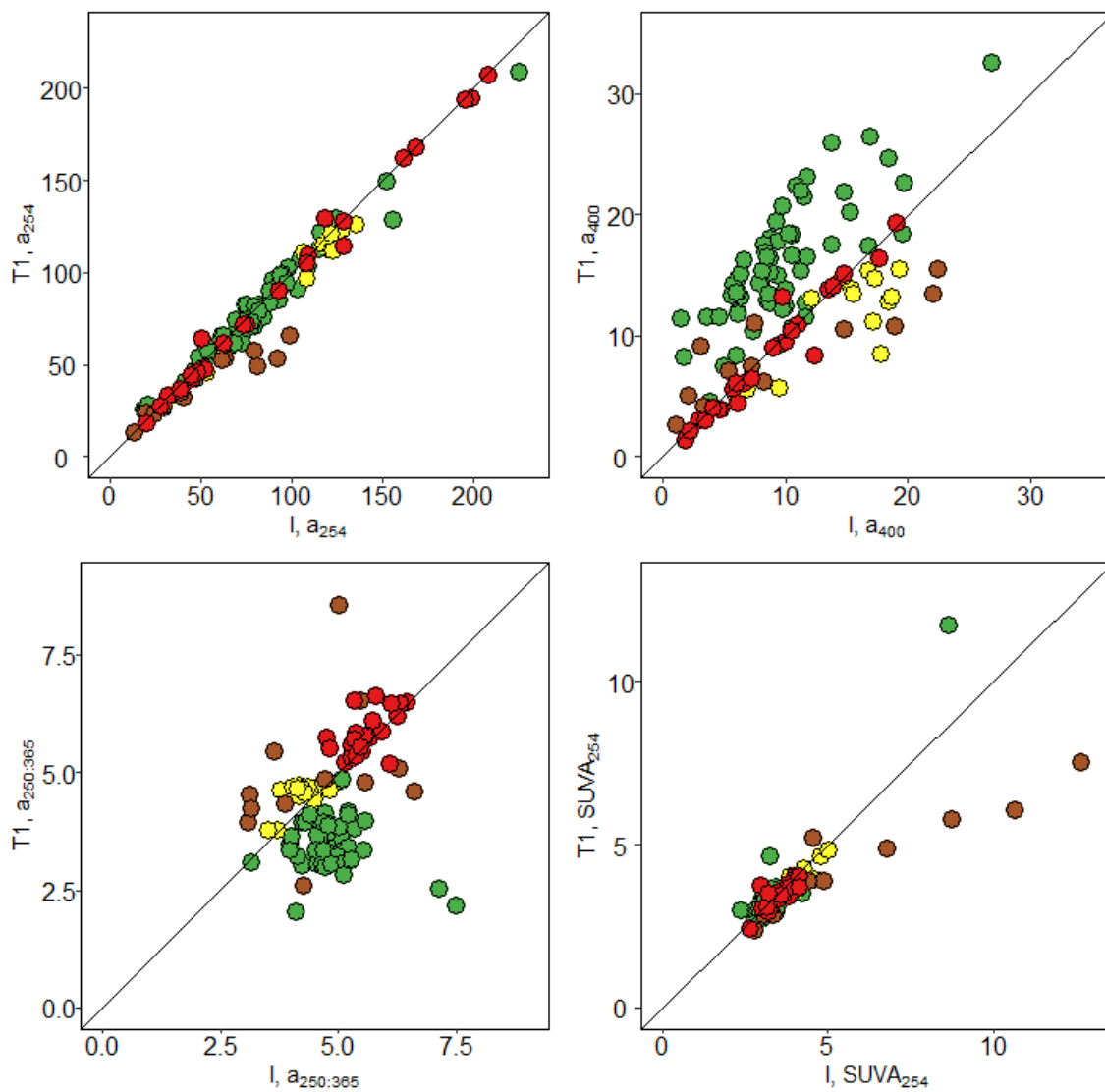Figure 3.4. CDOM from frozen filtered and sonified samples (T4) versus initial (I) measurements of a) a_{254}, b) a_{400}, c) $a_{250:365}$, and d) SUVA$_{254}$. Mackenzie, Texas, and Yukon samples were stored frozen for 3-4 months and sonified using microtip probe. Kolyma samples were stored frozen for 1 week, and sonified in a bath. Colors of points indicate river system: Red = Kolyma, Green = Mackenzie, Brown = Texas, Yellow = Yukon.
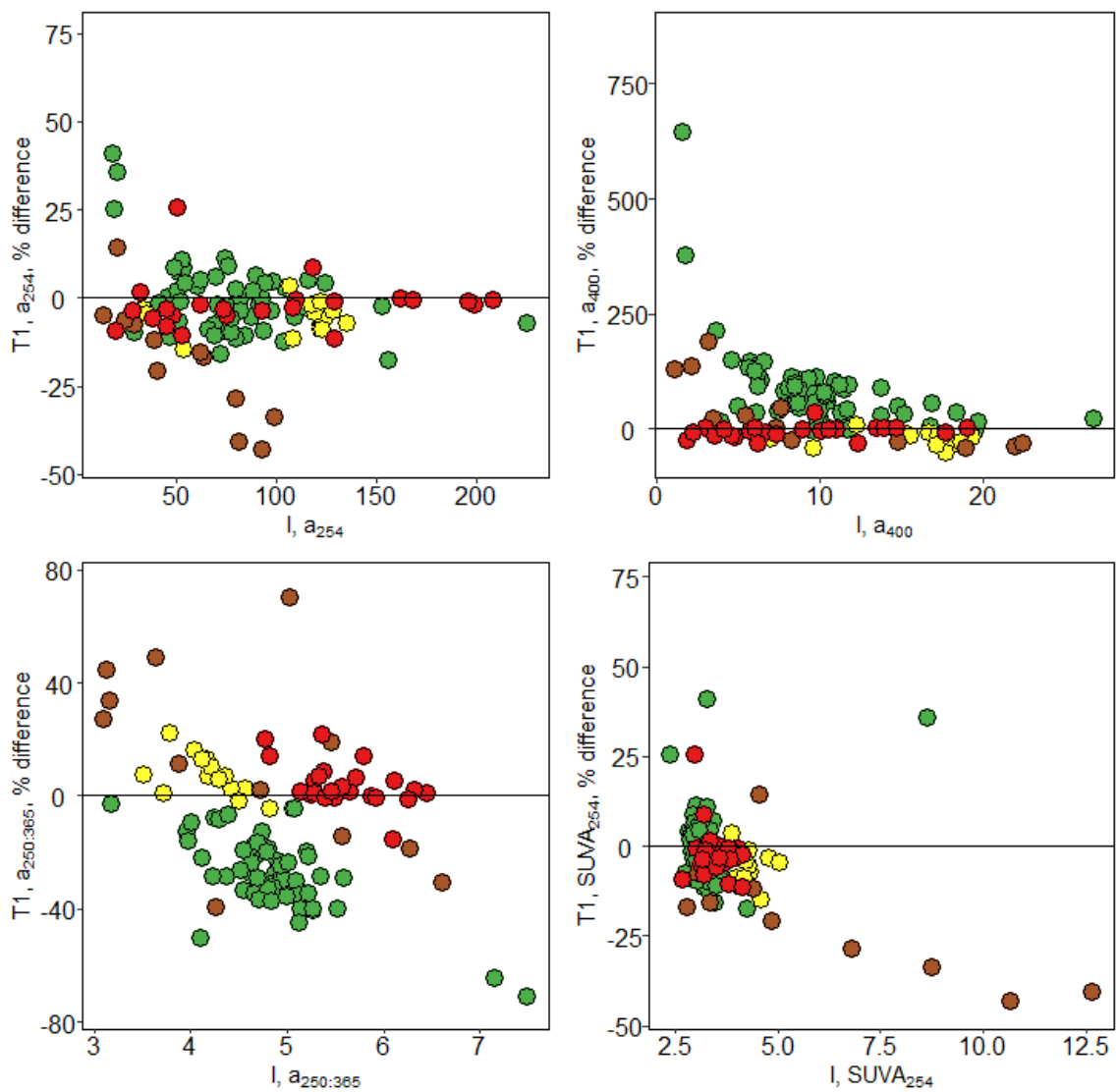
Figure 3.5. Comparison of initial CDOM measurements versus the percent difference of a) a_{254}, b) a_{400}, c) $a_{250:365}$, and d) SUVA$_{254}$ for frozen samples. Colors of points indicate river system: Red = Kolyma, Green = Mackenzie, Brown = Texas, Yellow = Yukon.
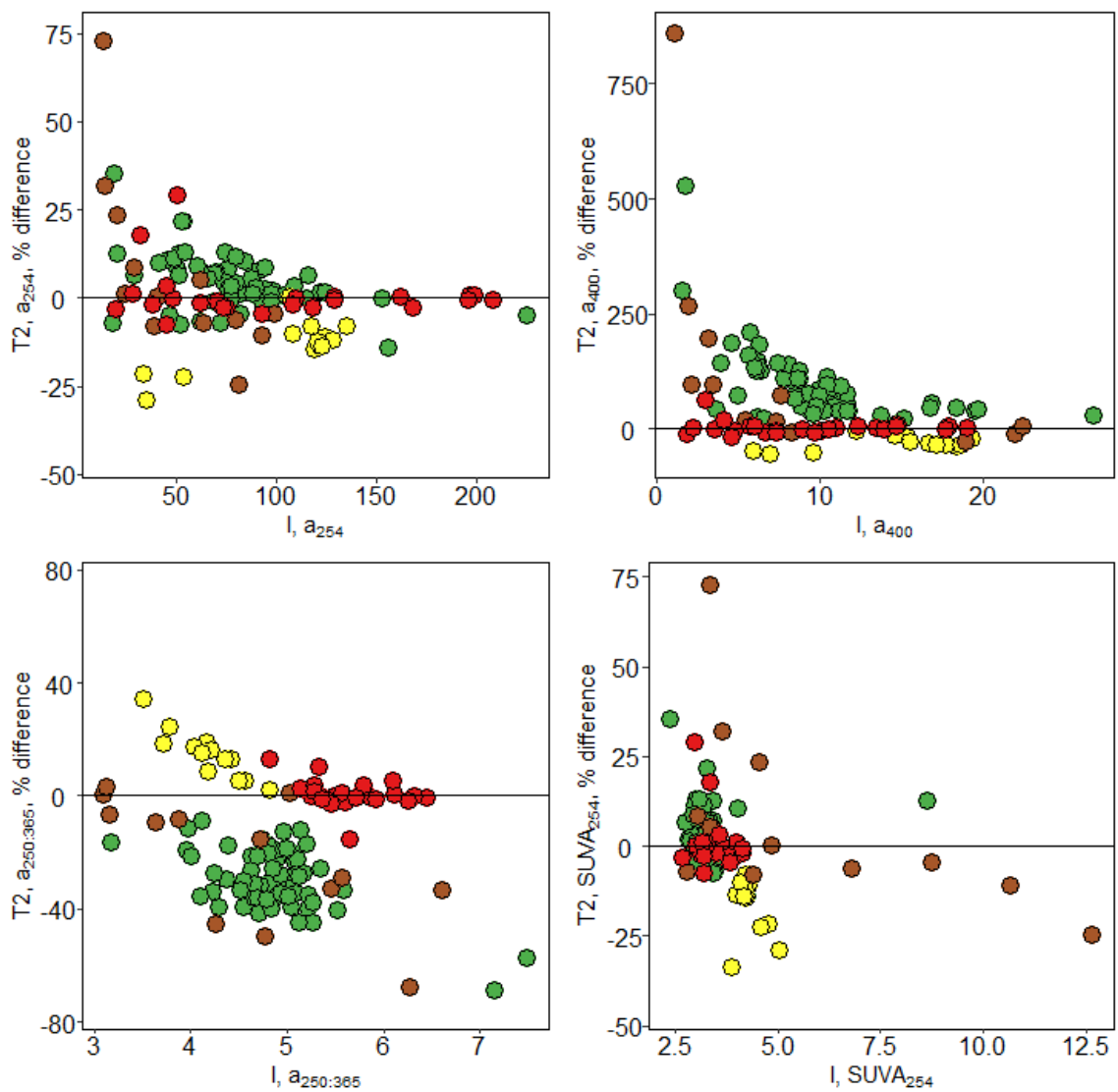
Figure 3.6. Comparison of initial CDOM measurements versus the percent difference of a) a_{254}, b) a_{400}, c) $a_{250:365}$, and d) SUVA$_{254}$ for sonified samples. Colors of points indicate river system: Red = Kolyma, Green = Mackenzie, Brown = Texas, Yellow = Yukon.

110

Figure 3.7.   Frozen sonified (T2) versus frozen (T1) CDOM measurements from archival Arctic-GRO samples. There are no CDOM measurements prior to freezing available for these samples. Archival samples were stored for 2 – 4 years before analyses. Colors of points indicate river: Red = Kolyma, Blue = Lena, Green = Mackenzie, Purple = Ob', Orange = Yenisey, Yellow = Yukon.
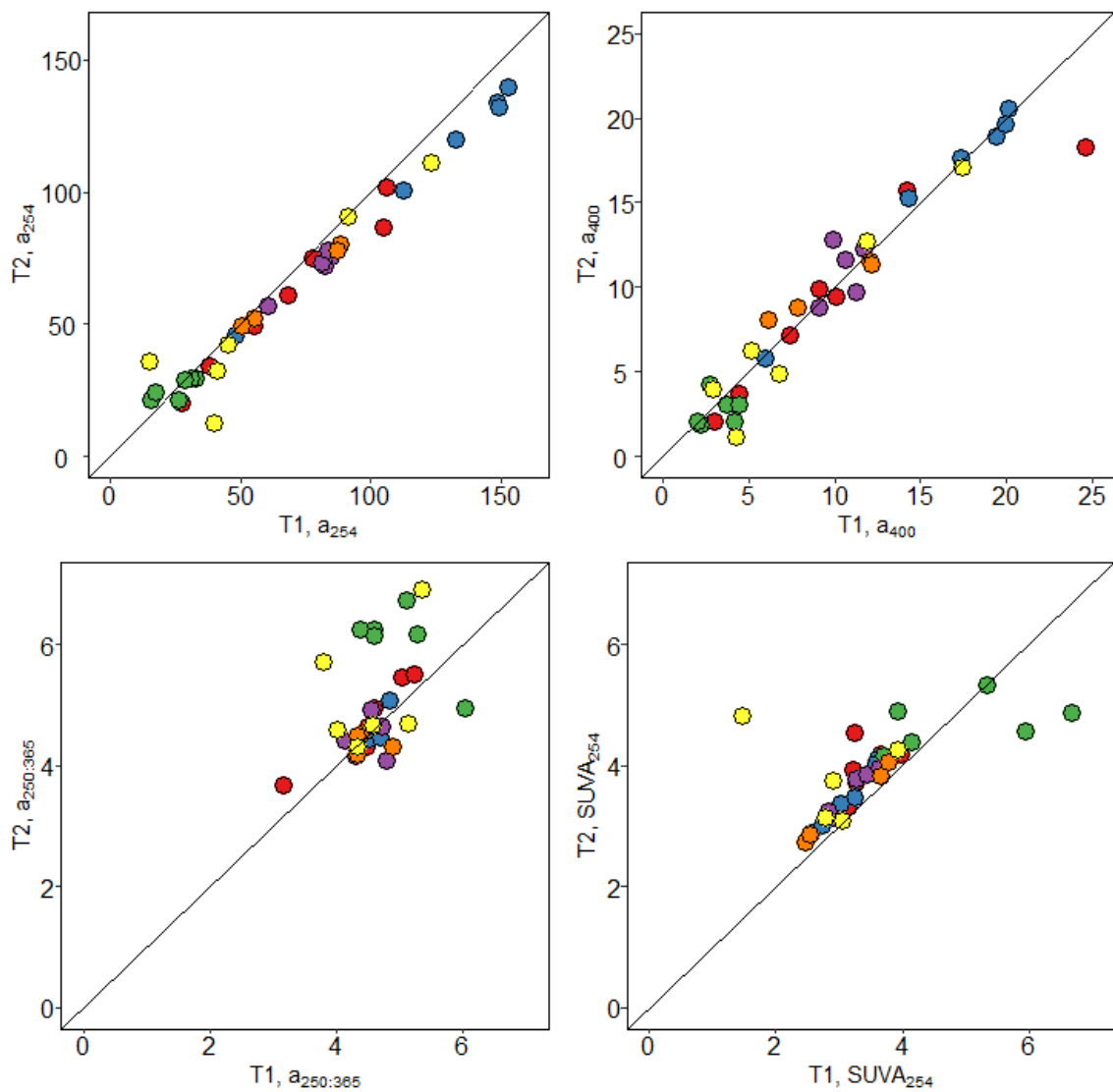
Concluding Remarks

Understanding the role of DOM in high latitude systems has been hampered by the difficult and expensive logistics required for sampling in remote regions across the Pan-Arctic. The studies presented within this dissertation represent a significant increase in our ability to monitor riverine DOM in the Arctic, both through remote sensing studies and laboratory measurements of CDOM. We now have well-established methods to estimate CDOM and DOC concentrations from multispectral satellite sensors that may be applied to both historical and new imagery. These results have been used to calculate fluxes of riverine DOM in multiple rivers. The highly seasonal nature of organic matter concentrations and fluxes were captured using satellite data, as well as potentially important ties to other environmental variables. For instance, these fluxes could be associated with the Arctic Oscillation in many rivers, demonstrating the importance of atmospheric teleconnections to regional carbon cycling. Furthermore, remote sensing methods were used to extend time series over the past thirty years. Multi-decadal records in the Ob' and Yenisey rivers showed shifts in discharge-CDOM relationships, suggesting potential climate change impacts associated with differential watershed characteristics. Experimental results from both Arctic and Texas rivers also improve our understanding of the impacts of cryopreservation on CDOM across many river systems, and whether further processing may improve CDOM results.Our understanding of terrestrial organic matter in aquatic Arctic systems has advanced drastically over the past decade as studies have revealed greater seasonality [*Finlay et al.*, 2006; *Raymond et al.*, 2007], higher lability [*Holmes et al.*, 2008; *Mann et al.*, 2015], and greater detail on the sources and quality of organic matter [*Neff et al.*, 2006; *Guo et al.*, 2007; *Wickland et al.*, 2007] than previously known. Large Arctic rivers integrate watershed scale processes, making them valuable indicators of possible widespread change. Within the Yenisey

River, for instance, there have potentially been decreases in CDOM concentration relative to discharge over a thirty year period. Such decreases may be linked to permafrost degradation, and deeper groundwater flowpaths and longer residence times through organic-poor mineral soils [*Walvoord and Striegl*, 2007; *Pokrovsky et al.*, 2015]. In order for such a shift to be observed within a system as large as the Yenisey, which delivers ~636 km^3 of water to the Arctic Ocean annually [*Holmes et al.*, 2012], extensive changes have likely occurred within the watershed. While monitoring the total CDOM or DOC flux is an important step in understanding land-ocean linkages and climate change impacts, these large rivers are likely less sensitive to climate than smaller streams and river [*Cole et al.*, 2007; *Spencer et al.*, 2015], or even lakes [*Tranvik et al.*, 2009]. However, synoptic sampling to understand linkages across spatial scales remains difficult in high latitude watersheds.

The work performed for the studies presented here has demonstrated the utility of remote sensing in monitoring CDOM through time, but has yet to fully leverage the spatial power of satellite observations. Further research linking remote sensing to ground observations throughout a watershed could substantially enhance our ability to understand how organic matter is transformed as it moves from land to sea. Just as our understanding of organic matter lability within Arctic rivers has shifted in recent years, our concept of terrestrial organic matter fate within estuaries and the coastal ocean has undergone revision [*Benner et al.*, 2004; *Alling et al.*, 2010]. Both biological and photochemical processes have been shown to contribute to DOM loss within nearshore environment [*Bélanger et al.*, 2006; *Letscher et al.*, 2011; *Manizza et al.*, 2011; *Tank et al.*, 2012b]. Here, too, remote sensing can increase our observational capacity greatly, as has been shown in several studies tracing CDOM in nearshore Arctic environments [*Belanger et al.*, 2008; *Matsuoka et al.*, 2012; *Fichot et al.*, 2013]. Such work remains

relatively novel, and has yet to be fully incorporated into process-level research exploring the ultimate fate of terrestrial materials in the Arctic Ocean.

Throughout recent research on organic carbon cycling in the Arctic, CDOM has proven to be a useful tool in assessing the quantity and quality of terrestrial organic matter. Experimental results also show that, while some samples may be transformed in unpredictable ways through freezing for preservation, most CDOM samples relatively stable at low UV wavelengths. However, CDOM absorption at wavelengths in the UV-C and visible spectrum often vary unpredictably after freezing, particularly for samples with low concentrations of CDOM. Additional sonifying of samples after thaw may help correct for flocculation that occurred during freezing, but such improvements are river-specific and may require statistical corrections. When possible, researchers should avoid cryopreservation, although the remote nature of many study regions – particularly in the Arctic – limits this option.Future research may more fully explore the linkages between Arctic CDOM quality and environmental processing of DOM. Already, remote sensing of spectral slope – a common proxy for relative molecular weight – has led to new insights into the transport of terrestrial DOM along Arctic continental shelves [*Fichot et al.*, 2013]. CDOM also plays an important role in the organic carbon cycle, in and of itself, as the primary portion of DOM to undergo photochemical transformation and an important factor in light penetration in aquatic environments [*Bélanger et al.*, 2006; *Osburn et al.*, 2009; *Xie et al.*, 2012]. The research presented in this dissertation lays the groundwork for future studies that will connect remote sensing of CDOM to the ultimate fate of terrestrial organic matter in aquatic and estuarine systems.

114

References

Aagard and E.C. Carmack, K., K. Aagard, and E.C.Carmack (1989), The role of sea ice and other fresh water in the Arctic circulation, *J. Geophys. Res.*, *94*(1), 14,414–485,498, doi:10.1029/JC094iC10p14485.

Alling, V. et al. (2010), Nonconservative behavior of dissolved organic carbon across the Laptev and East Siberian seas, *Global Biogeochem. Cycles*, *24*(4), 1–15, doi:10.1029/2010GB003834.

Battin, T. J., L. a. Kaplan, S. Findlay, C. S. Hopkinson, E. Marti, A. I. Packman, J. D. Newbold, and F. Sabater (2009), Biophysical controls on organic carbon fluxes in fluvial networks, *Nat. Geosci.*, *2*(8), 595–595, doi:10.1038/ngeo602.

Beaulieu, J. J. et al. (2011), Nitrous oxide emission from denitrification in stream and river networks., *Proc. Natl. Acad. Sci. U. S. A.*, *108*(1), 214–9, doi:10.1073/pnas.1011464108.

Beilman, D. W., G. M. MacDonald, L. C. Smith, and P. J. Reimer (2009), Carbon accumulation in peatlands of West Siberia over the last 2000 years, *Global Biogeochem. Cycles*, *23*(1), GB1012.

Bekryaev, R. V., I. V. Polyakov, and V. A. Alexeev (2010), Role of polar amplification in long-term surface air temperature variations and modern arctic warming, *J. Clim.*, *23*(14), 3888–3906, doi:10.1175/2010JCLI3297.1.

Belanger, S., M. Babin, and P. Larouche (2008), An empirical ocean color algorithm for estimating the contribution of chromophoric dissolved organic matter to total light absorption in optically complex waters, *J. Geophys. Res. Ocean.*, *113*(4), 1–14, doi:10.1029/2007JC004436.

Bélanger, S., H. Xie, N. Krotkov, P. Larouche, W. F. Vincent, and M. Babin (2006), Photomineralization of terrigenous dissolved organic matter in arctic coastal waters from 1979 to 2003: Interannual variability and implications of climate change, *Global Biogeochem. Cycles*, *20*, 1–13, doi:10.1029/2006GB02708.

Belzile, C., J. a. E. Gibson, and W. F. Vincent (2002), Colored dissolved organic matter and dissolved organic carbon exclusion from lake ice: Implications for irradiance transmission and carbon cycling, *Limnol. Oceanogr.*, *47*(5), 1283–1293, doi:10.4319/lo.2002.47.5.1283.

Benner, R., B. Benitez-Nelson, K. Kaiser, and R. M. . Amon (2004), Export of young terrigenous dissolved organic carbon from rivers to the Arctic Ocean, *Geophys. Res. Lett*, *31*(5).

Berner, L. T., P. S. A. Beck, A. G. Bunn, A. H. Lloyd, and S. J. Goetz (2011), High - latitude tree growth and satellite vegetation indices : Correlations and trends in Russia and Canada (1982 – 2008), , *116*, 1–13, doi:10.1029/2010JG001475.

Bertilsson, S., and L. J. Tranvik (2000), Photochemical transformation of dissolved organic matter in lakes, *Limnol. Oceanogr.*, *45*(4), 753–762, doi:10.4319/lo.2000.45.4.0753.

Brabets, T. P., and M. A. Walvoord (2009), Trends in streamflow in the Yukon River Basin from 1944 to 2005 and the influence of the Pacific Decadal Oscillation, *J.*

Hydrol., *371*(1-4), 108–119, doi:10.1016/j.jhydrol.2009.03.018.

Brezonik, P., K. Menken, and M. Bauer (2005), Landsat-based Remote Sensing of Lake Water Quality Characteristics, Including Chlorophyll and Colored Dissolved Organic Matter (CDOM), *Lake Reserv. Manag.*, *21*(4), 373–382, doi:10.1080/07438140509354442.

Brezonik, P. L., L. G. Olmanson, J. C. Finlay, and M. E. Bauer (2014), Factors affecting the measurement of CDOM by remote sensing of optically complex inland waters, *Remote Sens. Environ.*, *157*, 199–215, doi:10.1016/j.rse.2014.04.033.

Del Castillo, C. E., and R. L. Miller (2008), On the use of ocean color remote sensing to measure the transport of dissolved organic carbon by the Mississippi River Plume, *Remote Sens. Environ.*, *112*(3), 836–844, doi:10.1016/j.rse.2007.06.015.

Chavez, P. S. J. (1996), Image-based atmospheric corrections- revisited and improved, *Photogramm. Eng. Remote Sensing*, *62*, 1025–1035, doi:0099-1112/96/6209-1025.

Chen, J., S. Xue, Y. Lin, C. Wang, Q. Wang, and Q. Han (2015), Effect of freezing–thawing on dissolved organic matter in water, *Desalin. Water Treat.*, *3994*(April), 1–11, doi:10.1080/19443994.2015.1085913.

Coble, P. G. (2007), Marine optical biogeochemistry: the chemistry of ocean color., *Chem. Rev.*, *107*(2), 402–18, doi:10.1021/cr050350+.

Cole, J. J. et al. (2007), Plumbing the Global Carbon Cycle: Integrating Inland Waters into the Terrestrial Carbon Budget, *Ecosystems*, *10*(1), 172–185, doi:10.1007/s10021-006-9013-8.

Cooper, L. W., R. Benner, J. W. McClelland, B. J. Peterson, R. M. Holmes, P. A. Raymond, D. A. Hansell, J. M. Grebmeier, and L. A. Codispoti (2005), Linkages among runoff, dissolved organic carbon, and the stable oxygen isotope composition of seawater and other water mass indicators in the Arctic Ocean,

Denfeld, B., K. Frey, and W. Sobczak (2013), Summer CO 2 evasion from streams and rivers in the Kolyma River basin, north-east Siberia, *Polar …*, *1*, 1–15.

Dilling, J., and K. Kaiser (2002), Estimation of the hydrophobic fraction of dissolved organic matter in water samples using UV photometry, *Water Res.*, *36*(20), 5037–5044, doi:10.1016/S0043-1354(02)00365-2.

Dittmar, T., and G. Kattner (2003), The biogeochemistry of the river and shelf ecosystem of the Arctic Ocean: a review, *Mar. Chem.*, *83*(3-4), 103–120, doi:10.1016/S0304-4203(03)00105-1.

Dunton, K. H., S. V Schonberg, and L. W. Cooper (2012), Food Web Structure of the Alaskan Nearshore Shelf and Estuarine Lagoons of the Beaufort Sea, *Estuaries and coasts*, 416–435, doi:10.1007/s12237-012-9475-1.

Elmquist, M., I. Semiletov, L. Guo, and Ö.¨Gustafsson (2008), Pan-Arctic patterns in black carbon sources and fluvial discharges deduced from radiocarbon and PAH source apportionment markers in estuarine surface sediments, *Global Biogeochem. Cycles*, *22*(2), 1–13, doi:10.1029/2007GB002994.

Emmerton, C. a., L. F. W. Lesack, and P. Marsh (2007), Lake abundance, potential water storage, and habitat distribution in the Mackenzie River Delta, western Canadian Arctic, *Water Resour. Res.*, *43*(5), 1–14, doi:10.1029/2006WR005139.

Emmerton, C. a., L. F. W. Lesack, and W. F. Vincent (2008), Nutrient and organic matter patterns across the Mackenzie River, estuary and shelf during the seasonal recession of sea-ice, *J. Mar. Syst.*, *74*(3-4), 741–755, doi:10.1016/j.jmarsys.2007.10.001.

Fellman, J. B., D. V. D'Amore, and E. Hood (2008), An evaluation of freezing as a preservation technique for analyzing dissolved organic C, N and P in surface water samples, *Sci. Total Environ.*, *392*(2-3), 305–312, doi:10.1016/j.scitotenv.2007.11.027.

Ferrari, G. M., and M. D. Dowell (1998), CDOM Absorption Characteristics with Relation to Fluorescence and Salinity in Coastal Areas of the Southern Baltic Sea, *Estuar. Coast. Shelf Sci.*, *47*(1), 91–105, doi:10.1006/ecss.1997.0309.

Ficek, D., T. Zapadka, and J. Dera (2011), Remote sensing reflectance of Pomeranian lakes and the Baltic, *Oceanologia*, *53*(4), 959–970, doi:10.5697/oc.53-4.959.

Fichot, C. G., and R. Benner (2011), A novel method to estimate DOC concentrations from CDOM absorption coefficients in coastal waters, *Geophys. Res. Lett.*, *38*(3), 1–5, doi:10.1029/2010GL046152.

Fichot, C. G., K. Kaiser, S. B. Hooker, R. M. W. Amon, M. Babin, S. Bélanger, S. a Walker, and R. Benner (2013), Pan-Arctic distributions of continental runoff in the Arctic Ocean., *Sci. Rep.*, *3*, 1053, doi:10.1038/srep01053.

Finlay, J., J. Neff, S. Zimov, A. Davydova, and S. Davydov (2006), Snowmelt dominance of dissolved organic carbon in high-latitude watersheds: Implications for characterization and flux of river DOC, *Geophys. Res. Lett*, *33*, L10401.

Le Fouest, V., M. Babin, and J. E. Tremblay (2013), The fate of riverine nutrients on Arctic shelves, *Biogeosciences*, *10*, 3661–3677, doi:10.5194/bg-10-3661-2013.

Frey, K. E., and J. W. McClelland (2009), Impacts of permafrost degradation on arctic river biogeochemistry, *Hydrol. Process.*, *23*(1), 169–182, doi:10.1002/hyp.7196.

Frey, K. E., and L. C. Smith (2005), Amplified carbon release from vast West Siberian peatlands by 2100, *Geophys. Res. Lett.*, *32*(9), 2–5, doi:10.1029/2004GL022025.

Frey, K. E., J. W. McClelland, R. M. Holmes, and L. C. Smith (2007), Impacts of climate warming and permafrost thaw on the riverine transport of nitrogen and phosphorus to the Kara Sea, *J. Geophys. Res.*, *112*(G4), 1–10, doi:10.1029/2006JG000369.

Frey, K. E., W. V. Sobczak, P. J. Mann, and R. M. Holmes (2016), Optical properties and bioavailability of dissolved organic matter along a flow-path continuum from soil pore waters to the Kolyma River, Siberia, *Biogeosciences*, *12*(15), 12321–12347, doi:10.5194/bgd-12-12321-2015.

Gao, L., D. Fan, D. Li, and J. Cai (2010), Fluorescence characteristics of chromophoric dissolved organic matter in shallow water along the Zhejiang coasts, southeast China, *Mar. Environ. Res.*, *69*(3), 187–197, doi:10.1016/j.marenvres.2009.10.004.

Garneau, M.-È., S. Roy, C. Lovejoy, Y. Gratton, and W. F. Vincent (2008), Seasonal dynamics of bacterial biomass and production in a coastal arctic ecosystem: Franklin Bay, western Canadian Arctic, *J. Geophys. Res.*, *113*, 1–15, doi:10.1029/2007JC004281.

Giesy, J. P., and L. A. Briese (1978), Particulate formation due to freezing humic waters, *Water Resour. Res.*, *14*(3), 542–544, doi:10.1029/WR014i003p00542.

117

Gordon, H. R., and M. Wang (1994), Retrieval of water-leaving radiance and aerosol optical thickness over the oceans with SeaWiFS: a preliminary algorithm., *Appl. Opt.*, *33*(3), 443–452, doi:10.1364/AO.33.000443.

Griffin, C. G., K. E. Frey, J. Rogan, and R. M. Holmes (2011), Spatial and interannual variability of dissolved organic matter in the Kolyma River, East Siberia, observed using satellite imagery, *J. Geophys. Res. Biogeosciences*, *116*(May), 1–12, doi:10.1029/2010JG001634.

Griffin, C. G., J. W. McClelland, K. E. Frey, G. Fiske, R. M. Holmes (in preparation), Estimating dissolved organic matter concentrations in major Arctic rivers using Landsat data.

Griffin, C. G., J. W. McClelland, K. E. Frey, R. M. Holmes (in preparation), Decadal-scale dissolved organic matter concentrations and fluxes across the pan-Arctic from remote sensing (in preparation).

Griffin, C. G. and J. W. McClelland (in preparation), Chromophoric dissolved organic matter in cryopreserved samples: Quantifying changes after a freeze-thaw cycle and methods to ameliorate freezing effects.

Guo, L., C. L. Ping, and R. W. Macdonald (2007), Mobilization pathways of organic carbon from permafrost to arctic rivers in a changing climate, *Geophys. Res. Lett.*, *34*(13), L13603.

Guo, L., Y. Cai, C. Belzile, and R. W. Macdonald (2010), Sources and export fluxes of inorganic and organic carbon and nutrient species from the seasonally ice-covered Yukon River, *Biogeochemistry*, *107*(1-3), 187–206, doi:10.1007/s10533-010-9545-z.

Gustafsson, Ö., B. E. Van Dongen, J. E. Vonk, O. V Dudarev, and I. P. Semiletov (2011), Widespread release of old carbon across the Siberian Arctic echoed by its large rivers, *Biogeosciences*, *8*(6), 1737–1743, doi:10.5194/bg-8-1737-2011.

Hansen, M. C., P. V Potapov, R. Moore, M. Hancher, S. A. Turubanova, and A. Tyukavina (2013), High-Resolution Global Maps of 21st-Century Forest Cover Change, *Science (80-.).*, *342*(6160), 850–853, doi:10.1126/science.1244693.

Harrison, J. A., N. Caraco, and S. P. Seitzinger (2005), Global patterns and sources of dissolved organic matter export to the coastal zone: Results from a spatially explicit, global model, *Global Biogeochem. Cycles*, *19*(4), doi:10.1029/2005GB002480.

Hedges, J. I., R. G. Keil, and R. Benner (1997), What happens to terrestrial organic matter in the ocean?, *Org. Geochem.*, *27*(5-6), 195–212, doi:10.1016/S0146-6380(97)00066-1.

Heim, B. et al. (2014), Ocean colour remote sensing in the southern laptev sea: Evaluation and applications, *Biogeosciences*, *11*, 4191–4210, doi:10.5194/bg-11-4191-2014.

Helms, J. R., A. Stubbins, J. D. Ritchie, E. C. Minor, D. J. Kieber, and K. Mopper (2008), Absorption spectral slopes and slope ratios as indicators of molecular weight , source , and photobleaching of chromophoric dissolved organic matter, *October*, *53*(3), 955–969.

Holmes, R. M., B. J. Peterson, a V Zhulidov, V. V Gordeev, and P. N. Makkaveev

(2001), Nutrient chemistry of the Ob' and Yenisey Rivers, Siberia: results from June 2000 expedition and evaluation of long-term data sets, *Mar. C*, (June 2000), 4203–4203, doi:10.1016/S0304-4203(01)00038-X.

Holmes, R. M., J. W. McClelland, B. J. Peterson, I. a Shiklomanov, A. I. Shiklomanov, A. V Zhulidov, V. V Gordeev, and N. N. Bobrovitskaya (2002), A circumpolar perspective on fluvial sediment flux to the Arctic ocean, *Global Biogeochem. Cycles*, *16*(4), 14–45, doi:10.1029/2001GB001849.

Holmes, R. M., J. W. McClelland, P. a. Raymond, B. B. Frazer, B. J. Peterson, and M. Stieglitz (2008), Lability of DOC transported by Alaskan rivers to the Arctic Ocean, *Geophys. Res. Lett.*, *35*(3), 1–5, doi:10.1029/2007GL032837.

Holmes, R. M. et al. (2012), Seasonal and Annual Fluxes of Nutrients and Organic Matter from Large Rivers to the Arctic Ocean and Surrounding Seas, *Estuaries and Coasts*, *35*(2), 369–382, doi:10.1007/s12237-011-9386-6.

Holmes, R. M., A. I. Shiklomanov, S. E. Tank, J. W. McClelland, and M. Tretiakov (2015), *NOAA Arctic Report Card - River Discahrge*.

Hu, C. M., F. E. Muller-Karger, and R. G. Zepp (2002), Absorbance, absorption coefficient, and apparent quantum yield: A comment on common ambiguity in the use of these optical concepts, *Limnol. Oceanogr.*, *47*(4), 1261–1267, doi:10.4319/lo.2002.47.4.1261.

Hudson, N., A. Baker, D. M. Reynolds, C. Carliell-Marquet, and D. Ward (2009), Changes in freshwater organic matter fluorescence intensity with freezing/thawing and dehydration/rehydration, *J. Geophys. Res. Biogeosciences*, *114*(4), doi:10.1029/2008JG000915.

Hugelius, G. et al. (2013a), A new data set for estimating organic carbon storage to 3 m depth in soils of the northern circumpolar permafrost region, *Earth Syst. Sci. Data*, *5*, 393–402, doi:10.5194/essd-5-393-2013.

Hugelius, G., C. Tarnocai, G. Broll, J. G. Canadell, P. Kuhry, and D. K. Swanson (2013b), The northern circumpolar soil carbon database: Spatially distributed datasets of soil coverage and soil carbon storage in the northern permafrost regions, *Earth Syst. Sci. Data*, *5*, 3–13, doi:10.5194/essd-5-3-2013.

Jiang, X., and Z.-L. Yang (2012), Projected changes of temperature and precipitation in Texas from downscaled global climate models, *Clim. Res.*, *53*(3), 229–244, doi:10:3354/cr01093.

Joshi, I., and E. J. D. Sa (2015), Seasonal Variation of Colored Dissolved Organic Matter in Barataria Bay, Louisiana, Using Combined Landsat and Field Data, , 12478–12502, doi:10.3390/rs70912478.

Kaiser, M., and A. Asefaw Berhe (2014), How does sonication affect the mineral and organic constituents of soil aggregates? - A review, *J. Plant Nutr. Soil Sci.*, *177*(4), 479–495, doi:10.1002/jpln.201300339.

Kallio, K., J. Attila, P. Härmä, S. Koponen, J. Pulliainen, U.-M. Hyytiäinen, and T. Pyhälahti (2008), Landsat ETM+ Images in the Estimation of Seasonal Lake Water Quality in Boreal River Basins, *Environ. Manage.*, *42*(3), 511–522, doi:10.1007/s00267-008-9146-y.

119

Karlsson, E. S., A. Charkin, O. Dudarev, I. Semiletov, and J. E. Vonk (2011), Carbon isotopes and lipid biomarker investigation of sources , transport and degradation of terrestrial organic matter in the Buor-Khaya Bay , SE Laptev Sea, , 3463–3496, doi:10.5194/bgd-8-3463-2011.

Kicklighter, D. W., D. J. Hayes, J. W. Mcclelland, B. J. Peterson, A. D. Mcguire, and J. M. Melillo (2013), Insights and issues with simulating terrestrial DOC loading of Arctic river networks, *Ecol. Appl.*, *23*(8), 1817–1836, doi:10.1890/11-1050.1.

Kloiber, S. M., P. L. Brezonik, L. G. Olmanson, and M. E. Bauer (2002), A procedure for regional lake water clarity assessment using Landsat multispectral data, *Remote Sens. Environ.*, *82*(1), 38–47.

Koven, C. D., B. Ringeval, P. Friedlingstein, P. Ciais, P. Cadule, D. Khvorostyanov, G. Krinner, and C. Tarnocai (2011), Permafrost carbon-climate feedbacks accelerate global warming., *Proc. Natl. Acad. Sci. U. S. A.*, *108*(36), 14769–74, doi:10.1073/pnas.1103910108.

Kremenetski, K. V., A. A. Velichko, O. K. Borisova, G. M. MacDonald, L. C. Smith, K. E. Frey, and L. A. Orlova (2003), Peatlands of the Western Siberian lowlands: Current knowledge on zonation, carbon content and Late Quaternary history, *Quat. Sci. Rev.*, *22*(5-7), 703–723, doi:10.1016/S0277-3791(02)00196-8.

Kutser, T. (2012), The possibility of using the Landsat image archive for monitoring long time trends in coloured dissolved organic matter concentration in lake waters, *Remote Sens. Environ.*, *123*, 334–338, doi:10.1016/j.rse.2012.04.004.

Kutser, T., D. C. Pierson, K. Y. Kallio, A. Reinart, and S. Sobek (2005), Mapping lake CDOM by satellite remote sensing, *Remote Sens. Environ.*, *94*(4), 535–540, doi:10.1016/j.rse.2004.11.009.

Kutser, T., L. Tranvik, and D. C. Pierson (2009), Variations in colored dissolved organic matter between boreal lakes studied by satellite remote sensing, *J. Appl. Remote Sens.*, *3*(July), 033538, doi:10.1117/1.3184437.

Kutser, T., C. Verpoorter, B. Paavel, and L. J. Tranvik (2015), Estimating lake carbon fractions from remote sensing data, *Remote Sens. Environ.*, *157*, 138–146, doi:10.1016/j.rse.2014.05.020.

Larouche, J. R., B. W. Abbott, W. B. Bowden, and J. B. Jones (2015), The role of watershed characteristics, permafrost thaw, and wildfire on dissolved organic carbon biodegradability and water chemistry in Arctic headwater streams, *Biogeosciences Discuss.*, *12*(5), 4021–4056, doi:10.5194/bgd-12-4021-2015.

Lehner, B., and P. Doll (2004), Development and validation of a global database of lakes, reservoirs and wetlands, *J. Hydrol.*, *296*(1-4), 1–22, doi:10.1016/j.jhydrol.2004.03.028.

Letscher, R. T., D. A. Hansell, and D. Kadko (2011), Rapid removal of terrigenous dissolved organic carbon over the Eurasian shelves of the Arctic Ocean, *Mar. Chem.*, *123*(1-4), 78–87, doi:10.1016/j.marchem.2010.10.002.

Lobbes, J., and H. Fitznar (2000), Biogeochemical characteristics of dissolved and particulate organic matter in Russian rivers entering the Arctic Ocean, *Geochim. Cosmochim. Acta*, *64*(17), 2973–2983.

Lobo, F. L., M. P. F. Costa, and E. M. L. M. Novo (2014), Time-series analysis of Landsat-MSS/TM/OLI images over Amazonian waters impacted by gold mining activities, *Remote Sens. Environ.*, *157*, 170–184, doi:10.1016/j.rse.2014.04.030.

Long, C. M., and T. M. Pavelsky (2013), Remote sensing of suspended sediment concentration and hydrologic connectivity in a complex wetland environment, *Remote Sens. Environ.*, *129*, 197–209, doi:10.1016/j.rse.2012.10.019.

Macdonald, R. W., Z. A. Kuzyk, and S. C. Johannessen (2015), It is not just about the ice: a geochemical perspective on the changing Arctic Ocean, *J. Environ. Stud. Sci.*, *5*(3), 288–301, doi:10.1007/s13412-015-0302-4.

Manizza, M., M. J. Follows, S. Dutkiewicz, J. W. Mcclelland, D. Menemenlis, C. N. Hill, and B. J. Peterson (2009), Modeling transport and fate of riverine dissolved organic carbon in the Arctic Ocean, *Arctic*, *23*, 1–10, doi:10.1029/2008GB003396.

Manizza, M., M. J. Follows, S. Dutkiewicz, D. Menemenlis, J. W. Mcclelland, C. N. Hill, B. J. Peterson, and R. M. Key (2011), A model of the Arctic Ocean carbon cycle, *Carbon N. Y.*, *116*(January), 1–19, doi:10.1029/2011JC006998.

Mann, P. J., A. Davydova, N. S. Zimov, R. Spencer, S. Davydov, E. Bulygina, S. a. Zimov, and R. M. Holmes (2012), Controls on the composition and lability of dissolved organic matter in Siberia's Kolyma River Basin, *J. Geophys. Res.*, *117*, 1–15, doi:10.1029/2011JG001798.

Mann, P. J., T. I. Eglinton, C. P. McIntyre, N. Zimov, A. Davydova, J. E. Vonk, R. M. Holmes, and R. G. M. Spencer (2015), Utilization of ancient permafrost carbon in headwaters of Arctic fluvial networks, *Nat. Commun.*, *6*, 7856, doi:10.1038/ncomms8856.

Mann, P. J. et al. (2016), Pan-arctic trends in terrestrial dissolved organic matter from optical measurements, *Front. Earth Sci.*, *4*(25), 1–18, doi:10.3389/feart.2016.00025.

Mannino, A., M. E. Russ, and S. B. Hooker (2008), Algorithm development and validation for satellite-derived distributions of DOC and CDOM in the U.S. Middle Atlantic Bight, *J. Geophys. Res. Ocean.*, *113*(7), 1–19, doi:10.1029/2007JC004493.

Marsh, P., and M. Hey (1989), The flooding hydrology of Mackenzie Delta Lakes near Inuvik, N.W.T., Canada, *Arctic*, *42*(1), 41–49.

Masek, J. G., E. F. Vermote, N. E. Saleous, R. Wolfe, F. G. Hall, K. F. Huemmrich, F. Gao, J. Kutler, and T. K. Lim (2006), A landsat surface reflectance dataset for North America, 1990-2000, *IEEE Geosci. Remote Sens. Lett.*, *3*(1), 68–72, doi:10.1109/LGRS.2005.857030.

Matsuoka, A., A. Bricaud, R. Benner, J. Para, and R. Semp (2012), Tracing the transport of colored dissolved organic matter in water masses of the Southern Beaufort Sea : relationship with hydrographic characteristics, *Biogeosciences*, 925–940, doi:10.5194/bg-9-925-2012.

McClelland, J. W., R. M. Holmes, B. J. Peterson, and M. Stieglitz (2004), Increasing river discharge in the Eurasian Arctic: Consideration of dams, permafrost thaw, and fires as potential agents of change, *J. Geophys. Res. Atmos.*, *109*(18), doi:10.1029/2004JD004583.

McClelland, J. W., M. Stieglitz, F. Pan, R. M. Holmes, and B. J. Peterson (2007), Recent

changes in nitrate and dissolved organic carbon export from the upper Kuparuk River, North Slope, Alaska, *J. Geophys. Res.*, *112*(G4), 1–13, doi:10.1029/2006JG000371.

McClelland, J. W. et al. (2008), Development of a Pan-Arctic Database for River Chemistry, *Eos Trans. AGU*, *89*(24), doi:10.1029/2008EO240001.

McClelland, J. W., a. Townsend-Small, R. M. Holmes, F. Pan, M. Stieglitz, M. Khosh, and B. J. Peterson (2014), River export of nutrients and organicmatter from the North Slope of Alaska to the Beaufort Sea, *Water Resour. Res.*, 1823–1839, doi:10.1002/2013WR014722.Received.

McGuire, A. D. et al. (2010), An analysis of the carbon balance of the Arctic Basin from 1997 to 2006, *Tellus B*, *62*(5), 455–474, doi:10.1111/j.1600-0889.2010.00497.x.

Menard, H. L., and S. M. Smith (1966), Hypsometry of ocean provinces, *J. Geophys. Res.*, *71*, 4305–4325.

Menken, K. D., P. L. Brezonik, and M. E. Bauer (2006), Influence of Chlorophyll and Colored Dissolved Organic Matter (CDOM) on Lake Reflectance Spectra: Implications for Measuring Lake Properties by Remote Sensing, *Lake Reserv. Manag.*, *22*(3), 179–190, doi:10.1080/07438140609353895.

Meon, B., and R. M. W. Amon (2004), Heterotrophic bacterial activity and fluxes of dissolved free amino acids and glucose in the Arctic rivers Ob, Yenisei and the adjacent Kara Sea, *Aquat. Microb. Ecol.*, *37*(2), 121–135, doi:10.3354/ame037121.

Morel, A., and S. Bélanger (2006), Improved detection of turbid waters from ocean color sensors information, *Remote Sens. Environ.*, *102*, 237–249, doi:10.1016/j.rse.2006.01.022.

Morris, D. P., H. Zagarese, C. E. Williamson, E. G. Balseiro, D. P. Morris, and R. Moeller (1995), The Attenuation of Solar UV Radiation in Lakes and the Role of Dissolved Organic Carbon, *Limnol. Oceanogr.*, *40*(8), 1381–1391.

Müller, S., A. V. Vähätalo, M. A. Granskog, R. Autio, and H. Kaartokallio (2011), Behaviour of dissolved organic matter during formation of natural and artificially grown Baltic Sea ice, *Ann. Glaciol.*, *52*(57 PART 2), 233–241, doi:10.3189/172756411795931886.

Müller, S., A. V. Vähätalo, C. A. Stedmon, M. A. Granskog, L. Norman, S. N. Aslam, G. J. C. Underwood, G. S. Dieckmann, and D. N. Thomas (2013), Selective incorporation of dissolved organic matter (DOM) during sea ice formation, *Mar. Chem.*, *155*, 148–157, doi:10.1016/j.marchem.2013.06.008.

Murphy, K. R., C. A. Stedmon, T. D. Waite, and G. M. Ruiz (2008), Distinguishing between terrestrial and autochthonous organic matter sources in marine environments using fluorescence spectroscopy, *Mar. Chem.*, *108*(1-2), 40–58, doi:10.1016/j.marchem.2007.10.003.

Murphy, K. R., K. D. Butler, R. G. M. Spencer, C. A. Stedmon, J. R. Boehme, and G. R. Aiken (2010), Measurement of Dissolved Organic Matter Fluorescence in Aquatic Environments: An Interlaboratory Comparison RID B-8217-2009 RID B-5841-2008, *Environ. Sci. Technol.*, *44*(24), 9405–9412, doi:10.1021/es102362t.

Neff, J. C., J. C. Finlay, S. A. Zimov, S. P. Davydov, J. J. Carrasco, E. A. G. Schuur, and

A. I. Davydova (2006), Seasonal changes in the age and structure of dissolved organic carbon in Siberian rivers and streams, *Geophys. Res. Lett.*, *33*(23), L23401.

Novo, E. M. M., J. D. Hansom, and P. J. Curran† (1989), The effect of sediment type on the relationship between reflectance and suspended sediment concentration, *Int. J. Remote Sens.*, *10*(7), 1283–1289, doi:10.1080/01431168908903967.

Olmanson, L. G., M. E. Bauer, and P. L. Brezonik (2008), A 20-year Landsat water clarity census of Minnesota's 10,000 lakes, *Remote Sens. Environ.*, *112*(11), 4086–4097.

Olmanson, L. G., P. L. Brezonik, and M. E. Bauer (2014), Geospatial and temporal analysis of a 20-year record of Landsat-based water clarity in Minnesota's 10,000 lakes, *J. Am. Water Resour. Assoc.*, *50*(3), 748–761, doi:10.1111/jawr.12138.

Olmanson, L. G., P. L. Brezonik, J. C. Finlay, and M. E. Bauer (2016), Comparison of Landsat 8 and Landsat 7 for regional measurements of CDOM and water clarity in lakes, *Remote Sens. Environ.*, 1–10, doi:10.1016/j.rse.2016.01.007.

Osburn, C. L., and C. A. Stedmon (2011), Linking the chemical and optical properties of dissolved organic matter in the Baltic – North Sea transition zone to differentiate three allochthonous inputs, *Mar. Chem.*, *126*(1-4), 281–294, doi:10.1016/j.marchem.2011.06.007.

Osburn, C. L., L. Retamal, and W. F. Vincent (2009), Photoreactivity of chromophoric dissolved organic matter transported by the Mackenzie River to the Beaufort Sea, *Mar. Chem.*, *115*(1-2), 10–20, doi:10.1016/j.marchem.2009.05.003.

Otero, M., A. Mendona, M. Vellega, E. B. H. Santos, E. Pereira, V. I. Esteves, and A. Duarte (2007), Fluorescence and DOC contents of estuarine pore waters from colonized and non-colonized sediments: Effects of sampling preservation, *Chemosphere*, *67*(2), 211–220, doi:10.1016/j.chemosphere.2006.10.044.

Palmer, S. C. J., T. Kutser, and P. D. Hunter (2015), Remote sensing of inland waters: Challenges, progress and future directions, *Remote Sens. Environ.*, *157*, 1–8, doi:10.1016/j.rse.2014.09.021.

Pavelsky, T. M., and L. C. Smith (2009), Remote sensing of suspended sediment concentration, flow velocity, and lake recharge in the Peace-Athabasca Delta, Canada, *Water Resour. Res.*, *45*(11), 1–16, doi:10.1029/2008WR007424.

Peacock, M., C. Freeman, V. Gauci, I. Lebron, and C. D. Evans (2015), Investigations of freezing and cold storage for the analysis of peatland dissolved organic carbon (DOC) and absorbance properties, *Environ. Sci. Process. Impacts*, *17*, 1290–1301, doi:10.1039/C5EM00126A.

Pearson, R. G., S. J. Phillips, M. M. Loranty, P. S. a. Beck, T. Damoulas, S. J. Knight, and S. J. Goetz (2013), Shifts in Arctic vegetation and associated feedbacks under climate change, *Nat. Clim. Chang.*, *3*(7), 673–677, doi:10.1038/nclimate1858.

Peterson, B., E. Hobbie, and T. L. Corliss (1986), ow in a Tundra Stream Ecosystem, , (1978).

Peterson, B. J., R. M. Holmes, J. W. McClelland, C. J. Vörösmarty, R. B. Lammers, A. I. Shiklomanov, I. A. Shiklomanov, and S. Rahmstorf (2002), Increasing River Discharge to the Arctic Ocean, *Science (80-.).*, *298*(5601), 2171 –2173,

doi:10.1126/science.1077445.

Peterson, B. J., J. McClelland, R. Curry, R. M. Holmes, J. E. Walsh, and K. Aagaard (2006), Trajectory shifts in the Arctic and subarctic freshwater cycle., *Science*, *313*(5790), 1061–1066, doi:10.1126/science.1122593.

Peuravuori, J., and K. Pihlaja (1997), Molecular size distribution and spectroscopic properties of aquatic humic substances, *Anal. Chim. Acta*, *337*, 133–149, doi:10.1016/S0003-2670(96)00412-6.

Pithan, F., and T. Mauritsen (2014), Arctic amplification dominated by temperature feedbacks in contemporary climate models, *Nat. Geosci.*, *7*(February), 2–5, doi:10.1038/NGEO2071.

Pokrovsky, O. S. et al. (2015), Permafrost coverage, watershed area and season control of dissolved carbon and major elements in western Siberian rivers, *Biogeosciences*, *12*(21), 6301–6320, doi:10.5194/bg-12-6301-2015.

Poulin, B. A., J. N. Ryan, and G. R. Aiken (2014), The effects of iron on optical properties of dissolved organic matter., *Environ. Sci. Technol. Technol.*, *48*(17), 10098–10106, doi:10.1021/es502670r.

Quibell, G. (1991), The effect of suspended sediment on reflectance from freshwater algae, *Int. J. Remote Sens.*, *12*(1), 177–182, doi:10.1080/01431169108929642.

Raymond, P. A., and J. E. Bauer (2001), DOC cycling in a temperate estuary: A mass balance approach using natural 14 C and 13 C isotopes, *Limnol. Oceanogr.*, *46*(3), 655–667, doi:10.4319/lo.2001.46.3.0655.

Raymond, P. A., J. W. McClelland, R. M. Holmes, A. V. Zhulidov, K. Mull, B. J. Peterson, R. G. Striegl, G. R. Aiken, and T. Y. Gurtovaya (2007), Flux and age of dissolved organic carbon exported to the Arctic Ocean: A carbon isotopic study of the five largest arctic rivers, *Global Biogeochem. Cycles*, *21*(4), GB4011.

Reckhow, D. a, P. C. Singer, and R. L. Malcolm (1990), Chlorination of humic materials: Byproduct formation and chemical interpretations, *Environ. Sci. Technol.*, *24*(11), 1655–1664, doi:10.1021/es00081a005.

Runkel, R. L., C. G. Crawford, and T. a Cohn (2004), Load Estimator (LOADEST): A FORTRAN program for estimating constituent loads in streams and rivers. Techniques and Methods Book 4 , Chapter A5. U.S. Geological Survey., *World*, 69.

Santos, P. S. M., M. Otero, E. B. H. Santos, and A. C. Duarte (2010), Molecular fluorescence analysis of rainwater: Effects of sample preservation, *Talanta*, *82*(4), 1616–1621, doi:10.1016/j.talanta.2010.07.048.

Schmidt, G., C. Jenkerson, J. Masek, E. Vermote, and F. Gao (2013), *Landsat Ecosystem Disturbance Adaptive Processing System (LEDAPS) Algorithm Description*.

Schuur, E. a. G. et al. (2015), Climate change and the permafrost carbon feedback, *Nature*, *520*, 171–179, doi:10.1038/nature14338.

Slonecker, E. T., D. K. Jones, and B. A. Pellerin (2016), The new Landsat 8 potential for remote sensing of colored dissolved organic matter (CDOM), *Mar. Pollut. Bull.*, -, doi:http://dx.doi.org/10.1016/j.marpolbul.2016.02.076.

Smith, L. C., D. W. Beilman, K. V Kremenetski, Y. Sheng, G. M. Macdonald, R. B. Lammers, A. I. Shiklomanov, and E. D. Lapshina (2012), Short Communication

Influence of permafrost on water storage in West Siberian peatlands revealed from a new database of soil properties, *Methods*, *79*(February), 69–79, doi:10.1002/ppp.735.

Spence, C., S. V Kokelj, S. a Kokelj, M. Mccluskie, and N. Hedstrom (2015), Evidence of a change in water chemistry in Canada's subarctic associated with enhanced winter streamflow, *J. Geophys. Res. Biogeosciences*, *120*, 113–127, doi:10.1002/2014JG002809.Received.

Spencer, R., and G. Aiken (2009), Utilizing chromophoric dissolved organic matter measurements to derive export and reactivity of dissolved organic carbon exported to the Arctic Ocean: A case study, *Geophys. ...*, *36*, 1–6, doi:10.1029/2008GL036831.

Spencer, R. G. M., L. Bolton, and A. Baker (2007), Freeze/thaw and pH effects on freshwater dissolved organic matter fluorescence and absorbance properties from a number of UK locations., *Water Res.*, *41*(13), 2941–50, doi:10.1016/j.watres.2007.04.012.

Spencer, R. G. M., G. R. Aiken, K. P. Wickland, R. G. Striegl, and P. J. Hernes (2008), Seasonal and spatial variability in dissolved organic matter quantity and composition from the Yukon River basin, Alaska, *Global Biogeochem. Cycles*, *22*(4), 1–13, doi:10.1029/2008GB003231.

Spencer, R. G. M., P. J. Hernes, R. Ruf, A. Baker, R. Y. Dyda, A. Stubbins, and J. Six (2010), Temporal controls on dissolved organic matter and lignin biogeochemistry in a pristine tropical river, Democratic Republic of Congo, *J. Geophys. Res. Biogeosciences*, *115*(3), 1–12, doi:10.1029/2009JG001180.

Spencer, R. G. M., K. D. Butler, and G. R. Aiken (2012), Dissolved organic carbon and chromophoric dissolved organic matter properties of rivers in the USA, *J. Geophys. Res.*, *117*(G3), G03001, doi:10.1029/2011JG001928.

Spencer, R. G. M., G. R. Aiken, M. M. Dornblaser, K. D. Butler, R. M. Holmes, G. Fiske, P. J. Mann, and A. Stubbins (2013), Chromophoric dissolved organic matter export from U.S. rivers, *Geophys. Res. Lett.*, *40*(8), 1575–1579, doi:10.1002/grl.50357.

Spencer, R. G. M., P. J. Mann, T. Dittmar, T. I. Eglinton, C. McIntyre, R. M. Holmes, N. Zimov, and A. Stubbins (2015), Detecting the signature of permafrost thaw in Arctic rivers, *Geophys. Res. Lett.*, *42*(October), 2830–2835, doi:10.1002/2015GL063498.

Stedmon, C. A., R. M. W. Amon, A. J. Rinehart, and S. A. Walker (2011), The supply and characteristics of colored dissolved organic matter (CDOM) in the Arctic Ocean : Pan Arctic trends and differences, *Mar. Chem.*, doi:10.1016/j.marchem.2010.12.007.

Striegl, R. G., G. R. Aiken, M. M. Dornblaser, P. A. Raymond, and K. P. Wickland (2005), A decrease in discharge-normalized DOC export by the Yukon River during summer through autumn, *Geophys. Res. Lett.*, *32*(21), L21413.

Stubbins, A., J. Niggemann, and T. Dittmar (2012), Photo-lability of deep ocean dissolved black carbon, *Biogeosciences*, *9*(5), 1661–1670, doi:10.5194/bg-9-1661-2012.

Stubbins, A., R. G. M. Spencer, P. J. Mann, R. M. Holmes, J. W. McClelland, J. Niggemann, and T. Dittmar (2015), Utilizing colored dissolved organic matter to derive dissolved black carbon export by arctic rivers, *Front. Earth Sci.*, *3*(October), 1–11, doi:10.3389/feart.2015.00063.

Tank, S. E., L. F. W. Lesack, J. A. L. Gareis, C. L. Osburn, and R. H. Hesslein (2011), Multiple tracers demonstrate distinct sources of dissolved organic matter to lakes of the Mackenzie Delta, western Canadian Arctic, *Limnol. Oceanogr.*, *56*(4), 1297–1309, doi:10.4319/lo.2011.56.4.1297.

Tank, S. E., K. E. Frey, R. G. Striegl, P. A. Raymond, R. M. Holmes, J. W. McClelland, and B. J. Peterson (2012a), Landscape-level controls on dissolved carbon flux from diverse catchments of the circumboreal, *Global Biogeochem. Cycles*, *26*(3), 1–15, doi:10.1029/2012GB004299.

Tank, S. E., M. Manizza, R. M. Holmes, J. W. McClelland, and B. J. Peterson (2012b), The Processing and Impact of Dissolved Riverine Nitrogen in the Arctic Ocean, *Estuaries and Coasts*, *35*(2), 401–415, doi:10.1007/s12237-011-9417-3.

Tank, S. E., R. G. Striegl, J. W. McClelland, and S. V. Kokelj (in review), Multi-decadal increases in dissolved organic carbon and alkalinity flux from the Mackenzie drainage basin to the Arctic Ocean.

Tarnocai, C., J. G. Canadell, E. a. G. Schuur, P. Kuhry, G. Mazhitova, and S. Zimov (2009), Soil organic carbon pools in the northern circumpolar permafrost region, *Global Biogeochem. Cycles*, *23*(2), 1–11, doi:10.1029/2008GB003327.

Tfaily, M. M., D. C. Podgorski, J. E. Corbett, J. P. Chanton, and W. T. Cooper (2011), Influence of acidification on the optical properties and molecular composition of dissolved organic matter, *Anal. Chim. Acta*, *706*(2), 261–267, doi:10.1016/j.aca.2011.08.037.

Townsend-Small, A., J. W. McClelland, R. Max Holmes, and B. J. Peterson (2010), Seasonal and hydrologic drivers of dissolved organic matter and nutrients in the upper Kuparuk River, Alaskan Arctic, *Biogeochemistry*, *103*(1-3), 109–124, doi:10.1007/s10533-010-9451-4.

Tranvik, L. J., J. a. Downing, J. B. Cotner, S. a. Loiselle, R. G. Striegl, T. J. Ballatore, P. Dillon, K. Finlay, K. Fortino, and L. B. Knoll (2009), Lakes and reservoirs as regulators of carbon cycling and climate, *Limnol. Oceanogr.*, *54*(6_part_2), 2298–2314, doi:10.4319/lo.2009.54.6_part_2.2298.

Vodacek, A., S. A. Green, and N. V Blough (1994), An experimental model of the solar-stimulated fluorescence of chromophoric dissolved organic matter, *Limnol. Oceanogr.*, *39*(January), 1–11.

Vonk, J. E. et al. (2015), Reviews and syntheses: Effects of permafrost thaw on Arctic aquatic ecosystems, *Biogeosciences*, *12*(23), 7129–7167, doi:10.5194/bg-12-7129-2015.

Walker, S. a., R. M. W. Amon, and C. a. Stedmon (2013), Variations in high-latitude riverine fluorescent dissolved organic matter: A comparison of large Arctic rivers, *J. Geophys. Res. Biogeosciences*, *118*(4), 1689–1702, doi:10.1002/2013JG002320.

Walvoord, M. A., and R. G. Striegl (2007), Increased groundwater to stream discharge

from permafrost thawing in the Yukon River basin: Potential impacts on lateral export of carbon and nitrogen, *Geophys. Res. Lett.*, *34*(12), doi:10.1029/2007GL030216.

Weishaar, J., G. Aiken, B. Bergamaschi, M. Fram, R. Fujii, and K. Mopper (2003), Evaluation of specific ultra-violet absorbance as an indicator of the chemical content of dissolved organic carbon, *Environ. Sci. Technol.*, *37*(20), 4702–4708, doi:10.1021/es030360x.

White, D. et al. (2007), The arctic freshwater system: Changes and impacts, *J. Geophys. Res.*, *112*(G4), 1–21, doi:10.1029/2006JG000353.

Wickland, K. P., J. C. Neff, and G. R. Aiken (2007), Dissolved Organic Carbon in Alaskan Boreal Forest: Sources, Chemical Characteristics, and Biodegradability, *Ecosystems*, *10*(8), 1323–1340, doi:10.1007/s10021-007-9101-4.

Wickland, K. P., G. R. Aiken, K. Butler, M. M. Dornblaser, R. G. M. Spencer, and R. G. Striegl (2012), Biodegradability of dissolved organic carbon in the Yukon River and its tributaries: Seasonality and importance of inorganic nitrogen, *Global Biogeochem. Cycles*, *26*(3), 1–14, doi:10.1029/2012GB004342.

Woo, M. K., and R. Thorne (2003), Streamflow in the Mackenzie Basin, Canada, *Arctic*, *56*(4), 328–340.

Xie, H., N. Krotkov, P. Larouche, W. F. Vincent, and M. Babin (2006), Photomineralization of terrigenous dissolved organic matter in Arctic coastal waters from 1979 to 2003 : Interannual variability and implications of climate change, *Arctic*, *20*, 1–13, doi:10.1029/2006GB002708.

Xie, H., C. Aubry, S. Bélanger, and G. Song (2012), The dynamics of absorption coefficients of CDOM and particles in the St . Lawrence estuarine system : Biogeochemical and physical implications, *Mar. Chem.*, *128-129*, 44–56, doi:10.1016/j.marchem.2011.10.001.

Xue, S., Y. Wen, X. Hui, L. Zhang, Z. Zhang, J. Wang, and Y. Zhang (2015), The migration and transformation of dissolved organic matter during the freezing processes of water, *J. Environ. Sci. (China)*, *27*(C), 168–178, doi:10.1016/j.jes.2014.05.035.

Yamashita, Y., N. Maie, H. Brice??o, and R. Jaff?? (2010), Optical characterization of dissolved organic matter in tropical rivers of the Guayana Shield, Venezuela, *J. Geophys. Res. Biogeosciences*, *115*(G1), doi:10.1029/2009JG000987.

Yu, Q., Y. Q. Tian, R. F. Chen, A. Liu, G. B. Gardner, and W. Zhu (2010), Functional Linear Analysis of in situ Hyperspectral Data for Assessing CDOM in Rivers Winner of the AAG-RSSG 2010 Best Paper Award for Early Career Scholars in Remote Sensing 1, *Photogramm. Eng. Remote Sens.*, *76*(10), 1147–1158.